

C.P. No. 1337



C.P. No. 1337

PROCUREMENT EXECUTIVE, MINISTRY OF DEFENCE

AERONAUTICAL RESEARCH COUNCIL

CURRENT PAPERS

Design and Theoretical Assessment of  
Experimental Glide Path and Flare Systems  
for a BAC 1-11 Aircraft  
(Including Direct Lift Control)

by

*F. R. Gill and M. J. Corbin*

*Avionics Dept., R.A.E., Farnborough*

LONDON: HER MAJESTY'S STATIONERY OFFICE

1975

PRICE £2-60 NET

\*CP No.1337

January 1974

DESIGN AND THEORETICAL ASSESSMENT OF EXPERIMENTAL GLIDE PATH AND  
FLARE SYSTEMS FOR A BAC 1-11 AIRCRAFT  
(INCLUDING DIRECT LIFT CONTROL)

by

F. R. Gill

M. J. Corbin

SUMMARY

Two experimental glide path and flare systems are described, one using spoilers installed in the aircraft to provide direct lift control. The various longitudinal control modes, altitude hold, glide path and flare, have similar feedback control gains whose values were determined by parameter optimisation.

An assessment of the performance of these two systems is described. Using elevator and throttle control only, there was little improvement over current flare systems, but use of high gain direct lift control can give significant improvement.

CONTENTS

	<u>Page</u>
1 INTRODUCTION	3
2 DISPLACEMENT HOLD SYSTEM	3
2.1 Throttle control	3
2.2 Description of elevator only system	4
2.3 Description of elevator and DLC system	4
2.4 Pole positions	6
2.5 Turbulence and noise performance	6
2.6 Responses to step inputs	7
3 THE ILS GLIDE PATH MODE	7
3.1 Variation in pole positions with range-to-go	9
3.2 Turbulence and noise performance	10
4 FACTORS AFFECTING DESIGN OF FLARE	10
4.1 Ground effect	10
4.2 Factors affecting choice of control for flare trajectory	12
4.3 Change of vertical speed in displacement hold system	13
4.4 Exponential flare in the absence of ground effect	14
4.5 Exponential flare in the presence of ground effect	16
4.6 Terminal conditions	16
4.7 An alternative approach to the flare trajectory problem	17
5 PROPOSED FLARE SYSTEMS AND PERFORMANCE ASSESSMENT	19
5.1 Description of flare systems	19
5.2 Justification of design procedure	19
5.3 Effect of variations in mean wind speed and levels of turbulence	21
5.4 Changes in glide slope	22
5.5 Effect of runway undulations	23
5.6 Touchdown errors caused by turbulence and ILS noise before the start of flare	23
5.7 Responses to step gusts	23
6 GLIDE PATH ACQUIRE	24
7 DISCUSSION AND CONCLUSIONS	26
Appendix Description of simulation models and systems transfer functions	29
Tables 1-4	33
Symbols	40
References	42
Illustrations	Figures 1-23
Detachable abstract cards	-

## 1 INTRODUCTION

The results of a study of ILS glide path and flare systems for experimental evaluation in a BAC 1-11 aircraft are presented in this paper. One of the principal aims of the study was an assessment of the possible performance improvements to be attained using the spoilers now fitted to this aircraft.

Two 'starting' systems are defined in detail, one using elevator and throttle alone and the other using the spoilers in addition. Variations to these 'starting' systems are discussed, particularly where final choice is best made after certain flight tests. The BAC 1-11 is fitted with an analogue computer on which the experimental control laws are patched and can be rapidly changed; this facility should enable the indicated variations to be flight tested with minimal delay.

The study was carried out in 1972 by Controls and Displays Division, Avionics Department, close liaison being maintained with BLEU who are responsible for the forthcoming flight evaluation. A contract has been placed with industry to support the design studies and flight evaluation.

The aircraft's equations of motion and actuator characteristics assumed during the study are defined in the Appendix.

Reference is made to other papers<sup>1,2,3,7</sup> for details of the design procedure used during the present study.

## 2 DISPLACEMENT HOLD SYSTEM

Detailed description and assessment of the proposed experimental systems commences with a displacement hold system, i.e. a height hold mode in which the height error sensor has negligible lag.

### 2.1 Throttle control

For all systems described in this paper, the throttle control errors:

$$T_D = 0.4 \left( 1 + \frac{0.05}{5} \right) (u + u_g) \quad (1)$$

where  $(u + u_g)$  is the airspeed error. No account was taken in this study of the problem of throttle activity. Detailed investigations were made with the possible use of other terms; none was found to be advantageous.

## 2.2 Description of elevator only system

A detailed block diagram of the elevator control is given in Fig.1. The 'optimum' values of the control parameters being chosen using a parameter optimisation technique described elsewhere.

Because a rate servo has been installed in the BAC 1-11, it is necessary to derive a rate of change of elevator demand,  $s\eta_D$ . In order to offset datum errors in the rate servo amplifier, a double integral term is desirable:

$$s\eta_{D5} = \frac{G}{h} \int y_3 dt$$

where  $y_3$  is the displacement error. Otherwise the system is identical to one for a positional servo system with the same characteristics.

In the design, component shortage on the analogue computer in the BAC 1-11 was considered and led to selecting time constants not less than 0.1 s. There was a resulting loss of performance but this was small for the relatively slow acting elevator servo characteristics.

## 2.3 Description of elevator and DLC system

The solution presented is one in which performance is never worse than the elevator only case. When the spoiler demand or its rate is zero, the control is that described in section 2.2 and Fig.1, except for a slow acting spoiler trim adjust loop. When the spoiler demand or its rate are not limited, the additional control is that shown in Fig.2.

The spoiler control has vertical motion terms only:

$$\left. \begin{aligned} \delta_{D2} &= (k_{m\eta}/k_{m\delta})\eta_{D2} \\ \delta_{D3} &= (k_{m\eta}/k_{m\delta})\eta_{D3} \end{aligned} \right\} \quad (2)$$

where  $k_{m\eta}$  and  $k_{m\delta}$  are the pitching moment coefficients of elevator and spoiler respectively. The data available on the spoiler characteristics suggest that  $(k_{m\eta}/k_{m\delta})$  is 8.6 which leads to the large gains defined in Fig.2. Such high gains are feasible only if severe limits can be applied to the spoiler demand and its rate during initial flying with the system. It was this consideration that led to the form of DLC given in Fig.2.

The design included an assessment of the advantages of all possible feed-back terms to the spoilers and elevator (pitch rate, pitch attitude, integral of pitch attitude; normal acceleration, normal velocity, height error and its integral; forward speed error and acceleration). If ideal spoilers are assumed with zero pitching and drag coefficients, it has been shown that pitch terms ( $G_q$ ,  $G_\theta$ ) should be fed to elevator and vertical motion terms ( $B_h$ ,  $B_h^\bullet$  and  $B_h^{\bullet\bullet}$ ) to the spoilers. The gain  $B_h^\bullet$  must be greater than  $13^\circ$  per m/s in order to improve vertical motion performance compared with the elevator only case. Pitching performance is much better than the elevator only case.

The loss of pitching performance incurred when the spoilers are assumed to possess a representative pitching moment can be recovered by feeding vertical motion terms ( $G_h$ ,  $G_h^\bullet$  and  $G_h^{\bullet\bullet}$ ) to the elevator as well as to the spoilers. Almost complete elimination of the effect of pitching moment is obtained if:

$$B_h^\bullet = (k_{m\eta}/k_{m\delta})G_h^\bullet$$

$$B_h = (k_{m\eta}/k_{m\delta})G_h \quad .$$

Therefore, by increasing ( $B_h^\bullet$ ,  $B_h$ ) until ( $G_h^\bullet$ ,  $G_h$ ) take on the 'optimum' elevator only values, good performance in both pitching and vertical motion is attained; and, in addition, when the rate or amplitude limits on the DLC are exceeded, performance is not worse than the elevator only case.

Because the spoiler authority is limited, it is desirable to apply an automatic trim,  $K_\delta$  in Fig.2. In the absence of  $G_h^\bullet$ , necessary only to adjust for datum errors in the rate servo,  $K_\delta$  can be increased to  $0.1 \text{ s}^{-1}$  without much loss in performance and the automatic trim is fast. However, it was found impossible to use simultaneously sufficiently high values of  $G_h^\bullet$  and  $K_\delta$  that would be effective during the duration of the approach. The tentative solution proposed is based on previous experience<sup>5</sup>; that the elevator servo drift is constant during an approach. During the highest hold prior to glide path join, it is proposed to fly the system on elevator only for a sufficient time to allow a signal to be generated ( $G_h^\bullet = 0.04^\circ/\text{m s}^2$ ) that should offset the rate servo datum error. This signal is 'frozen' before the DLC is used and remains 'frozen' during the approach and landing; thus allowing use of a high  $K_\delta$  during the approach.

## 2.4 Pole positions

The positions of all poles of the controlled system in the s-plane describe best the modal characteristics, particularly relative damping and settling times. These are given in Fig.3a and b for the elevator only and DLC cases respectively. A log-log scale is used in order to facilitate plotting all poles. On this scale, lines of equal relative damping are parallel; the 0.5 and 0.3 relative damping lines have been drawn.

All modes are within the design criterion, 0.5 relative damping and 20s settling time except for a long period pole, 10s settling time which is slightly underdamped. In the DLC case, Fig.3b, this case for  $G_h = 0.01^\circ/\text{m s}^2$  and  $K_\delta = 0.01 \text{ s}^{-1}$  has been selected to indicate the unacceptable long period mode for the 'best' compromise between offsetting the drift due to rate servo and automatic spoiler trim; this compromise solution was discarded (see section 2.3).

## 2.5 Turbulence and noise performance

The standard deviations in height error, vertical velocity and pitch attitude given in Table 2 were obtained for the models of horizontal and vertical turbulence and displacement error sensor noise defined in Table 1. These values were obtained by sampling the respective state variables at the end of each of 500 runs on the hybrid computer.

A qualitative illustration of this data is given in Fig.4 which present time histories of relevant state variables for the horizontal turbulence model. The principal features are:

- (a) the small effect of elevator control non-linearities,  $\pm 0.1^\circ$  dead-zone and  $\pm 0.25^\circ$  backlash (see Appendix)
- (b) the small effect of the applied spoiler demand limits on the performance of the DLC system
- (c) the improvement in pitching and vertical motion performance using DLC although the spoiler demands are limited.

This improvement and the slight effect of non-linearities is illustrated again in Fig.5 which shows the distribution of vertical velocity errors due to horizontal turbulence for (a) elevator only, and (b) DLC. The reason for presenting histograms is to demonstrate the satisfactory nature of the error distributions. There are no significant irregularities in the distributions shown in Fig.5.

## 2.6 Responses to step inputs

The systems' responses to step inputs are presented to demonstrate properties not revealed by responses to turbulence and noise inputs which, because they possess zero mean, do not produce a change in steady state (trim) of the control signals. The time responses in Fig.6 were obtained for the step inputs defined in Table 1, non-linearities being neglected.

### 3 THE ILS GLIDE PATH MODE<sup>4,5</sup>

This mode is a special case of the displacement hold system in which the ILS error signal  $y_{32}$  is considered as the displacement error.

The ILS is an angular system so that the ILS signal for a constant linear displacement from the glide slope varies with range-to-go to the glide slope origin. Any signal path in the control system relating elevator (or spoiler) deflection to the ILS signal has a gain to true displacement which increases as range-to-go decreases; by 1:40 in approaching from 12 km to 300m range. The dynamic characteristics of the control system depend on these gains referred to true displacement and, therefore, the dynamic characteristics change during the approach, i.e. the system is non-stationary.

In order to attain 'best' performance at the end of the glide path mode, at the runway threshold, the ILS gearings are selected to produce gains to true displacement at 300m range (threshold) equal to the 'best' displacement hold system, i.e. the system described in section 2. The amount of scheduling of the ILS signals and the choice of other control parameters must then be selected to provide acceptable settling time, damping and other performance features during the approach.

The ILS signal is used in three signal paths in the two 'starting' systems:

- (a) mixed with an accelerometer signal to produce a measure of velocity error normal to the glide slope
- (b) a displacement term
- (c) an integral of displacement to offset displacement errors due to datum errors.

An alternative possibility employs barometric height error in the mixing filter, as in the Hunter's experimental autopilot<sup>7</sup>.



In order to experience acceptable settling time at range, it is necessary to vary the ILS gearing (degrees of elevator per  $\mu\text{A}$  beam error) in the displacement signal path, (b) above, so as to partially compensate for the 1:40 change in the displacement gain (degrees of elevator per m displacement error). Complete compensation is not recommended because this would lead to an unnecessary increase in the effects on the system of ILS noise, e.g. course bends. A scheduled change of 8:1, varying linearly with barometric height was used previously<sup>4,5</sup> and, although there are other possibilities, this is proposed for the 'starting' systems.

Referring to Figs.1 and 2, the signal  $y'_3$  is replaced by:

$$y'_{32} = \frac{1}{(1 + \tau_3 s)} \left\{ 0.82 + 0.0036 H \right\} y_{32} \quad (3)$$

where  $H$  is barometric height in feet and  $y_{32}$  the ILS error signal. This law is valid for a  $3^\circ$  glide path only.

Because the gain to true displacement is a factor 5 down at range compared with the displacement hold system, the integral term, (c) above, must be more than a factor 40 down otherwise the damping of a long period mode is unacceptable. The solution proposed is a decrease in gain of  $G_h^-$  to  $0.01^\circ/\text{m s}$  experienced at 300m range and the application of no scheduling to the ILS signal from which this control term is derived. With this low value of integral gain, it is not possible to use a significant value of the double integral. This term is not applied during glide path hold (or flare) and it is therefore important to compute the necessary voltage that offsets the rate servo drift prior to glide path acquire (see section 2.3).

Finally, for the ILS signal fed to the mixing filter, the solution proposed was found as a compromise between conflicting interests:

(i) as the degree of scheduling of this signal was increased, the effects of ILS noise or the effects of accelerometer datum error increased depending on the mixing filter parameter  $B_0$

(ii) as the degree of scheduling was decreased, damping of the dominant mode decreased depending on  $B_0$ .

The experimental system flown in the Comet 3B appeared to be just satisfactory from the viewpoint of ILS noise. The ILS noise performance of the proposed systems is not worse than the Comet 3B: this is illustrated in Fig.7.

However, it was necessary to improve the performance with respect to accelerometer datum error since signals from an inertial platform were available in the Comet 3B whereas a strapped-down accelerometer only is available in the BAC 1-11.

The solution proposed applies no scheduling to the ILS signal fed to the mixing filter which has a parameter value  $B_0 = 0.5 \text{ s}^{-1}$ . Performance with respect to accelerometer datum error is unacceptable unless an approximate correction for attitude changes is applied:

$$y_5 = y_5' + g \left( \frac{\theta^2}{2} + \frac{\phi^2}{2} \right) \quad (4)$$

where  $y_5$  is the signal fed to the control system, Figs.1 and 5,  
 $y_5'$  is the output of the accelerometer, and  
 $\theta, \phi$  are approximate changes in pitch and bank.

### 3.1 Variation of pole positions with range-to-go

The modal characteristics of the system vary with range-to-go  $R$ , being identical with the displacement hold system, section 2, at  $R = 300 \text{ m}$  (except for the effects of the lower values of  $G_{\bar{h}}$  and  $G_{\bar{h}}$ ). The variation is shown in Fig.8 for the two cases, (a) elevator only, and (b) with DLC.

In order to obtain these pole positions, the system was linearised at different ranges-to-go, applying equation (3). The approximation is valid even at short range because the rate of gain change referred to true displacement is small compared with the frequency of the mode of interest. Justification for the linearisation is given below.

For both elevator only and DLC cases, the 0.5 relative damping criterion is exceeded by a mode associated with the mixing filter. At the expense of poorer performance with respect to accelerometer datum errors, the damping can be increased by decreasing  $B_0$ , the mixing filter parameter; or, at the expense of increasing the effects of ILS noise, by applying scheduling to the ILS signal fed to the mixing filter. Alternatively, improved damping can be obtained by replacing the ILS signal to the mixing filter by the signal from a barometric altimeter but due allowance must be made for the lag on this signal and the noise of the signal. Flight tests alone, using the starting control systems, will produce the improved models of noise, lags and datum errors necessary to make a better compromise between conflicting interests.

### 3.2 Turbulence and noise performance

The standard deviations in pitch attitude, displacement error and its rate given in Table 3 were obtained for the models of turbulence and ILS noise defined in Table 1. This data was obtained by sampling the respective state variables at the end of 200 runs.

The equations of motion for cases (1)-(3) in Table 3 were linearised at the given range-to-go  $R$ , using equation (3). The changes in performance with range-to-go are not significant.

Case (4) in Table 3 was obtained with a simulation of the beam tightening effect. Comparison of performance under the non-stationary conditions with that under linearised conditions is given in Case (4), Table 3, to justify the assumption made during the design and analysis that the non-stationary property has little effect on turbulence and noise performance.

The small effects of control non-linearities are illustrated in Fig.9 which are time histories of relevant state variables during height hold, ILS acquire, ILS hold and 'flare'. Horizontal turbulence was applied and the proposed procedure for glide path acquire (section 6) and 'flare' (section 4 and 5) were simulated, the 'flare' system being one appropriate for negligible ground effect.

Further information is presented in Fig.10 in which the standard deviations in pitch attitude and velocity error are plotted against the reciprocal of range-to-go  $R$ . Comparison is made between the elevator only and DLC cases, useful in providing the expected advantage of using DLC during the glide path hold mode.

## 4 FACTORS AFFECTING DESIGN OF FLARE

### 4.1 Ground effect

The aircraft's equations of motion during flare, as modified by ground effect, are non-linear (Appendix). It has been shown that<sup>8</sup> the equations of motion can be linearised, ground effect causing:

- (a) changes to the aerodynamic derivatives with height above runway
- (b) 'inputs' such as a pitching moment which vary with height above the runway.

The changes to the aerodynamic derivations cause a change to the modal characteristics of the controlled system and it is necessary to ensure that all modes are well damped at all times during the flare. Otherwise, a particular disturbance may excite unnecessarily an underdamped mode with a consequential poor touchdown performance.

These modal characteristics are best defined by the variation in pole positions with height above runway, using the linearised equations of motion. The pole plots shown in Fig.11 were obtained with the displacement hold system defined in section 2, except that the integral gains ( $G_{\bar{h}}$  and  $G_{\bar{h}}$ ) were zero. The modal characteristics are satisfactorily showing that the effect of ground effect is small.

With certain reservations, the displacement hold system defined in section 2 and used to obtain the modal characteristics in Fig.11 is one that minimises the effects of external disturbances, i.e. horizontal and vertical turbulence and an external pitching moment such as experienced during flare. The reservations apply only to the elevator only case and are associated with whether it is pitching errors or vertical motion errors about a prescribed trajectory that are important. Given that pitch errors are within acceptable limits, the minimisation of displacement errors from the prescribed trajectory is required for flare; and it is this objective that was used in the design of the displacement hold system.

Therefore, the displacement hold system is an 'optimum' basis for a flare system to which is added the control needed to define the trajectory in a fashion that does not affect the continuous closed loop performance of the hold control. An improvement would have been obtained if, in the design of the displacement hold system, allowance had been made for the change in modal characteristics; in a previous study of flare<sup>6</sup>, the control parameters were selected to minimise the effects of turbulence subject to all modes possessing 0.5 relative damping at the start and end of flare and this technique is recommended.

The use of an acceleration term in the control complicates the flare system and it is important to assess its importance. The aircraft equations of motion of the BAC 1-11 are such that hold performance without the acceleration term (elevator only case) is little inferior to that with the term. However, this is not the case with other aircraft so that, for the starting systems, it was decided to develop systems using the acceleration term.

#### 4.2 Factors affecting choice of control of flare trajectory

In order to produce the flare trajectory, it is necessary to add control terms to the displacement hold system. In a linear system, this implies that the additional signals are applied at the start of flare,  $t = t_f$ . Flare performance is then determined by:

- (a) when flare is started
- (b) how the control system is initialised at the start of flare
- (c) the means of achieving the required trajectory
- (d) terminal conditions at the end of flare.

A brief comparison study of a number of different types of system was made and, although not exhaustive, the systems proposed appeared to be best taking into account certain practical problems.

The basic elements of the proposed flare control is shown in Fig.12, the signal paths associated with the displacement terms are not shown in order to simplify presentation. The outputs  $y_{42}$  and  $y_{43}$  of the two mixing filters are measures of the aircraft's velocity normal to the ILS beam and to the ground respectively.

The time of flare start is determined by:

$$y_{43} - y_{42} + ky_{33} = 0 \quad (5)$$

where  $y_{33}$  is the height above runway measured by the radio altimeter and  $k$  is the flare time constant. Under undisturbed conditions this equation reduces to:

$$\dot{H} + kH = 0$$

where  $H$  and  $\dot{H}$  are height and velocity relative to a perfect horizontal runway. The ideal flare start occurs therefore when the aircraft lies on the ideal exponential trajectory:

$$H = H_f e^{-kt}, \quad \dot{H} = -kH_f e^{-kt}.$$

This choice of the time for flare start reduces the effects of variations in mean vertical speed prior to flare start and leads to a system useful for steep approaches.

At this time,  $t = t_f$ , defined by equation (5), vertical speed control is switched from one mixing filter to the other, switch one from A to B, Fig.12. In order to overcome the undesirable transient that would be caused by the step  $(y_{43} - y_{42})$ , the value  $X_1$  of the difference between mixing filters is stored at  $t = t_f$  and the negative applied to the mixing filter output. A similar technique is applied to the displacement error signal path (not shown in Fig.12).

Command signals are now applied to the elevator and throttle through a lag with time constant  $\tau_f$ . These command signals are proportional to  $X_1$ , the stored values of  $(y_{43} - y_{42})$  at flare start. They are distinguished in Fig.12 by the subscript  $c$  and are defined as follows:

- (a)  $\dot{h}_c$ , the expected change in vertical velocity during flare
- (b)  $\eta_c$ , an additional elevator command that offsets the opposing effect of the pitch attitude feedback (ground effect neglected)
- (c)  $\Delta\eta_c$ , an additional elevator command that corrects for the ground effect 'input'
- (d)  $u_c$ , a throttle command necessary to ensure that the aircraft pitches up by the desired amount
- (e)  $h_c$ , the desired trajectory in height.

In the DLC system, the commands  $\dot{h}_c$  and  $h_c$ , are applied to both spoilers and elevator through the respective gains  $B_h^*$ ,  $G_h^*$ ,  $B_h$  and  $G_h$ .

Results are presented in the following sub-sections to demonstrate the separate effects of these signals which produce the flare trajectory.

#### 4.3 Change of vertical speed in displacement hold system (elevator only)

Computer results are presented first on the response of the displacement hold system to a command  $\dot{h}_c$ , a step of 10 m/s lagged by a first order lag, time constant  $\tau_f = 2.33$  s. The flare system outlined in section 4.2 is based on such a command.

The response to such a command is shown in Fig.13a, the displacement gains being zero. The system is underdamped but the main interest is in the

steady state performance. The steady state error in  $\dot{h}$  is caused by the change in  $\theta$  and  $u$  which, through the control, opposes the command  $\dot{h}_c$ . If  $G_\theta$  is decreased, the steady state in  $\dot{h}$  decreases, as illustrated in Fig.13b.

The addition of an elevator demand  $\eta_c$  eliminates the opposing action of  $G_\theta\theta$  (applicable to both systems, with and without DLC). Ignoring the effect of changes in  $u$ , the value of  $\eta_c$  is:

$$\eta_c = \dot{h}_c \left( \frac{57.3}{V_T} \right) G_\theta = \dot{h}_c \left( \frac{G_\theta}{1.14} \right) . \quad (6)$$

The result of adding this signal is shown in Fig.13c; the steady state error in  $\dot{h}$  is small. The residual steady state error can be eliminated by adding a term  $A_\theta\theta = 0.17\theta$ ; or by adjusting  $\eta_c$  or adding a command  $u_c$  depending on what change in pitch attitude or forward speed is required.

Given zero steady state error in  $\dot{h}$  without using displacement terms, the latter can be added, i.e.  $G_h(h - h_c)$  where  $h_c$  is the integral of the command  $\dot{h}_c$ . The result is shown in Fig.13d. The steady state errors in  $(\dot{h} - \dot{h}_c)$  and  $(h - h_c)$  are negligible and the overshoots in the responses are small.

Instead of the application of the additional  $\eta_c$  command, it is possible to attain zero steady state in  $(\dot{h} - \dot{h}_c)$  by applying the control term

$G_h \int (\dot{h} - \dot{h}_c) dt$ . The speed with which the steady state in  $(\dot{h} - \dot{h}_c)$  is

achieved depends on the gain  $G_h$ , the value of which is restricted from stability considerations. The response of  $\dot{h}$  to the command is more sluggish and exhibits greater overshoots than in the recommended solution, *viz.* the addition of  $\eta_c$ . Moreover, there is a steady state error in  $(h - h_c)$  which

can be eliminated by the application of the integral,  $G_h \int (h - h_c) dt$ , but

only at the expense of a further deterioration in the transient response of  $(\dot{h} - \dot{h}_c)$  and  $(h - h_c)$ .

#### 4.4 Exponential flare in the absence of ground effect

Consider next the design of an exponential flare trajectory in the absence of ground effect, starting from  $H_f = 15.2$  m,  $\dot{H}_f = 3.4$  m/s on the ideal flare trajectory. The terminal conditions required are assumed to be  $H = 0$  and

$\dot{H} = 0$ ; this defines an exponential flare:

$$H = H_f e^{-kt}, \quad \dot{H} = \dot{H}_f e^{-kt}, \quad k = 0.225 \text{ s}^{-1} .$$

Referring to Fig.12, when the mixing filters are changed over, switch one from position A to B, the required step of 3.4 m/s occurs in the vertical speed signal path.

Following a similar approach to that discussed in section 4.3, the system's responses to this step, displacement gains zero, are shown in Fig.14a. Ignoring the underdamped nature of the response, there is a steady state error in  $\dot{H}$ . In addition, the system's response is too rapid to obtain the desired trajectory in  $H$ . The system's speed of response could be decreased by decreasing  $G_h$  but only at the expense of a deterioration in turbulence performance. (The vertical motion responses in Fig.14 are referred to displacement error from the glide slope before start of flare and to runway after the start of flare.)

When the negative of the difference between the mixing filter outputs  $X_1$  is applied at  $t = t_f$ , the responses shown in Fig.14b were obtained. The transient effect of the changeover has been eliminated.

The command  $\dot{h}_c$  is derived from  $X_1$  through a first order lag, time constant  $\tau_f$ , Fig.12. The responses shown in Fig.14c were obtained for  $\tau_f = 2.23 \text{ s}$ . The important feature is the steady state error in  $\dot{H}$ .

Application of the additional signal  $\eta_c$ , equation (6), and a term  $A_\theta \theta$  to the throttle ( $A_\theta = 0.17$ ) produced the responses in Fig.14d. The steady state error in  $\dot{H}$  is zero although there is a steady state error in  $H$ . The latter can be eliminated by changing the time constant  $\tau_f$ . An acceptable solution is  $\tau_f = 3.0 \text{ s}$ , Fig.14e.

Finally, the displacement error term is added,  $G_h(H - h_0 + h_c)$ , where  $h_0 = X_1/k$  and  $h_c = \dot{h}_c/k$ . The resulting responses in Fig.14f show that  $\dot{H}$  and  $H$  are exponential to the runway, as required, and that the elevator and acceleration responses are small.

It will be noticed that the time constant  $\tau_f$  (3.0 s) is less than the flare time constant  $1/k$  (4.45 s). The reason for this is believed to be due mainly to the opposing action of the acceleration and pitch rate feedback terms.

It will also be noticed that the pitch attitude at 'touchdown' is zero, an undesirable feature in a practical flare system. This results from the use,



during this particular part of the investigation of the throttle term  $0.17\theta$  applied to produce zero change in forward speed.

#### 4.5 Exponential flare in the presence of ground effect

The problem is a little more complicated when ground effect is included. Consider first the case when the displacement error gain is zero, the responses without ground effect being those given in Fig.14e. The addition of ground effect modifies the responses, Fig.14g. The steady state error in  $\dot{H}$  is negligible but the steady state errors in  $H$  and  $\theta$  are not acceptable.

Instead of applying a throttle term  $A_\theta\theta$ , a throttle command

$$u_c = c_3 \dot{h}_c$$

is added; and the additional elevator command is modified:

$$\eta_c = (c_1 + c_2) \dot{h}_c \quad (7)$$

$c_1 = G_\theta/1.14$  being the command for no ground effect. Adjustment of  $c_2$  and  $c_3$  yielded the desired zero steady state in  $H$  and an acceptable steady state in  $\theta$ , Fig.14h. When the displacement error term was applied, the responses in Fig.14i were obtained.

#### 4.6 Terminal conditions

Conversion of the flare system exponential to the runway to one which yields acceptable undisturbed touchdown performance can be made in several ways. Two were considered:

- (a) aim to exponentially flare to a horizontal plane below the runway surface such that the rate of descent at touchdown is 0.6 m/s
- (b) aim to produce a steady state rate of descent of 0.6 m/s just before touchdown.

From an assessment of performance with each method, using the conventional band-limited noise model of turbulence, there appeared to be little benefit in applying the slightly more complicated method (b).

The starting systems described in more detail in section 5 were therefore based on (a). A small adjustment to the additional command signal  $\eta_c$ , through the parameter  $c_2$ , is all that is necessary to convert from the flare

trajectory exponential to the runway to the flare trajectory exponential to a horizontal plane below the runway level, terminal condition (a).

In the light of results<sup>9</sup> obtained since this study was completed, it is believed now that method (b) is more attractive. These further results were obtained during investigations into defining the gust time histories yielding worst touchdown errors. Applying terminal condition (a), gusts of reasonable amplitude were found which produced large range errors, the aircraft 'floating' along the runway. The addition of an integral term of the form:

$$G_h^- \int (y_{33} - h_0 + h_c) dt \quad G_h^- \leq 0.4^\circ/\text{m s}$$

would prevent this floating,  $y_{33}$  being the radio altimeter output. It was found, however, that the 'floating' did not occur when terminal condition (b) was applied.

#### 4.7 An alternative approach to the flare trajectory problem

Many in-service systems do not employ 'command' signals but form the flare trajectory from signals available in the system itself. Because such systems are less complex, it was appropriate to comment on these systems in the light of the results discussed above.

When the mixing filters are changed over at  $t = t_c$ , the step on the elevator demand can be eliminated by applying a term  $G_h' y_{33}$  instead of  $G_h y_{33}$  where  $G_h'$  is determined from the relation:

$$G_h' = k G_h \quad . \quad k = 0.223 \text{ s}^{-1}$$

For  $G_h = 5.1^\circ$  per m/s,  $G_h' = 1.1^\circ/\text{m}$  slightly less than that in the proposed system.

Due to the opposing action of the pitch attitude term and, to a lesser extent, of other feedback terms, the flare trajectory has a much longer time constant than the required 4.4 s.

It is necessary to decrease the error:

$$\epsilon = (y_{43} + ky_{33}) \sim \dot{H} + kH \quad . \quad (8)$$

One method used in some in-service systems is to integrate  $\epsilon$ , preferably with a wash-out of about 3 s so as to decrease effects of errors earlier in the trajectory; and apply this as an additional signal. For the low value of  $G'_h$  ( $1.1^\circ/\text{m}$ ), it is not possible to apply a sufficiently strong integral gain otherwise very poor damping is experienced. It is found necessary to start the flare earlier than the runway threshold. This leads to problems at some airports where the undershoot area is not sufficiently flat for the system to be used.

An interesting modification which requires more study is to apply a signal  $G''_h y_{33}$  instead of  $G'_h y_{33}$  where:

$$G''_h = \left( \frac{1}{\tau'_3} \right) G'_h \quad . \quad \tau'_3 = 3.0 \text{ s}$$

There will be a step

$$G''_h y_{33} + G'_h (y_{43} - y_{42}) \sim G''_h H_f + G'_h \dot{H}_f$$

which should be removed by storing the value of this step at  $t = t_f$  and applying an equal and opposite signal to the elevator demand. For  $G'_h = 5.1^\circ$  per m/s,  $\tau'_3 = 3.0$  s,  $G''_h = 1.7^\circ$  (still less than the  $G'_h$  value in the proposed system). As  $\tau'_3$  is decreased, the time constant of the flare trajectory increases, compensating for the opposing action of the pitch attitude feedback and other terms.

The parameter  $\tau'_3$  must be selected after deciding how the throttle control (and in the DLC case, how the elevator control) should be applied to attain the desired change in pitch attitude.

Preliminary results have indicated that flare performance is not inferior to the more complex 'command' system. However, there are two reasons for recommending this command system for experimental flight tests in the BAC 1-11:

(a) there are more parameters that can be selected independently to adjust different aspects of performance, e.g. if the ground effect model is incorrect, changing  $c_2$  should yield the required correction,

(b) in the future application with MLS (microwave landing system), it is possible that flare should start using the glide path of the MLS. A 'command' system appears to be the only possible solution to a smooth transfer from MLS to radio altimeter during flare.

## 5 PROPOSED FLARE SYSTEMS AND PERFORMANCE ASSESSMENT

Two of the many possible flare systems were selected for detailed assessment, one for elevator only and the other for DLC. These systems are defined in detail before discussing the following aspects of flare performance:

- (a) touchdown errors due to the conventional turbulence model,
- (b) effect of variations in mean wind and levels of turbulence,
- (c) changes in glide slope (steep approaches),
- (d) runway undulations,
- (e) touchdown errors caused by disturbances before the start of flare,
- (f) step gusts.

### 5.1 Description of flare systems

The system(s) are drawn in Fig.15. The basic system is identical to the hold systems described in Figs.1 and 2. For clarity, the additional applied limits to the spoiler demand have been omitted in Fig.15.

During the ILS glide path mode, switches 1 and 2 are in the A position and switch 3 is off. The integral ( $G_h^-$ ) is operative.

The comparator should yield a positive output when:

$$y_{33} + c_4(y_{43} - y_{42}) > 1$$

i.e. after reaching the runway threshold. To avoid premature flare engagement, the comparator signal should be AND gated with the minimum expected height of engagement.

At  $t = t_f$  defined by the comparator:

- (a) amplifier  $A_1$  is set to store
- (b) switches 1 and 2 are changed from A to B positions
- (c) switch 3 is closed.

The necessary command signals are then applied to the system.

### 5.2 Justification of design procedure

Results are presented to justify certain assumptions made during the design of the flare systems:

(a) that ground effect requires a change to the trajectory control only, so that inaccuracies in the ground effect model require adjustments to that control alone ( $c_2$  and  $c_3$ )

(b) that the control for best displacement hold performance is that for best touchdown performance with respect to turbulence.

(Reference is made to the reservation regarding damping discussed in section 4.1.)

Means and standard deviations of touchdown rate of descent, pitch attitude and range are presented in Table 4 for two cases:

Case (1): a system designed, with no ground effect, to produce an undisturbed touchdown rate of descent of 0.7 m/s, without regard for pitch attitude or forward speed of touchdown ( $c_2 = c_3 = 0$ ).

Case (2): by adding commands  $u_c$  and  $\Delta\eta_c$  to Case (1), to correct the trajectory for ground effect and produce, in still air, a mean rate of descent of 0.7 m/s, pitch attitude  $+1.0^\circ$  together with an associated decrease in forward speed.

Because the same command time constant  $\tau_f$  was used for elevator only and DLC, the pitch attitude at touchdown for the DLC case was  $1.3^\circ$ .

There is little difference between Cases (1) and (2) in the standard deviations due to turbulence models given in Table 1. Histograms for Case (2) are presented in Fig.16 to show the acceptable distribution of touchdown errors due to horizontal turbulence (similar results were obtained for vertical turbulence). These results demonstrate that the scatter in touchdown errors due to turbulence is unchanged by ground effect provided the necessary adjustments are made to correct the trajectory control.

The distribution of touchdown rate of descent for Case (2) is compared in Fig.17 with the distribution of vertical velocity errors for the displacement hold system on which the flare system was based. Except for a tendency for touchdown errors to have a skewed distribution, the statistical properties are very similar thereby indicating that, if the displacement hold system is 'optimum' so also is the flare system based upon it.

The data discussed above was obtained without the control non-linearities simulated. The data given in Table 4, Case (3), was obtained for the flare system defined as Case (2) above with the following control non-linearities:

- (a) elevator only;  $0.1^\circ$  dead-zone and  $0.25^\circ$  backlash (Appendix)
- (b) DLC; as (a) with  $10^\circ/\text{s}$  rate limit and:
- (i)  $7^\circ$ , (ii)  $10^\circ$ , (iii)  $15^\circ$ ,

amplitude limits applied to the spoiler demand signal.

For the elevator only case, the non-linearities have little effect on performance. As the amplitude limit is increased in the DLC case, performance changes from being little better than the elevator only case to being little worse than the linear DLC case.

This is illustrated in more detail by the histograms in Fig.18 for which, in order to reduce the amount of information presented, the changes in the distribution of rate of descent for horizontal turbulence have been chosen for illustration. The time histories of relevant state variables shown in Fig.19 illustrate further the effects of these non-linearities. (The computer was put into hold at touchdown in order to show touchdown values.)

The fact that the non-linearities do not affect performance significantly justifies the use of a linear system in the design: this was desirable in order to use a number of design techniques. It also justifies the separate investigation of the effects of different disturbances and other causes of error. Unless otherwise stated, therefore, further results were obtained with the non-linearities not simulated.

### 5.3 Effect of variations in mean wind speed and levels of turbulence

The following results show the effects of applying a step change in wind,  $+10\text{m/s}$  headwind,  $-10\text{m/s}$  tailwind at a range-to-go to flare start of 1000 m. The flare system was that defined as Case (2), Fig.15, i.e. control non-linearities neglected but ground effect simulated.

Table 5

Touchdown value of:	(a) Elevator only		(b) DLC	
	(i) Headwind	(ii) Tailwind	(i) Headwind	(ii) Tailwind
Vertical speed, m/s	0.72	0.60	0.65	0.62
Range, m (estimated)	497	484	502	487
Pitch attitude, deg	1.20	1.10	1.27	1.37
Forward speed, m/s change	-16	-4	-15	-5

The effect is small due to the fact that, through the way in which flare start is defined, the effects of changes in the mean rate of descent before flare are approximately eliminated.

The effect of changing the level of turbulence is more interesting. Data for horizontal turbulence only is given in Table 4, the flare systems being those defined in Case (2) with:

Case (4): level of turbulence twice that in Table 1, rms 2 m/s

Case (5): 3 times, rms 3 m/s

Case (6): 4 times, rms 4 m/s.

The histograms in Figs.20 and 21 show the changes in distributions in touchdown rate of descent and range from threshold for the two extreme cases of horizontal turbulence, 1 m/s and 4 m/s rms. The rate of descent distributions tend to be skew, the mean value increasing with turbulence. In Fig.22, the variations of the mean and standard deviation of the touchdown rate of descent with level of turbulence are illustrated more clearly. The approximate linear variation of the standard deviation of touchdown rate of descent with level of turbulence justifies further the approximate linear characteristics assumed.

#### 5.4 Changes in glide slope

Results are presented on touchdown performance for the systems defined (without alteration) for the following steep approaches:

Table 6

	(a) Elevator only			(b) DLC		
	3°	4.5°	6°	3°	4.5°	6°
Vertical speed, m/s	0.64	0.84	2.6	0.64	0.75	0.74
Range, m	478	402	207	443	396	325
Pitch attitude, deg	1.07	1.65	0.50	1.30	1.63	0.50
Forward speed, m/s	-5.7	-7.8	-0.5	-5.3	-7.7	-4.6

The approach speed was constant (65 m/s) and still air conditions simulated. The resulting changes in touchdown parameters are measures of the merit of the trajectory control and the law defining the start of flare. The result is fair but further correction for glide slope change would lead to a more acceptable solution for the elevator only case.

### 5.5 Effect of runway undulations

There is interest in extending the use of autoflare to runways exhibiting relative large changes in gradient. Complex models of runway profiles have been produced but, in order to compare systems, a simplified model of undulations is used; the complex models were interpreted in terms of maximum mean gradients and curvatures.

The maximum mean gradient variation is equivalent to a vertical velocity datum change of  $\pm 0.6$  m/s. Provided this datum occurs before the start of flare, the change in mean gradient produces touchdown errors equal to the errors produced by the same change in rate of descent before start of flare, i.e. approximately those shown in Table 5, section 5.3.

The maximum change in mean runway curvature is equivalent to a vertical acceleration datum change of  $\pm 0.03$  m/s<sup>2</sup>. The touchdown errors were:

Table 7

	(a) Elevator only		(b) DLC	
	+0.03 m/s <sup>2</sup>	-0.03 m/s <sup>2</sup>	+0.03 m/s <sup>2</sup>	-0.03 m/s <sup>2</sup>
Vertical speed, m/s	0.72	0.41	0.75	0.50
Range, m	455	530	427	483
Pitch attitude, deg	0.98	1.12	1.20	1.40
Forward speed, m/s	-1.2	-6.1	-4.8	-5.6

The addition of an integral term, integrating the error from the required trajectory, did not improve performance significantly.

### 5.6 Touchdown errors caused by turbulence and ILS noise before start of flare

The applied turbulence and ILS noise was switched off at the start of flare to obtain the data given in Case (7), Table 4. The touchdown errors are small compared with errors due to turbulence applied during flare.

### 5.7 Responses to step gusts

Touchdown errors caused by step or pulse gusts are an alternative way of describing the turbulence performance of flare systems. The results presented in this paper are restricted to step gusts applied at different times  $t$  from a range-to-go of 1.5 km to the glide path origin. Other results are referred to:



(a) investigations<sup>10</sup> at BLEU of the performance to 'square' pulses, i.e. a step applied at  $t_1$  and an equal and opposite step applied at  $t_1 + t_2$ . Both  $t_1$  and  $t_2$  are varied in order to define the variation of touchdown errors with gust characteristic,

(b) investigations<sup>9</sup> in Controls and Displays Division of the gust shape which produces the maximum error at touchdown.

The variation of touchdown rate of descent with the time  $t$  of applying the step horizontal gust is shown in Fig.23. Maximum error occurs for the step applied about 2 s before touchdown. It will be recalled that there is a delay of 2.3 s in the controlled system response in rate of descent. This is decreased using the high gain DLC system.

For small amplitudes of gust, the systems behave approximately linearly. From Fig.23, therefore, the square pulse yielding the greatest error in touchdown rate of descent is one for which the first step is applied at  $t_1 = 5$  s and the second at  $t_2 = 2$  s before touchdown. This result agrees approximately with the investigations at BLEU, (a) above. It also agrees well with results from the 'worst gust' investigations which were limited to gusts within the band-limited white noise model. These investigations showed that:

(i) the gust producing the maximum error in rate of descent consists of two ramps of opposite signs,

(ii) the shape of the gust producing maximum error in rate of descent differed from that producing maximum error in range.

## 6 GLIDE PATH ACQUIRE

The problems of joining the glide path from height hold were not studied sufficiently in the design of the experimental glide path hold system flown in the Comet 3B, the principal aim of that design study was glide path hold performance. The difficulties experienced in flight were traced after the flight experiment to the method used to initialise the experimental control system. These difficulties produced errors in the latter stages of the approach and affected significantly assessment of ILS hold performance.

A more detailed study was made therefore on the glide path acquire for the experimental systems to be flown in the BAC 1-11. This study aimed to provide the means to acquire glide path from difficult heights down to 200 ft and from different rates of descent prior to acquire.

The procedure proposed entails:

(a) Initialising the experimental systems on the patchable analogue computer during height or vertical speed hold prior to glide path acquire. Sufficient time in height hold is required to produce the steady state trim signals needed to offset accelerometer and rate servo amplifier errors. When using DLC, the elevator only control is applied first, the automatic spoiler trim loop being applied in order to zero spoiler position.

(b) A smooth exponential trajectory is provided by starting the acquire phase at a time  $t = t'_f$  before the ILS signal is zero. This time is decided in a similar manner to flare start; when:

$$y_{32} + k(\dot{\beta}_e) = 0 \quad k = 0.223 \text{ s}^{-1}$$

where  $\dot{\beta}_e$  is a preselected estimate of the rate of change of ILS error, and  $y_{32}$  is the ILS error signal.

(During height or vertical speed hold, the parametric signal  $y_{31}$  is fed to filter B, Fig.5, in place of the radio altimeter signal.)

(c) At  $t = t'_f$ , the mixing filters are not changed over but the commands  $h_c$ ,  $\eta_c$  and  $\dot{h}_c$  are applied. This overcomes problems associated with the fact that the output of the mixing filter A is not a good measure of velocity error normal to the ILS beam. These commands are best referred to a pre-selected estimate  $X_{1e}$  of the required change in vertical velocity in contrast to the 'closed-loop' estimate employed in flare.

(d) The integral term is placed in hold during flare in order to prevent unnecessary overshoots in the trajectory.

(e) At a time  $t = t'_f + 20 \text{ s}$ , the acquire is complete and the mixing filters can be switched over,  $-X_{1e}$  being applied to eliminate the transient.

Much of the circuitry required to effect the glide path acquire is common to that used for flare. The main increase in complexity is associated with switching in the different displacement error signals.

An example of the glide path acquire performance is shown in Fig.9.

7 DISCUSSION AND CONCLUSIONS

Two systems are defined in this paper, one using the spoilers installed in the aircraft to provide DLC. These systems are considered as 'starting' systems for experimental flight tests in the BAC 1-11 insofar as a more accurate specification of performance requirements is needed before the 'best' system is defined. Engineering judgement rather than an absolute criterion was applied in selecting the compromise between different conflicting performance aspects. It is proposed that flight tests should be made to improve current performance specifications; and subsequent changes be made to the experimental systems to produce the 'best' solution.

It is intended that the two systems, with and without DLC, should be patched simultaneously on the airborne analogue computer. A comparative assessment of performance would be obtained, under the conditions experienced during the same sortie, by switching on the spoiler control loops on alternate approach and landings.

The design procedure, methods of assessment and subsequent deeper understanding of the problems involved are applicable to any aircraft. These aspects of the study are, perhaps, more important than the specific results for the BAC 1-11.

Glide path acquire and hold, and flare were based on a 'displacement' hold system, designed to minimise errors from a specified trajectory. An additional non-continuous control defines the trajectory during glide path acquire and flare. Ground effect during flare requires a change to this trajectory control alone and, because the latter does not greatly affect the modal characteristics or performance of the basic displacement hold system, turbulence performance is not changed by ground effect. Moreover, changes in the mean touchdown values of rate of descent, pitch attitude and forward speed are made by adjustments to the trajectory control alone.

Glide path acquire is a smooth exponential trajectory, time constant 5 s, with no beam overshoot and acceptable acceleration. With some additional circuitry, the acquire system can be used for joining the glide path beam from variable vertical speeds and heights (down to 200 ft). This could be useful in flight tests associated with terminal area problems.

Minimising beam error was assumed as the prime requirement for the ILS glide path hold phase. The ILS signal remains coupled to the system down to the

start of flare which was selected to be the runway threshold. There is adequate gain margin at the end of this phase to allow for expected variations of ILS sensitivity from site to site, day to day, etc.

Turbulence performance of the flare systems is directly related to the turbulence performance of the basic displacement hold system. Because all modes are well damped, control non-linearities do not significantly change flare performance. Using the DLC, a decrease of more than 2:1 was achieved in the standard deviations of touchdown errors in rate of descent, range and pitch attitude.

The standard deviation of errors in rate of descent and range due to moderate turbulence are no better with the experimental elevator plus throttle system than in-service systems, although there was a decrease, by a factor of 2.5, in the standard deviation of pitch errors at touchdown due to moderate turbulence. As the level of turbulence is increased, the experimental system yields standard deviations proportional to level of turbulence, an improvement on the performance of in-service systems.

The distribution of touchdown errors due to turbulence is, perhaps, more important than their standard deviations. From the limited information on some in-service systems, these distributions are irregular due, it is believed, to poor damping of long period modes. The distributions for the experimental systems are near-Gaussian except for a tendency to skew and the distributions remain near-Gaussian as the level of turbulence is increased.

The other aspects of flare performance are related to the effects on touchdown performance of initial conditions at the start of flare and a change of runway datum during flare. The method of deciding when to start flare and the additional control to define the trajectory has been chosen to reduce touchdown errors due to:

- (a) disturbances at the end of glide path hold
- (b) variations in headwind and tailwind experienced during the approach
- (c) variations in glide slope (possible steep approaches for VSTOL investigations).

Further studies are required but the performance with respect to these features is expected to be much better than in-service systems. Touchdown errors due to runway undulations are acceptable.

There are certain reservations on the systems as defined. Firstly, it is necessary to correct the output of the strapped-down accelerometer for attitude effects, pitch and bank angle. Without this correction, variations of  $3^\circ$  rms in bank angle cause displacement errors with a standard deviation equal to that for moderate turbulence. Secondly, the use of an elevator rate servo system rather than the more conventional positional servo requires the addition of a double integral of displacement term; this reduces the performance of glide path hold and, in the DLC case, causes difficulty in achieving a satisfactory spoiler trim facility.

The study has shown clearly that there are limitations to performance directly due to the use of linear control policies. In particular, many conflicts between the control needed to optimise different performance aspects are due to coupling between linear control loops most of which are needed only when certain conditions are experienced.

Appendix

DESCRIPTION OF SIMULATION MODELS AND SYSTEMS TRANSFER FUNCTIONS

A.1 Models of aircraft and control equipment

The small perturbation, pitch axis equations of motion for the BAC 1-11 are:

$$\dot{u} = -0.058(u + u_g) + 0.065(w + w_g) - 0.171\dot{\theta} - T$$

$$\dot{w} = -0.303(u + u_g) - 0.686(w + w_g) + 1.11\dot{\theta} - 0.054\eta + 0.0736\delta$$

$$\ddot{\theta} = -0.82(w + w_g) - 0.236\dot{w} - 0.685\dot{\theta} - 1.14\eta + 0.133\delta$$

$$\ddot{h} = 1.14\dot{\theta} - \dot{w}$$

$$\dot{h} = 1.14\theta - w$$

where  $u$  (m/s) is the forward speed perturbation

$u_g$  (m/s) is a horizontal gust

$w$  (m/s) is the rate of descent perpendicular to  $u$

$w_g$  (m/s) is a vertical gust

$\theta$  (degrees) is the pitch angle

$h$  (m) is the height perturbation.

The aircraft is in approach configuration:

Airspeed,  $v_T = 65$  m/s

45° Flaps

Undercarriage lowered

The autothrottle law is most conveniently expressed as an equation in Laplace transform space:

$$T = (0.4/(1.15s))(u + u_g)(1 + 0.05/s)$$

where the lag of 1.5s time constant represents the combined lag of the engine and throttle actuator.

The elevator hydraulic system is rate-rate in nature, so that the signal applied to the actuator ( $\dot{\eta}_D$ ) is required to be the derivative of the demanded elevator movement. The signal  $\dot{\eta}_D$  is derived from  $\eta_D$  by means of a washout circuit considered to be part of the control system. The transfer function of the actuator is assumed to be:

$$400/(s^2 + 28s + 400)$$

and the transfer function of the power control unit is assumed to be:

$$1/(1 + 0.1s) \quad .$$

The elevator mechanical control linkage is assumed to have non-linearities between actuator and power control unit, which are:

- a deadzone of  $\pm 0.1^\circ$  directly after the actuator, followed by
- a backlash of  $\pm 0.25^\circ$  - within the simulated PCU.

The Direct Lift Control (DLC) spoilers have a position actuator. The combined transfer function of this and the power control unit is assumed to be:

$$1/(1 + 0.1s) \quad .$$

The spoiler angle ( $\delta$ ) is limited to  $\pm 20^\circ$ , and its rate of application ( $\dot{\delta}$ ) is limited to  $\pm 25^\circ/s$ . It is proposed to impose additional limits of  $\pm 7^\circ$  on  $\delta_D$  and  $\pm 10^\circ/s$  on  $\dot{\delta}_D$  within the control system. These can be reduced to limit its authority during initial flying. Possible non-linearities of the DLC aerodynamic derivatives have not been simulated.

#### A.2 Models of ground effect

The additional inputs to the aerodynamic equations when the aircraft is near the ground are proportional to a non-linear function:

$$f(H) = 1/(3.28H + 4) - 1/54$$

where  $H$ ,

$$15 > H \geq 2.13 \text{ m}$$

is the height of the centre of gravity above the runway.

The additional inputs are:

$$\Delta \dot{u} = + (6.17 + 0.685(w + w_g))f(H)$$

$$\Delta \dot{w} = - 11.1f(H)$$

$$\Delta \ddot{\theta} = - (11.3 + 1.87(w + w_g))f(H) \quad .$$

For stability analyses these equations are linearised according to a method described elsewhere<sup>8</sup>, giving a first order approximation which is:

$$\Delta \dot{u} = 6.17 \left( \frac{df(H)}{dH} \right)_{H=H_0} \dot{h} + 0.685f(H_0)(w + w_g)$$

$$\Delta \dot{w} = - 11.1 \left( \frac{df(H)}{dH} \right)_{H=H_0} \dot{h}$$

$$\Delta \ddot{\theta} = - 11.3 \left( \frac{df(H)}{dH} \right)_{H=H_0} \dot{h} - 1.87f(H_0)(w + w_g)$$

where  $h$  is the height perturbation about a reference height  $H_0$ . It has been assumed that the reference value of  $w$  is approximately zero.

### A.3 Transfer functions of control laws

The elevator plus throttle height hold system has a transfer function which is:

$$s\eta_D = (s/(1 + 0.1s)) \left( \eta_{D1} + (1/(1 + 0.5s))(\eta_{D2} + \eta_{D3} + \eta_{D4}) \right) + G_h^- y_3/s$$

where:  $\eta_{D1} = 2.25y_6 + 2.35(y_6 + 0.05y_7)/(0.05 + s)$

$$\eta_{D2} = 1.81y_5 + 5.1(0.25sy_3 + (1 + s)y_5)/(0.5 + s)^2$$

$$\eta_{D3} = 2.35y_3/(1 + 0.5s)$$

$$\eta_{D4} = G_h^- y_3/s \quad ;$$



For the displacement hold system

$$G_h^- = 0.4^\circ/\text{m s}; \quad G_h^+ = 0.04^\circ/\text{m s}^2$$

and  $y_3$  is the displacement error signal

$y_5$  is the accelerometer signal

$y_6$  is the pitch rate gyro signal

$y_7$  is a pitch reference obtained from the air data computer.

The DLC plus elevator displacement hold system has the additional terms:

$$\text{Spoiler actuator input} = 0.01(\delta_0 - \delta)/s + \delta_D$$

$$s\delta_D = (15.4y_5 + 43.6(0.25sy_3 + (1 + s)y_5)/(0.5 + s)^2 + 20.1y_3)(s/(1 + 0.53))$$

with the value of  $G_h^-$  changed to  $0.02^\circ/\text{m s}^2$ .

The positions of the rate and amplitude limits are shown in the block diagram, Fig.2.

The glide path control systems for elevator with and without DLC are obtained from the above by changing the integral terms to:

$$G_h^- = 0.1^\circ/\text{m s}; \quad G_h^+ = 0$$

and by replacing the displacement error signal  $y_3$ , with a scheduled ILS displacement signal:

$$(0.82 + 0.0036H)y_{32}$$

where  $H$  is barometric height in ft referred to the centre of gravity of the aircraft

$$y_{32} = \beta(\mu\text{A}) / \left( \text{beam sensitivity at 290m range } (\mu\text{A/m}) \right)$$

Table 1DISTURBANCES AND INPUTS APPLIED IN ASSESSMENT(a) Noise type disturbances

Band limited white noise filtered by first order lag of time constant  $\tau_n$  given and rms quoted.

Input	Time constant $\tau_n$ sec	rms
Horizontal turbulence	2.6	1.0 m/s
Vertical turbulence	0.13	0.5 m/s
Height error sensor noise (ILS noise)	0.5 (0.5)	0.125 m (5 $\mu$ A)

NOTE: Turbulence models appropriate to current ARB specification for mean wind at 100ft height. The vertical turbulence is added to  $w$  in the aerodynamic equations (Appendix).

(b) Step inputs

Input	Size
Horizontal gust $e_1$	5.0 m/s
Vertical gust $e_2$	1.0 m/s
Height error $e_3$	1.0 m
Acceleration datum error $e_5$	0.1 m/s <sup>2</sup>
Elevator rate datum error $e_8$	0.3 <sup>o</sup> /s
Spoiler datum error $e_9$	10 <sup>o</sup>

Table 2TURBULENCE AND SENSOR NOISE PERFORMANCE: DISPLACEMENT HOLD SYSTEM(A) Elevator only case(a) Linearised equations: Fig.4a

rms of:	Horizontal gusts, $n_1$	Vertical gusts, $n_2$	Height error sensor noise, $n_3$
Height error, m	0.45	0.16	0.10
Vertical velocity error, m/s	0.28	0.13	0.068
Pitch attitude, deg	0.35	0.15	0.091

(b) Non-linear elevator control (Appendix): Fig.4b

Height error, m	0.5	0.18	0.15
Vertical velocity error, m/s	0.33	0.16	0.12
Pitch attitude, deg	0.42	0.2	0.17

(B) DLC case(a) Linearised equations: Fig.4c

Height error, m	0.145	0.06	0.087
Vertical velocity error, m/s	0.094	0.06	0.052
Pitch attitude, deg	0.05	0.04	0.013

(b) Limits applied to rate and amplitude of spoiler demand: Fig.4d

Height error, m	0.20	0.07	0.087
Vertical velocity error, m/s	0.125	0.08	0.054
Pitch attitude, deg	0.13	0.089	0.087

Table 3

TURBULENCE AND SENSOR NOISE PERFORMANCE: ILS GLIDE PATH

Except for Case (4), measurements were made with linearised equations, see equation (3). Control non-linearities neglected.

Case (1) R = 10 km

(a) Elevator only

rms of:	Horizontal turbulence, $n_1$	Vertical turbulence, $n_2$	ILS noise $n_3$
Height error, m	0.52	0.37	1.1
Vertical velocity, m/s	0.21	0.13	0.21
Pitch attitude, deg	0.23	0.13	0.33

(b) DLC

Height error, m	0.27	0.18	1.40
Vertical velocity, m/s	0.078	0.065	0.23
Pitch attitude, deg	0.03	0.029	0.065

Case (2) R = 3.3 km

(a) Elevator only

Height error, m	0.5	0.57	0.4
Vertical velocity, m/s	0.2	0.12	0.1
Pitch attitude, deg	0.22	0.14	0.14

(b) DLC

Height error, m	0.26	0.15	0.5
Vertical velocity, m/s	0.083	0.062	0.1
Pitch attitude, deg	0.025	0.032	0.03

Table 3 (concluded)

Case (3)  $R = 0.67$  km(a) Elevator only

	Horizontal turbulence, $n_1$	Vertical turbulence, $n_2$	ILS noise $n_3$
Height error, m	0.46	0.2	0.13
Vertical velocity, m/s	0.22	0.12	0.057
Pitch attitude, deg	0.25	0.14	0.08

(b) DLC

Height error, m	0.17	0.065	0.15
Vertical velocity, m/s	0.088	0.063	0.059
Pitch attitude, deg	0.033	0.035	0.019

Case (4): The performance at  $R = 0.29$  km measured with the beam tightening effect simulated is compared with the performance at  $R = 0.29$  km measured using the linearised equations. The latter, in brackets, is the data from Table 2.

(a) Elevator only

Height error, m	0.4 (0.45)	0.19 (0.16)	0.14 (0.10)
Vertical velocity, m/s	0.28 (0.28)	0.13 (0.13)	0.07 (0.068)
Pitch attitude, deg	0.35 (0.35)	0.16 (0.15)	0.095 (0.091)

(b) DLC

Height error, m	0.14 (0.145)	0.06 (0.06)	0.12 (0.087)
Vertical velocity, m/s	0.092 (0.094)	0.065 (0.06)	0.064 (0.052)
Pitch attitude, deg	0.04 (0.05)	0.035 (0.04)	0.025 (0.013)

Table 4

FLARE PERFORMANCECase (1) Ground effect neglected,  $u_c = 0$  (Control non-linearities neglected)(a) Elevator only

Touchdown parameter	Horizontal turbulence		Vertical turbulence	
	Mean	SD	Mean	SD
Vertical speed, m/s	0.78	0.26	0.71	0.15
Range, m	427	55	417	18
Pitch attitude, deg	-0.44	0.28	-0.42	0.13

(b) DLC

Vertical speed, m/s	0.69	0.096	0.7	0.072
Range, m	444	20	442	5
Pitch attitude, deg	-0.64	0.055	-0.64	0.02

Case (2) Ground effect simulated (Control non-linearities neglected)(a) Elevator only

Vertical speed, m/s	0.68	0.3	0.76	0.13
Range, m	504	45	492	13
Pitch attitude, deg	1.05	0.12	1.07	0.07

(b) DLC

Vertical speed, m/s	0.65	0.097	0.61	0.072
Range, m	462	18	460	6
Pitch attitude, deg	1.32	0.07	1.33	0.02

Table 4 (continued)

Case (3) Ground effect simulated, control non-linearities simulated(a) Elevator only

	Horizontal turbulence, $n_1$		Vertical turbulence, $n_2$	
	Mean	SD	Mean	SD
Vertical speed, m/s	0.80 *(0.78)	0.28 (0.28)	0.68	0.15
Range, m	471 (488)	44 (44)	469	15
Pitch attitude, deg	0.97 (1.00)	0.12 (0.11)	0.9	0.08

(b) DLC

	Horizontal turbulence, $n_1$				Vertical turbulence, $n_2$	
	Mean	SD			Mean	SD
		** (i) 7°	** (ii) 10°	** (iii) 15°		
Vertical speed, m/s	0.67 *(0.62)	0.15 (0.095)	0.13	0.1	0.66	0.07
Range, m	446 (445)	24 (18)	21	18	441	5
Pitch attitude, deg	1.18 (1.30)	0.1 (0.04)	0.1	0.11	1.15	0.03

\* Figures in brackets correspond to the linear case.

\*\* Amplitude limits on spoiler demand.

Table 4 (concluded)

Cases (4) to (6): Changes in level of horizontal turbulence(a) Elevator only

	(4) 2 m/s rms		(5) 3 m/s rms		(6) 4 m/s rms	
	Mean	rms	Mean	rms	Mean	rms
Vertical speed, m/s	1.01	0.44	1.32	0.62	1.85	0.87
Range, m	495	90	472	120	443	136
Pitch, deg	1.01	0.2	1.12	0.37	1.2	0.48

(b) DLC

Vertical speed, m/s		0.86	0.34
Range, m		453	76
Pitch, deg		1.2	0.27

Case (7): Disturbances (Table 1) switched off at flare start(a) Elevator only

	Horizontal turbulence		Vertical turbulence		ILS noise	
	Mean	SD	Mean	SD	Mean	SD
Vertical speed, m/s	0.63	0.04	0.63	0.008	0.62	0.006
Range, m	479	18	478	5	479	3
Pitch, deg	1.05	0.04	1.04	0.01	1.04	0.02

b) DLC

Vertical speed, m/s	0.63	0.02	0.63	0.002	0.63	0.002
Range, m	444	10	443	1.0	443	2
Pitch, deg	1.3	0.01	1.27	0.01	1.28	0.03



SYMBOLS

$A_u$	gain: airspeed error to throttle
$A_u^-$	gain: integral airspeed to throttle
$B_h$	gain: displacement error to spoiler
$B_h^\cdot$	gain: vertical velocity error to spoiler
$B_h^{\cdot\cdot}$	gain: vertical acceleration to spoiler
$B_0$	mixing filter parameter
$e_1$ to $e_9$	step inputs (see Table 1)
$G_h$	$\left. \begin{array}{l} G_h \\ G_h^\cdot \\ G_h^{\cdot\cdot} \\ G_q \\ G_\theta \end{array} \right\} \text{gains to elevator} \left\{ \begin{array}{l} \text{displacement} \\ \text{vertical velocity} \\ \text{vertical acceleration} \\ \text{pitch rate} \\ \text{pitch} \end{array} \right\} \text{errors}$
$G_h^\cdot$	
$G_h^{\cdot\cdot}$	
$G_q$	
$G_\theta$	
$h$	displacement error (ideal)
$\dot{h}$	vertical velocity error (ideal)
$\ddot{h}$	acceleration (ideal)
$H, \dot{H}$	height error and its rate during ideal trajectory
$H_c, \dot{H}_c$	height error and its rate at start of ideal trajectory
$h_0, h_c$	initial and command for height error during trajectory
$\dot{h}_0, \dot{h}_c$	initial and command for velocity error during trajectory
$k$	flare time constant
$k_{m\eta}, k_{m\delta}$	aerodynamic derivations, moment due to elevator and spoiler deflection
$K_\delta$	spoiler trim gearing
$R$	range-to-go to glide path origin
$t_f, t_f'$	time of flare start, glide path acquire start
$T_D$	throttle demand
$U_g$	general wind gust (horizontal)
$\Delta u_c$	airspeed command in flare

SYMBOLS (concluded)

$X_1$	stored value of mean rate of descent for flare commands etc
$X_{1e}$	estimated change of rate of descent for glide path acquire demands
$y_3$	displacement error signal $y_{31}$ baro $y_{32}$ ILS (= $\beta$ ideally) $y_{33}$ radio altimeter
$y_4$	displacement rate error signal $y_{41}$ referred to baro $y_{42}$ referred to ILS $y_{43}$ referred to RA
$y_5'$	accelerometer signal
$y_5$	accelerometer signal after attitude corrections (eliminate g effects)
$y_6$	pitch rate gyro signal
$y_7$	pitch attitude reference
$\beta$	perfect ILS signal
$\delta_D$	spoiler demand signal $\delta_{D2}$ accelerometer plus velocity terms $\delta_{D3}$ displacement terms
$\eta_c$	elevator command for exponential flare without ground effect
$\Delta\eta_c$	additional elevator command which, with $\Delta\eta_c$ , produces correct mean touchdown coordinates with ground effect
$\eta_D$	elevator demand $\eta_{D1}$ pitch rate and attitude $\eta_{D2}$ acceleration and velocity $\eta_{D3}$ displacement $\eta_{D4}$ integral displacement $\eta_{D5}$ double integral displacement
$\tau_f$	time constant of command signals for flare and glide path acquire

REFERENCES

<u>No.</u>	<u>Author</u>	<u>Title, etc.</u>
1	F.R. Gill A.M. Whitehead	Hybrid computer programme for parameter optimisation of flight control systems. RAE Technical Report 70043 (ARC 32275) (1970)
2	F.R. Gill M.R. Watts	Problems in the design of linear flight control systems with particular reference to the height hold and glide path modes. RAE Technical Memorandum Avionics 82 (1971)
3	D.E. Fry F.R. Gill	A geometric search procedure with particular application to optimisation of flight control systems. RAE Technical Report 70018 (1970)
4	P. Robinson D.E. Fry	The theoretical performance of optimised glide path controllers for the Comet 3B. RAE Technical Report 71095 (ARC 33836) (1971)
5	A.M. Whitehead T.P. Asberry	Flight assessment of an optimised glide path control law for the Comet 3B. RAE Technical Report 72209 (ARC 34673) (1973)
6	P. Robinson D.E. Fry	A design study of the automatic flare manoeuvre including the use of direct lift control. RAE Technical Report 72033 (ARC 33711) (1972)
7	F.R. Gill M.R. Watts	Studies on the Hunter flight control system. RAE Technical Memorandum Avionics 81, 83, 84, 85 Parts I-IV (1971)
8	P. Robinson	A linearised analysis of ground effect with particular reference to the design of automatic flare systems. RAE Technical Memorandum Avionics 91 (1971)
9	M.J. Corbin	Turbulence time-histories causing greatest touchdown errors following an automatic flare. RAE Technical Memorandum Avionics 152 (1973)
10	M.J. Corbin K.F. Goddard	The design of automatic flight control systems to reduce the effects of atmospheric disturbances. RAE Technical Memorandum Avionics 140 (1973)

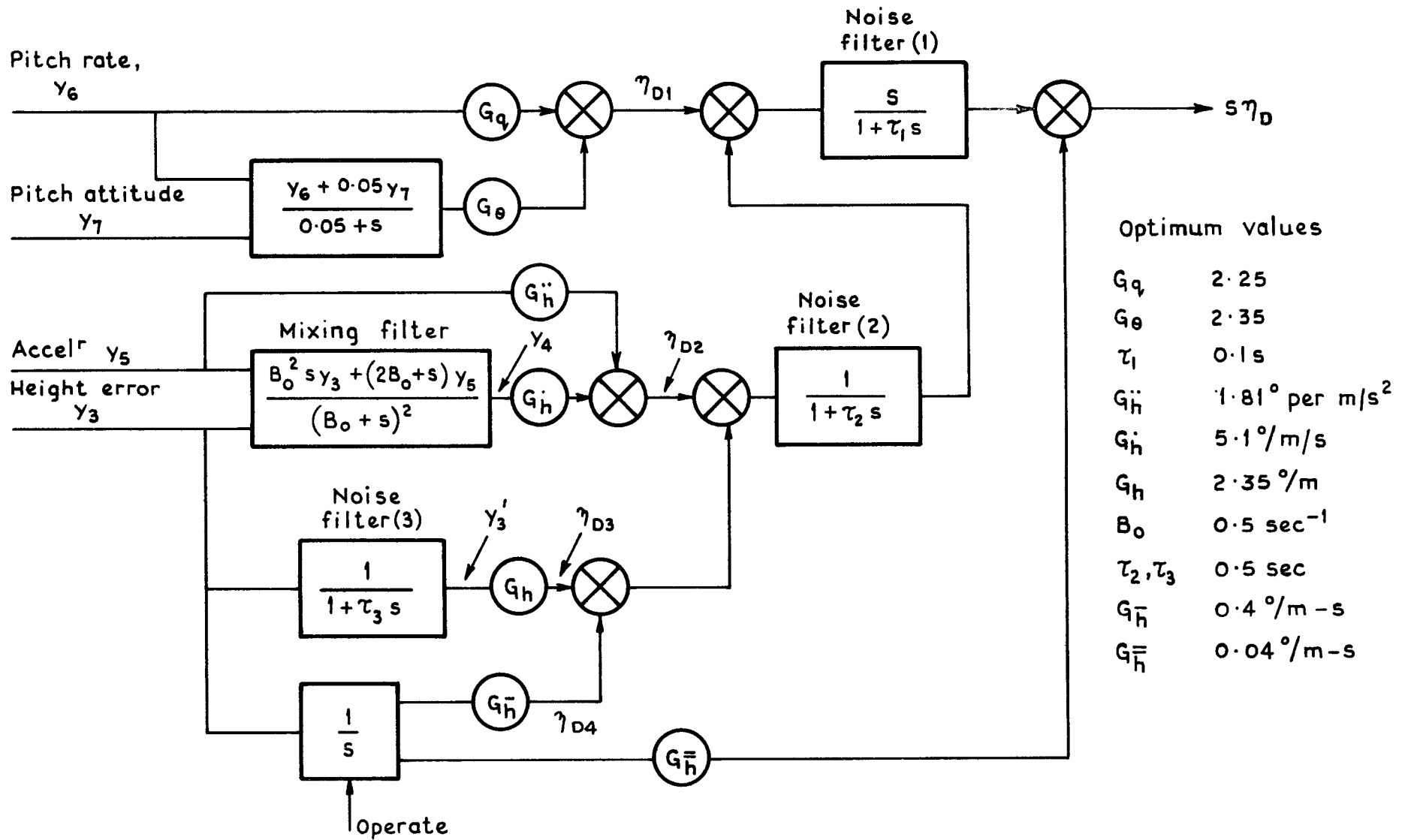
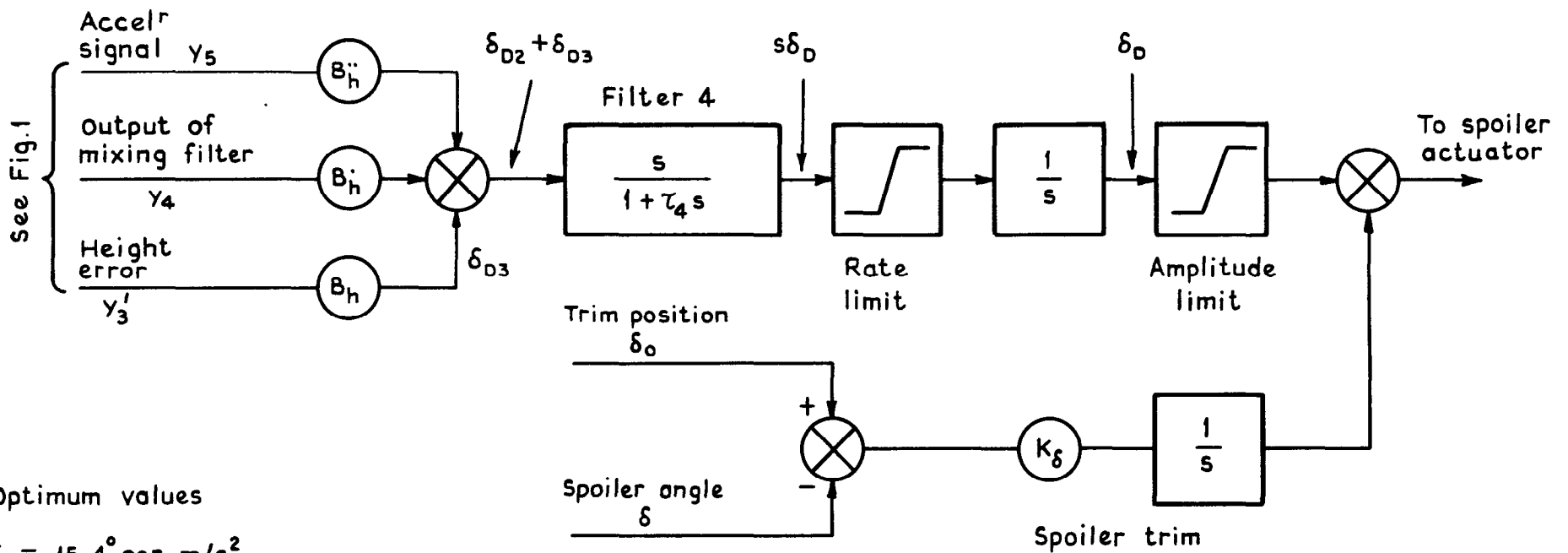


Fig.1 Detailed schematic of elevator only height hold system



Optimum values

$B_h'' = 15.4^\circ \text{ per } m/s^2$

$B_h' = 43.6^\circ \text{ per } m/s$

$B_h = 20.1^\circ \text{ per } m$

$\tau_4 = 0.5 \text{ sec}$

$K_\delta = 0.1 \text{ sec}^{-1}$

NB  $G_h^- = 0.4^\circ/ms$

$G_h^+ = 0.0^\circ/ms^2$

Fig.2 Additional control to elevator only for proposed DLC height hold

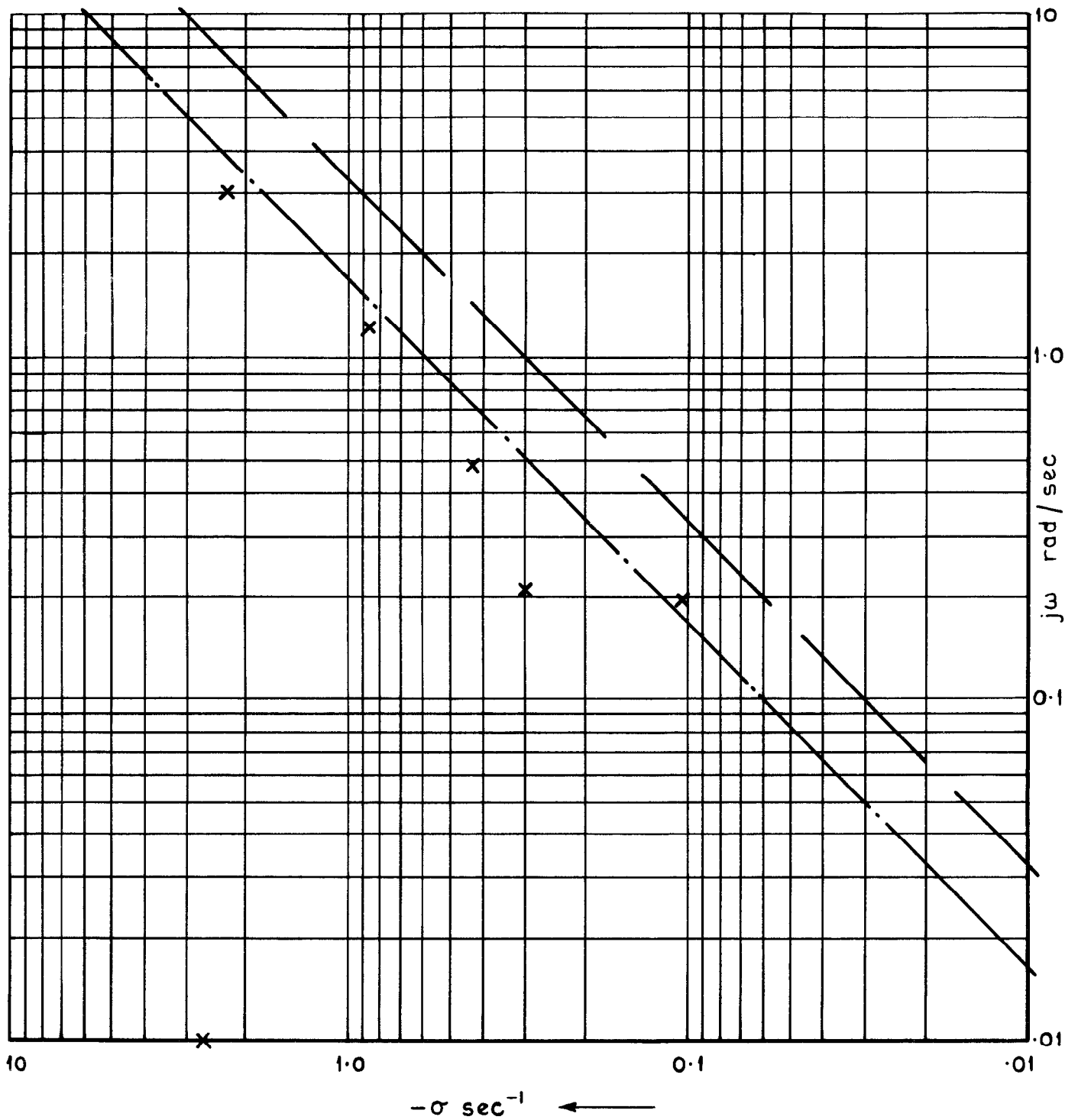


Fig.3a Pole positions for elevator only height hold system

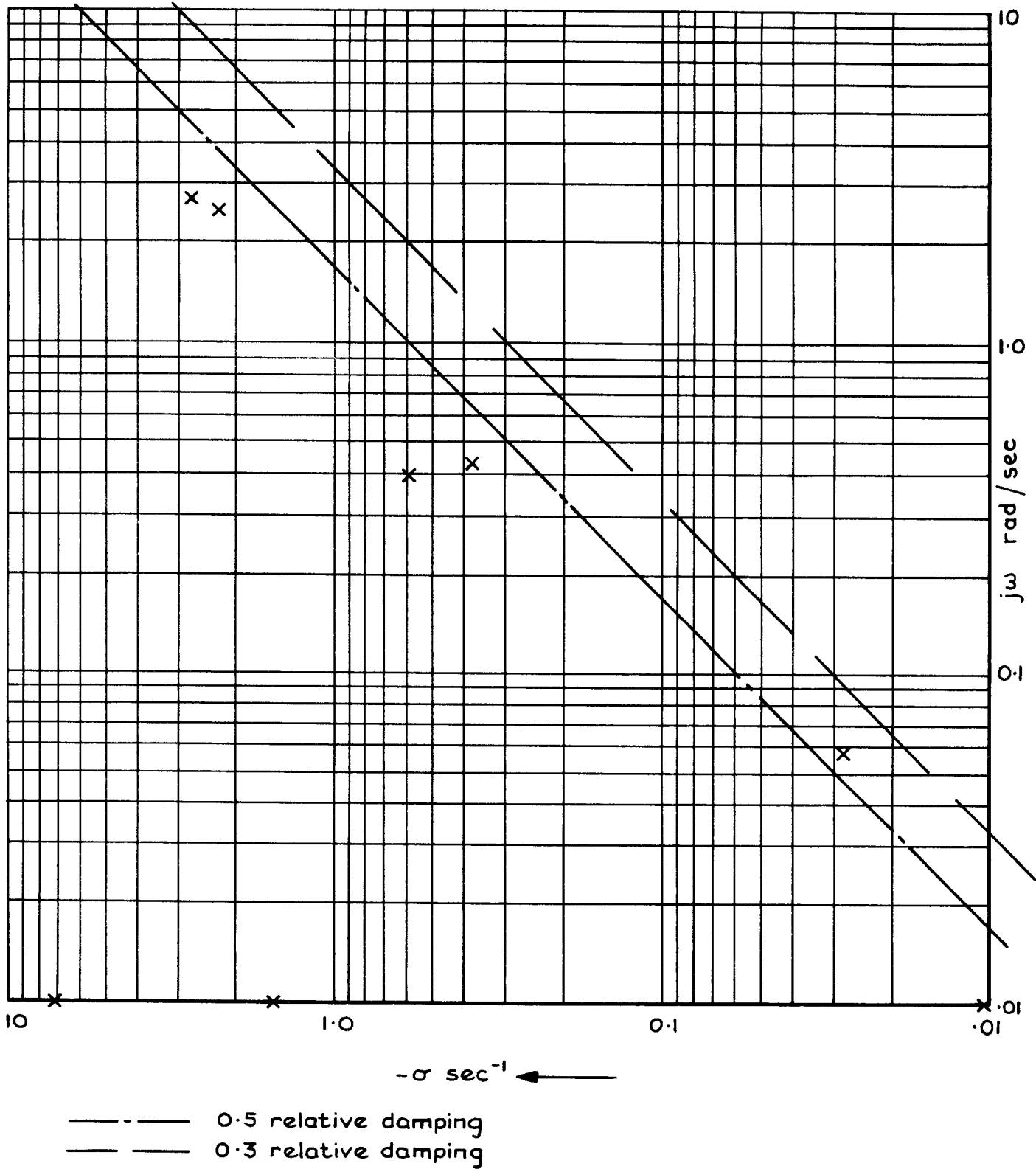


Fig. 3b Pole positions for DLC height hold system

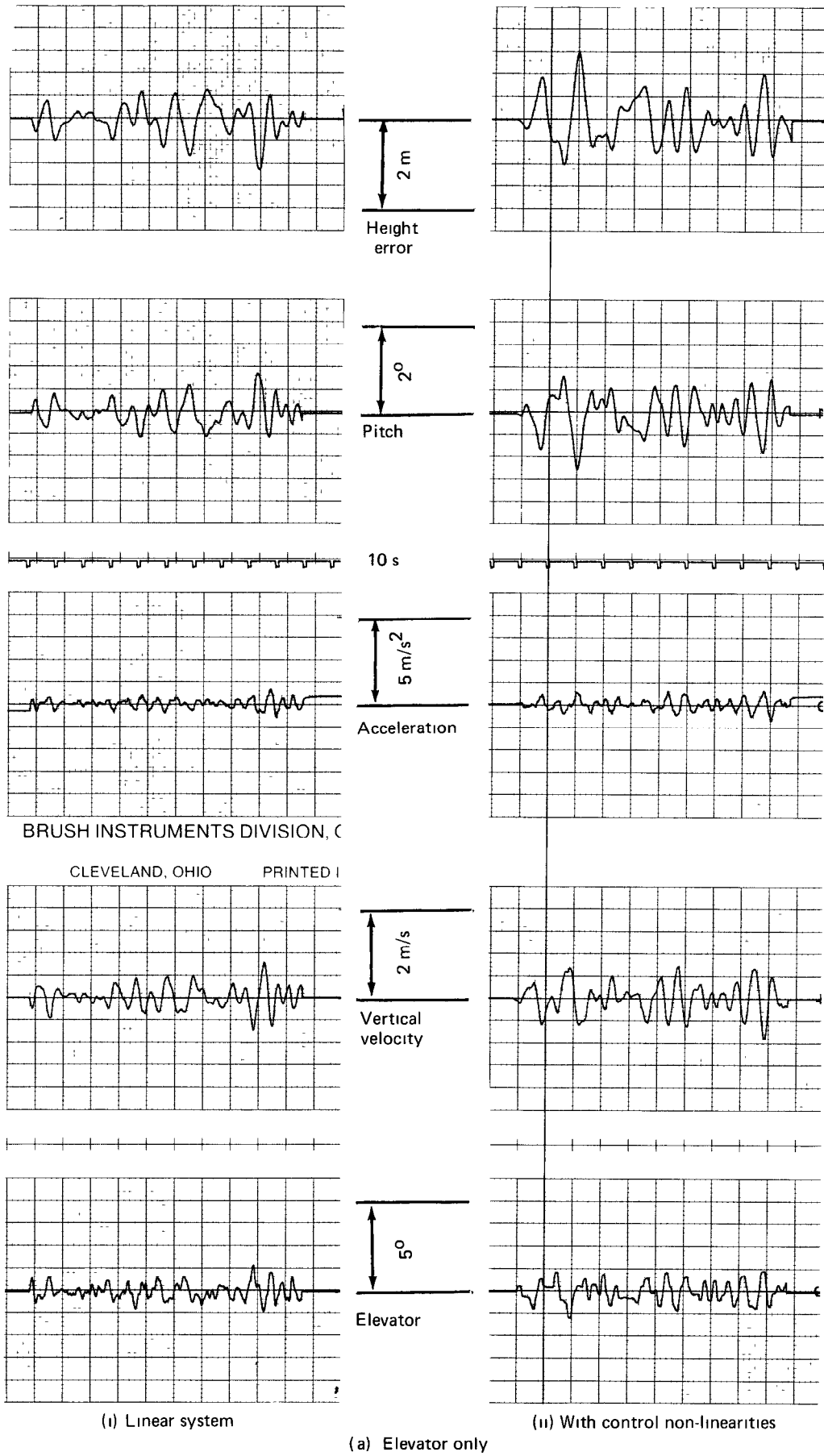


Fig.4 Response of height hold system to horizontal turbulence



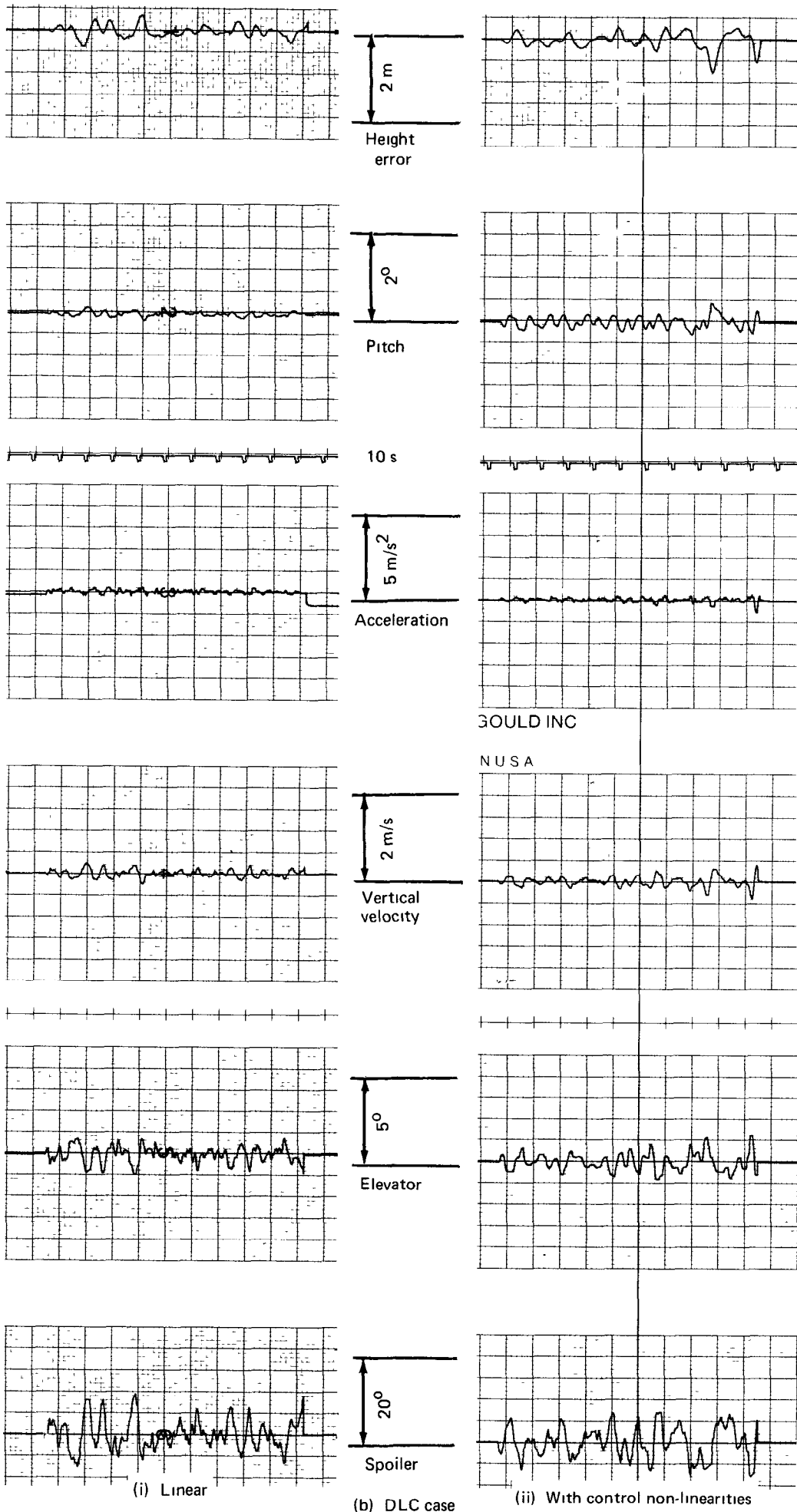


Fig.4 (cont'd.)

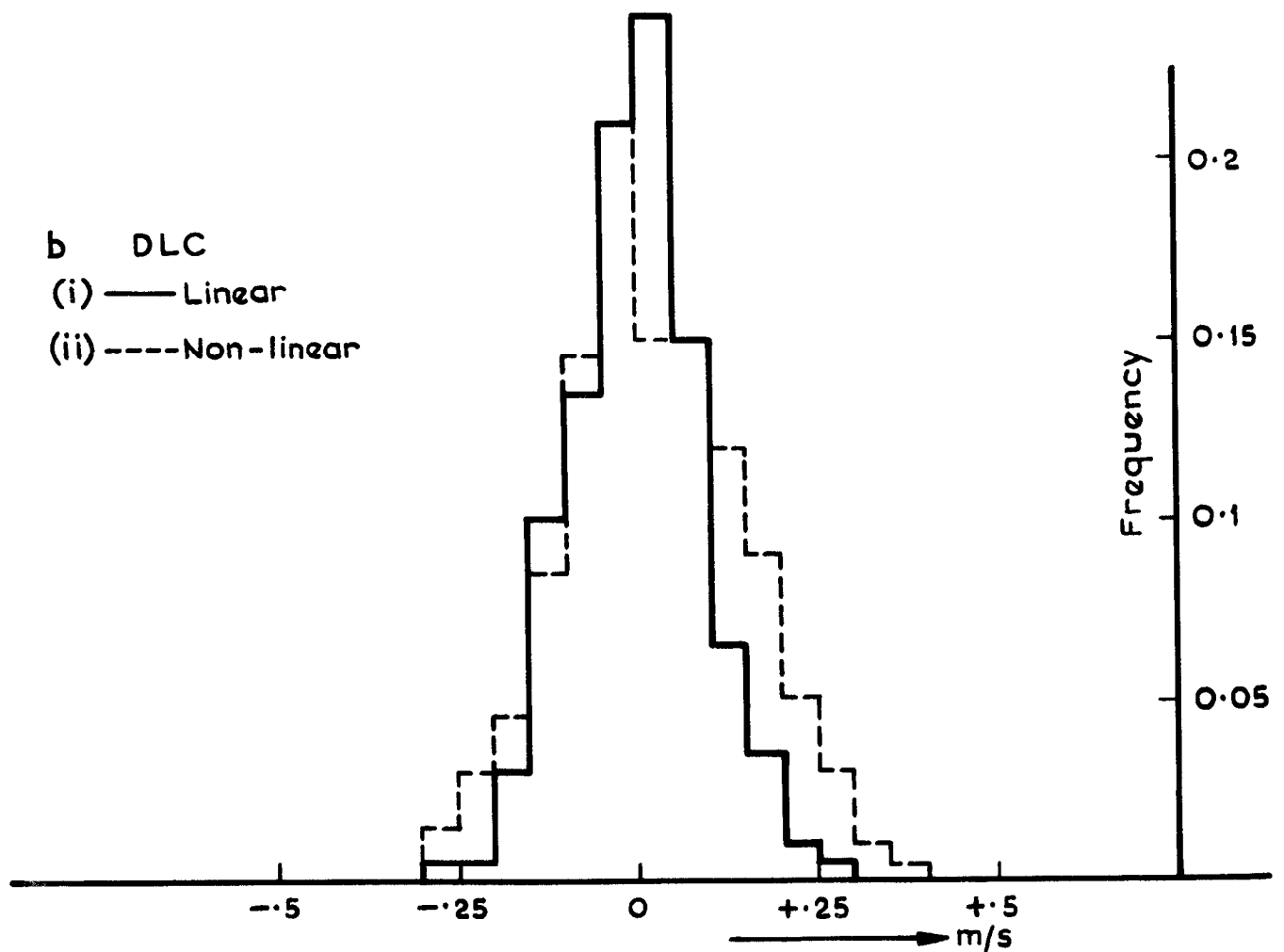
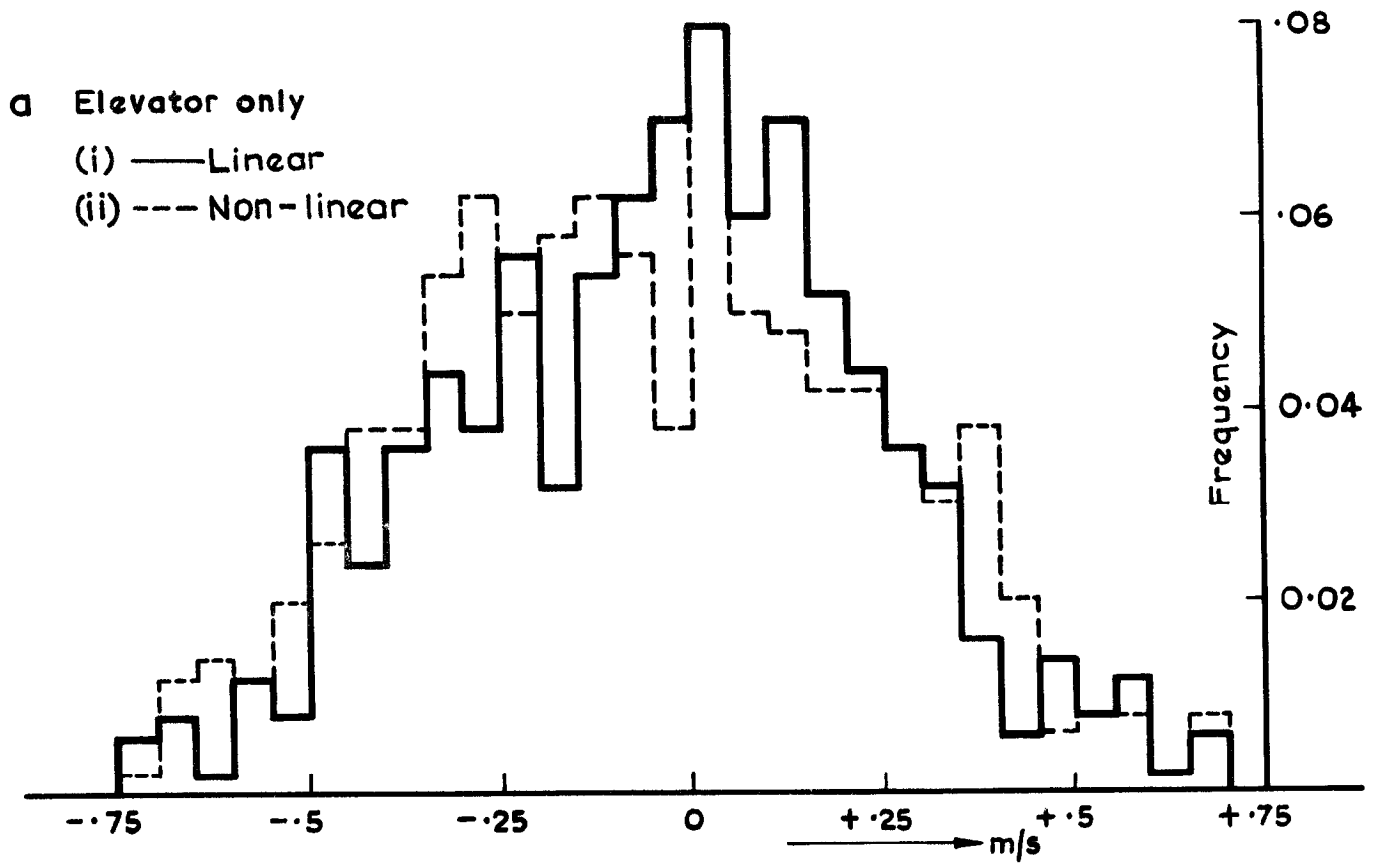


Fig.5 a&b Histograms for vertical velocity error: height hold due to horizontal turbulence

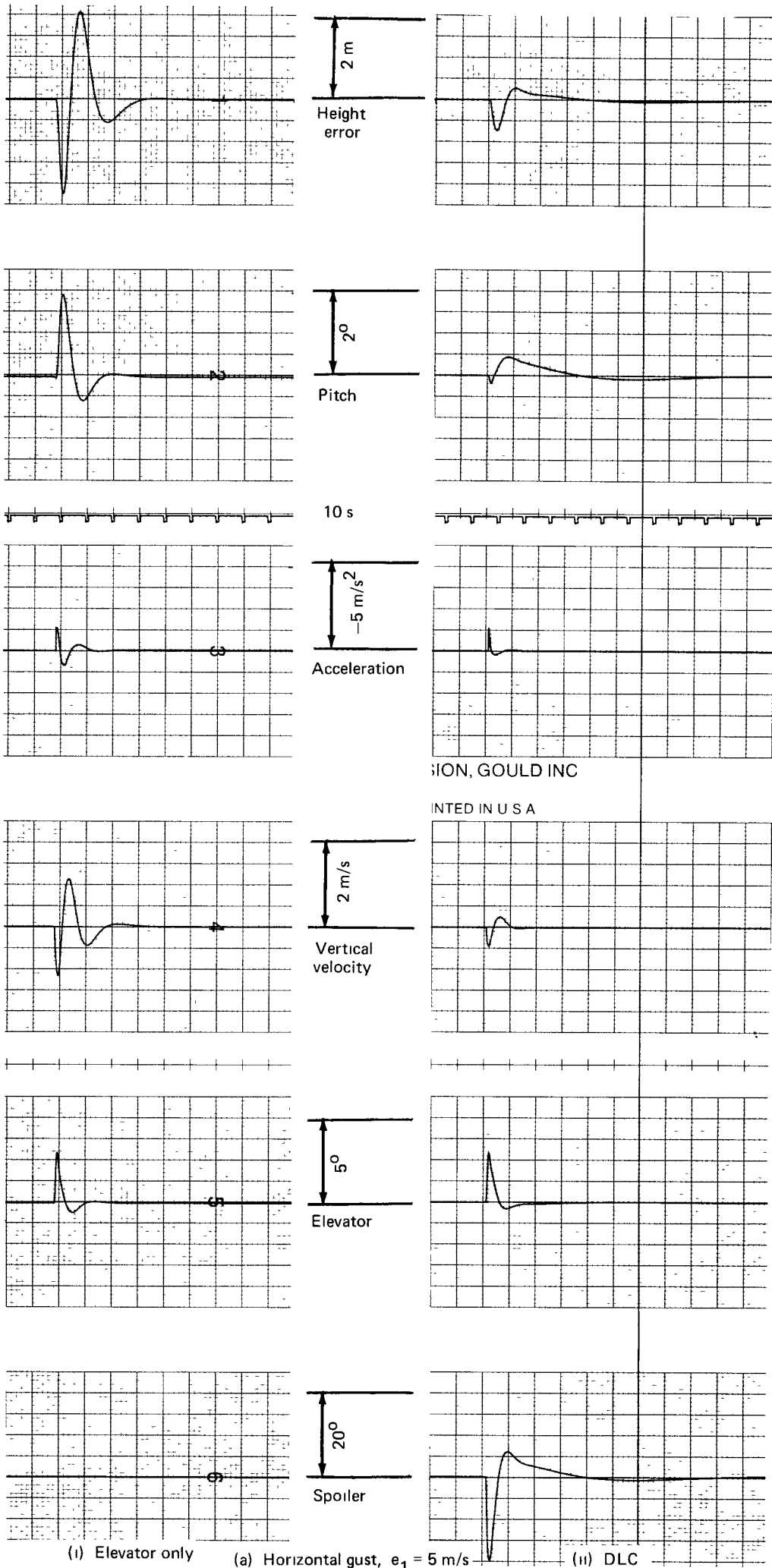


Fig.6 Step responses for height hold

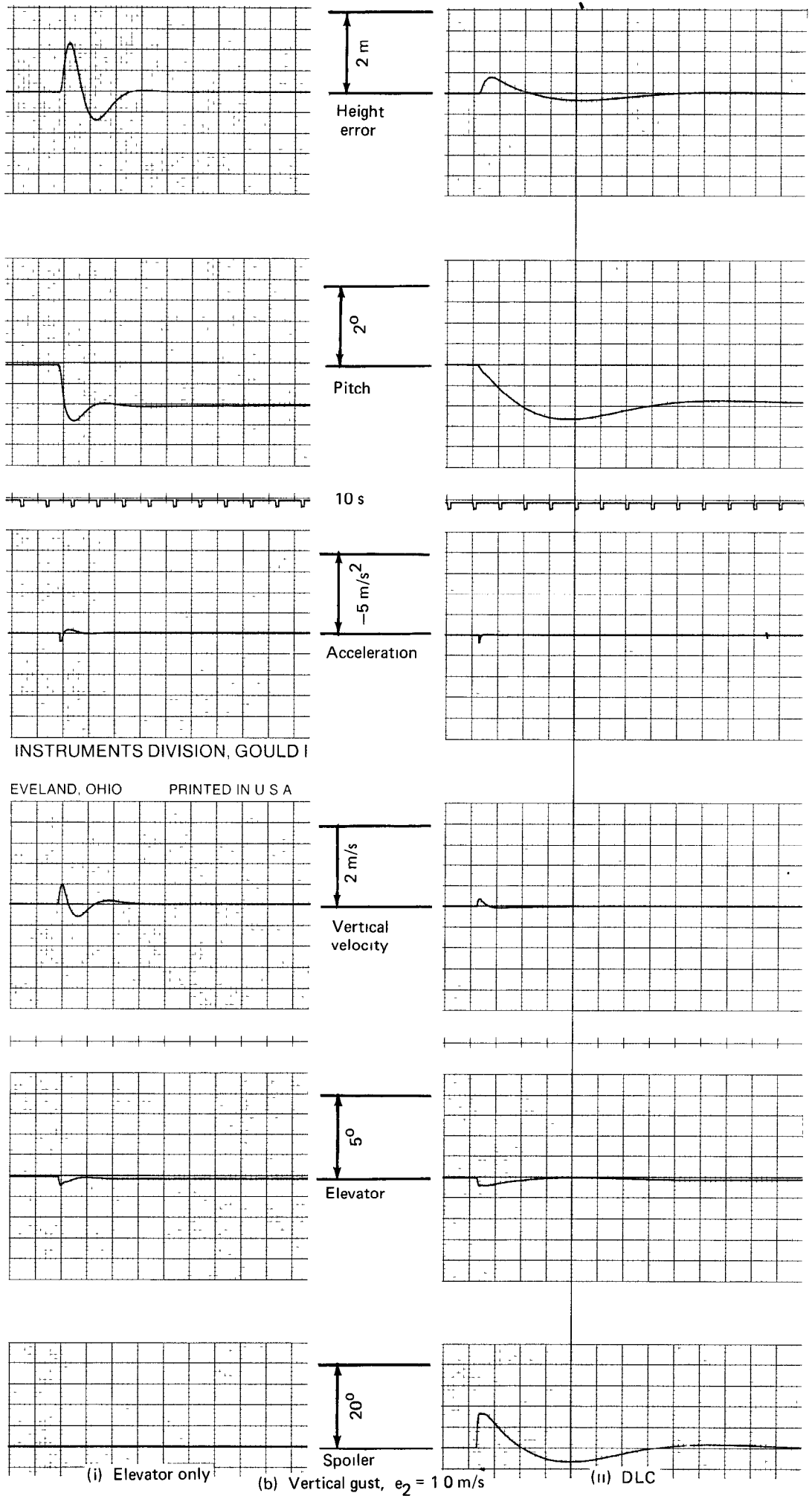
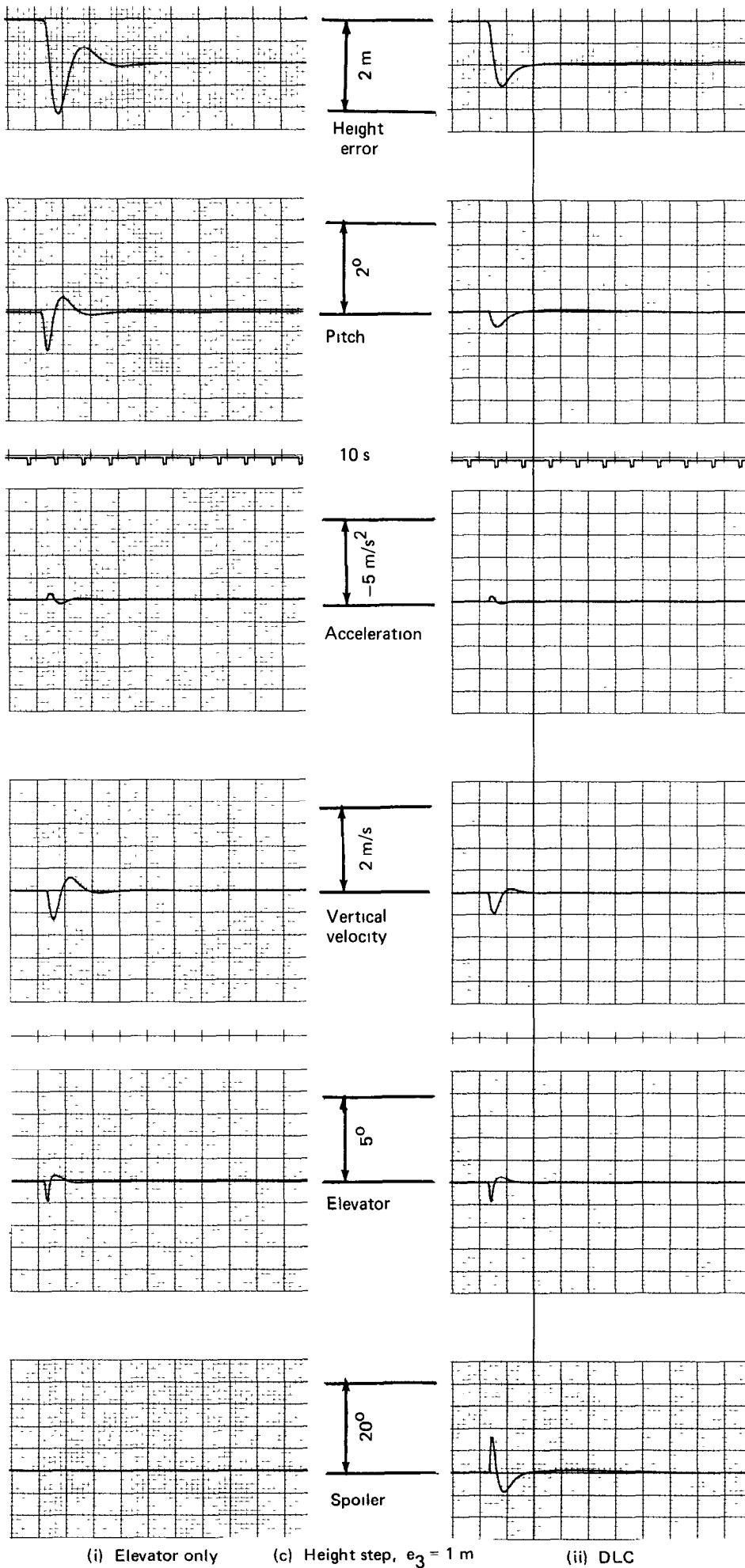


Fig.6 (cont'd.)

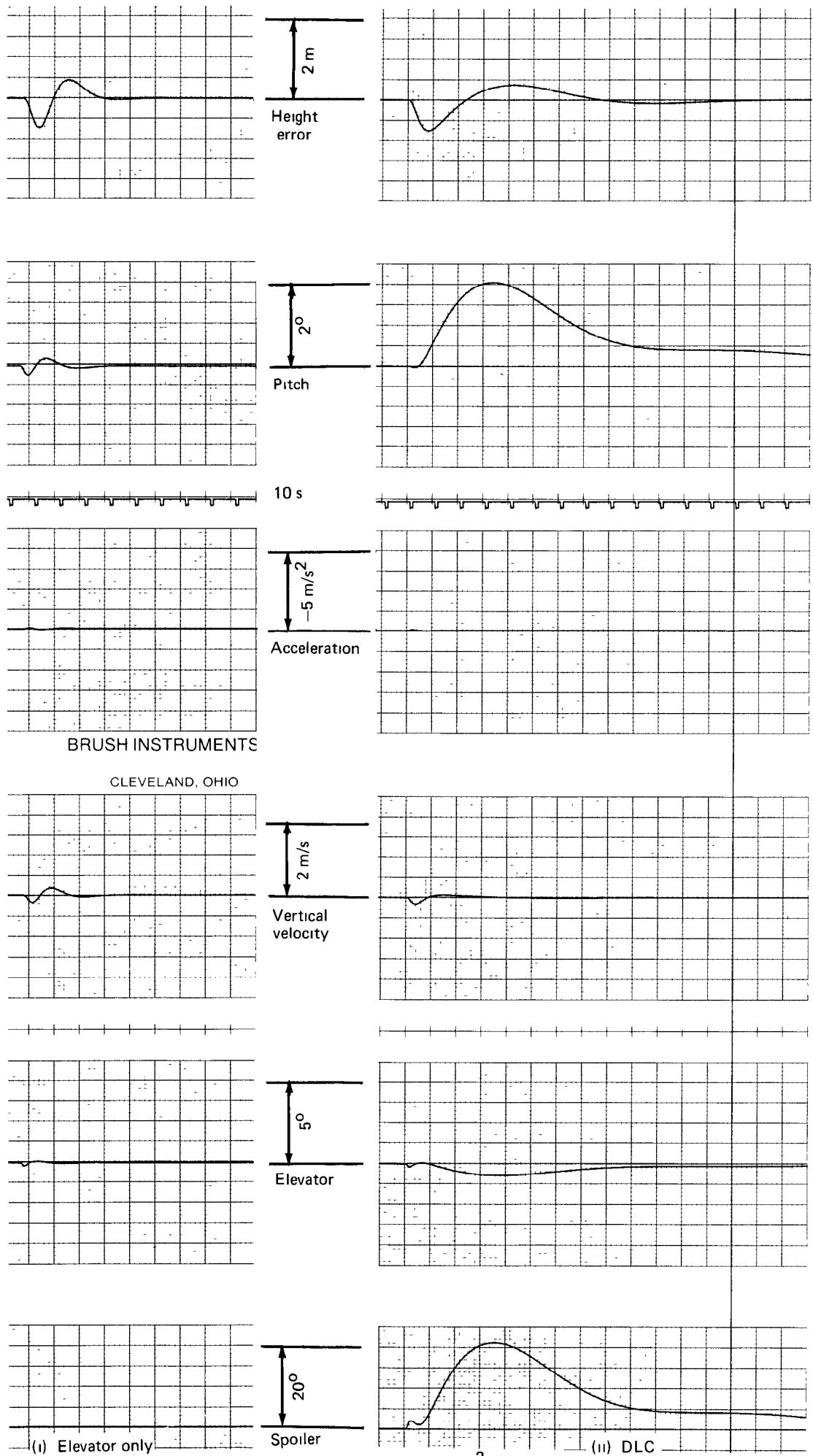


(i) Elevator only

(c) Height step,  $e_3 = 1$  m

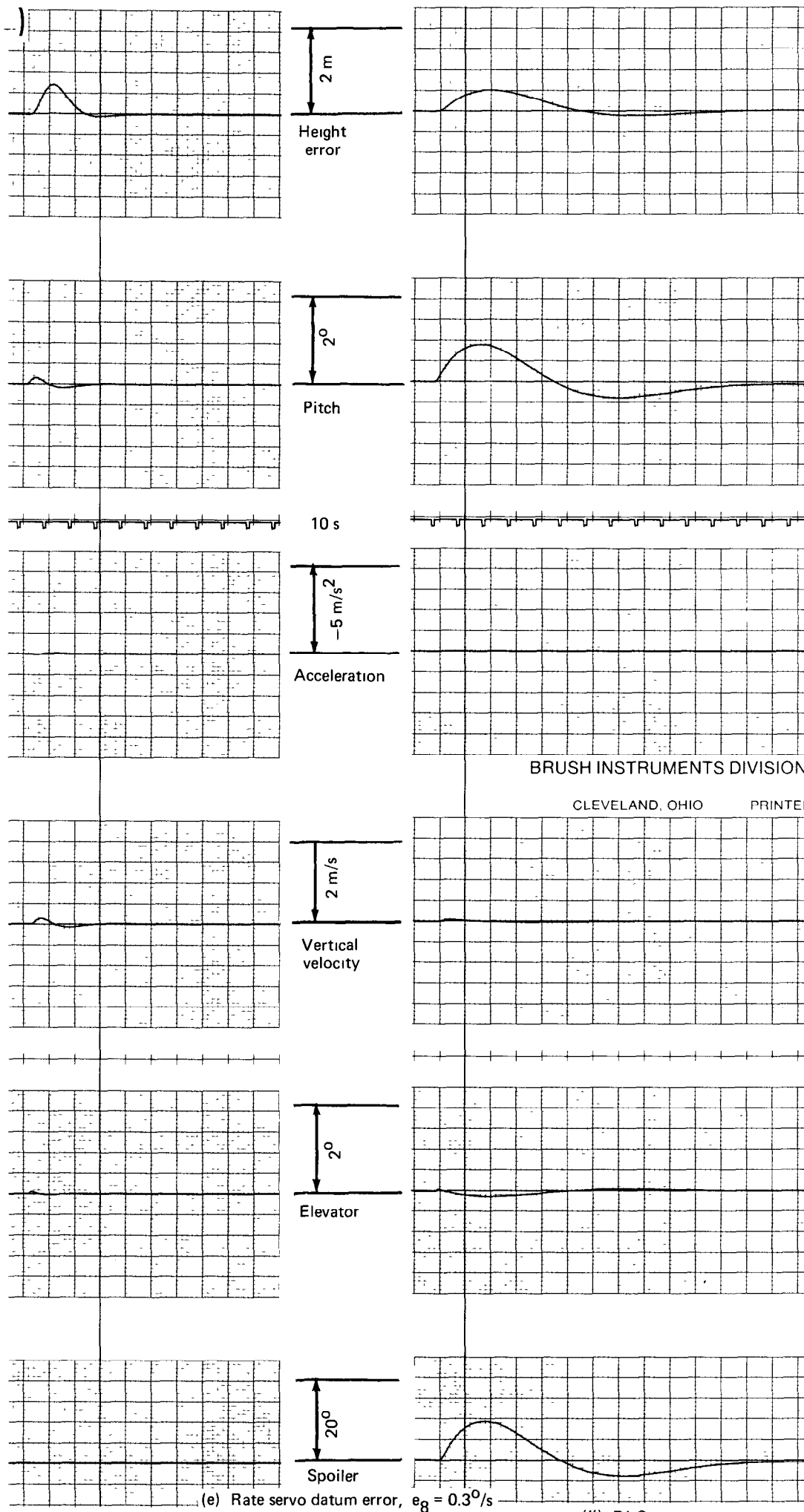
(ii) DLC

Fig.6 (cont'd.)



(d) Acceleration datum error,  $e_5 = 0.1 \text{ m/s}^2$

Fig.6 (cont'd.)



BRUSH INSTRUMENTS DIVISION

CLEVELAND, OHIO PRINTED

Fig.6 (concl'd.)

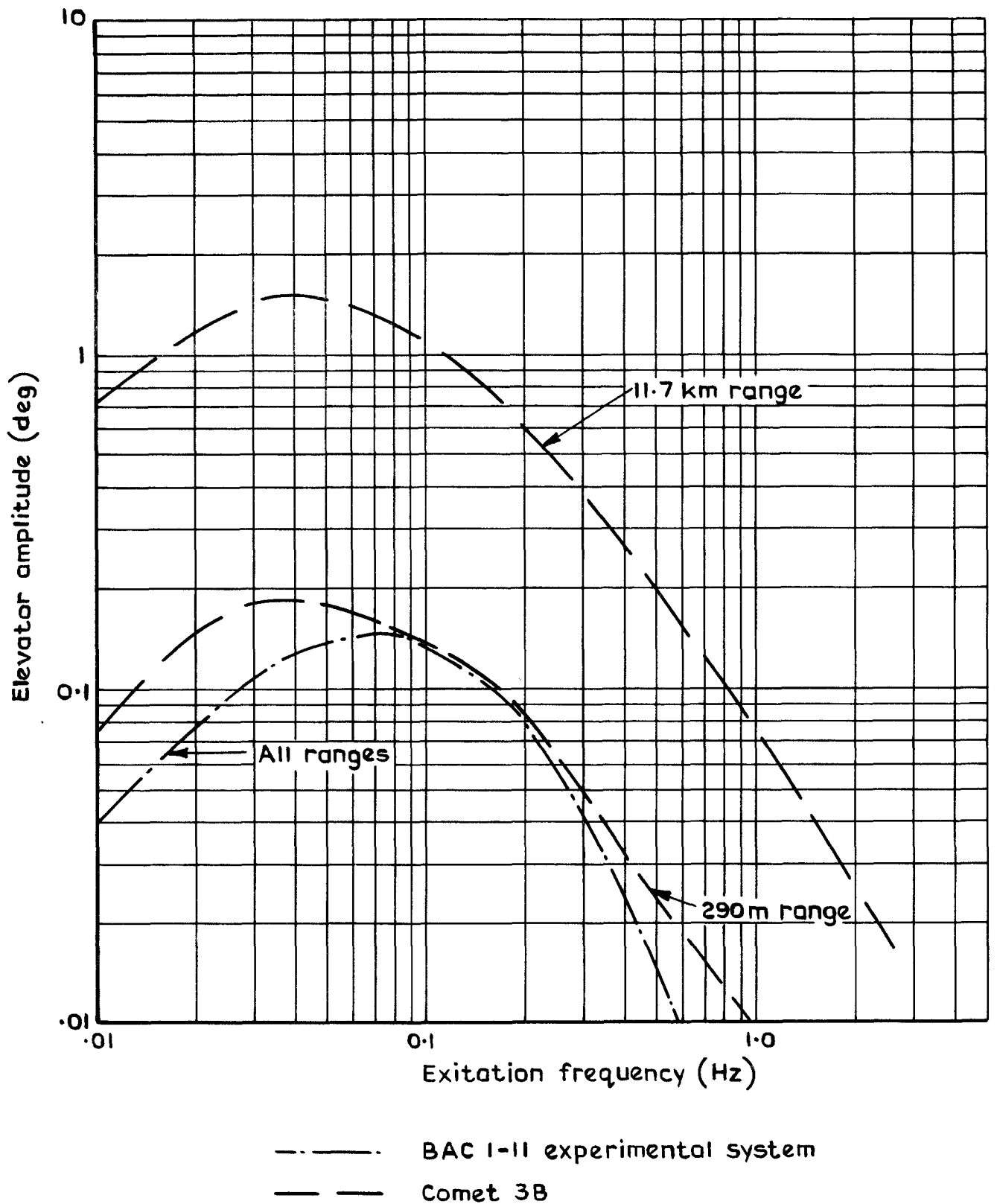
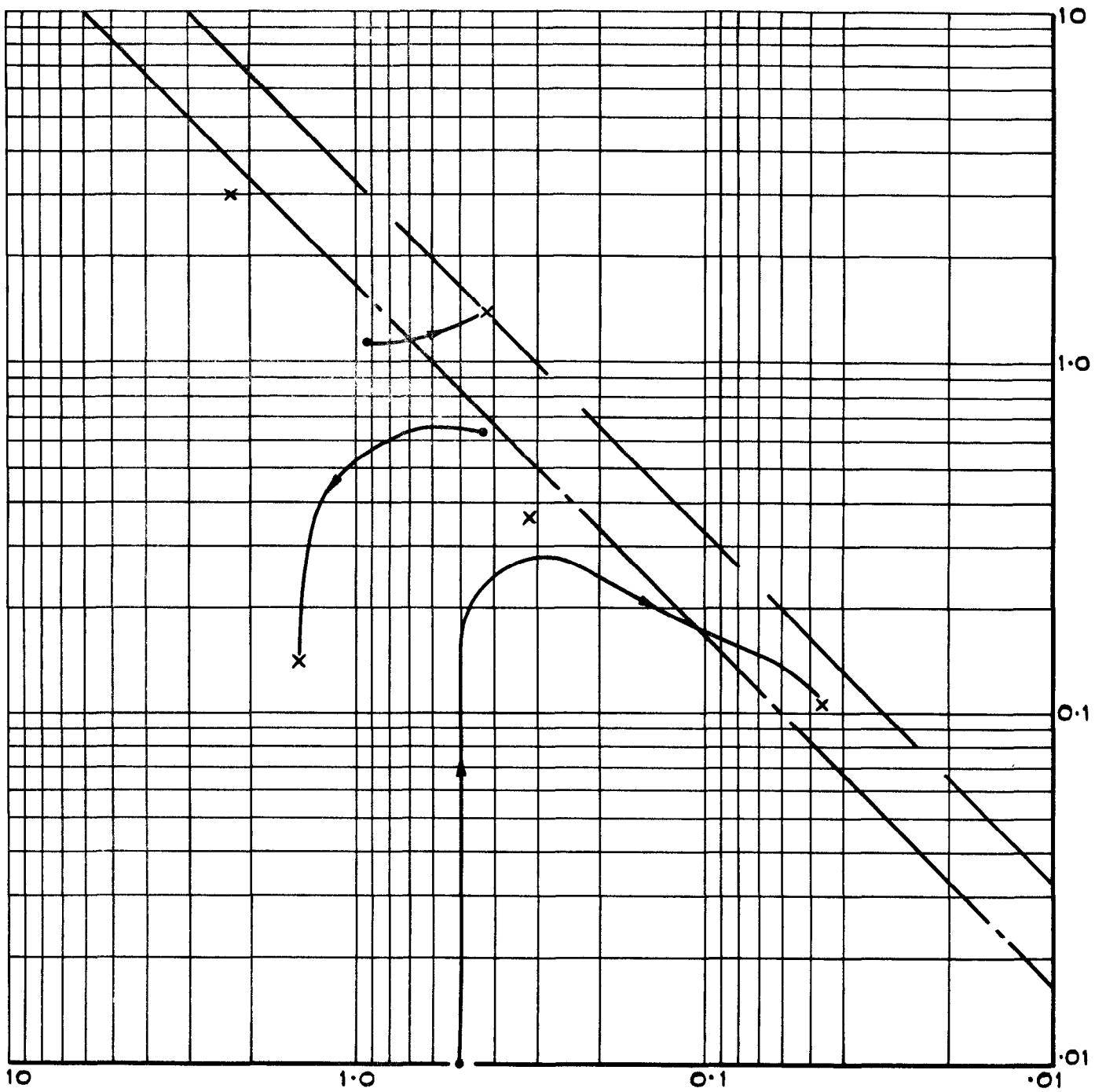


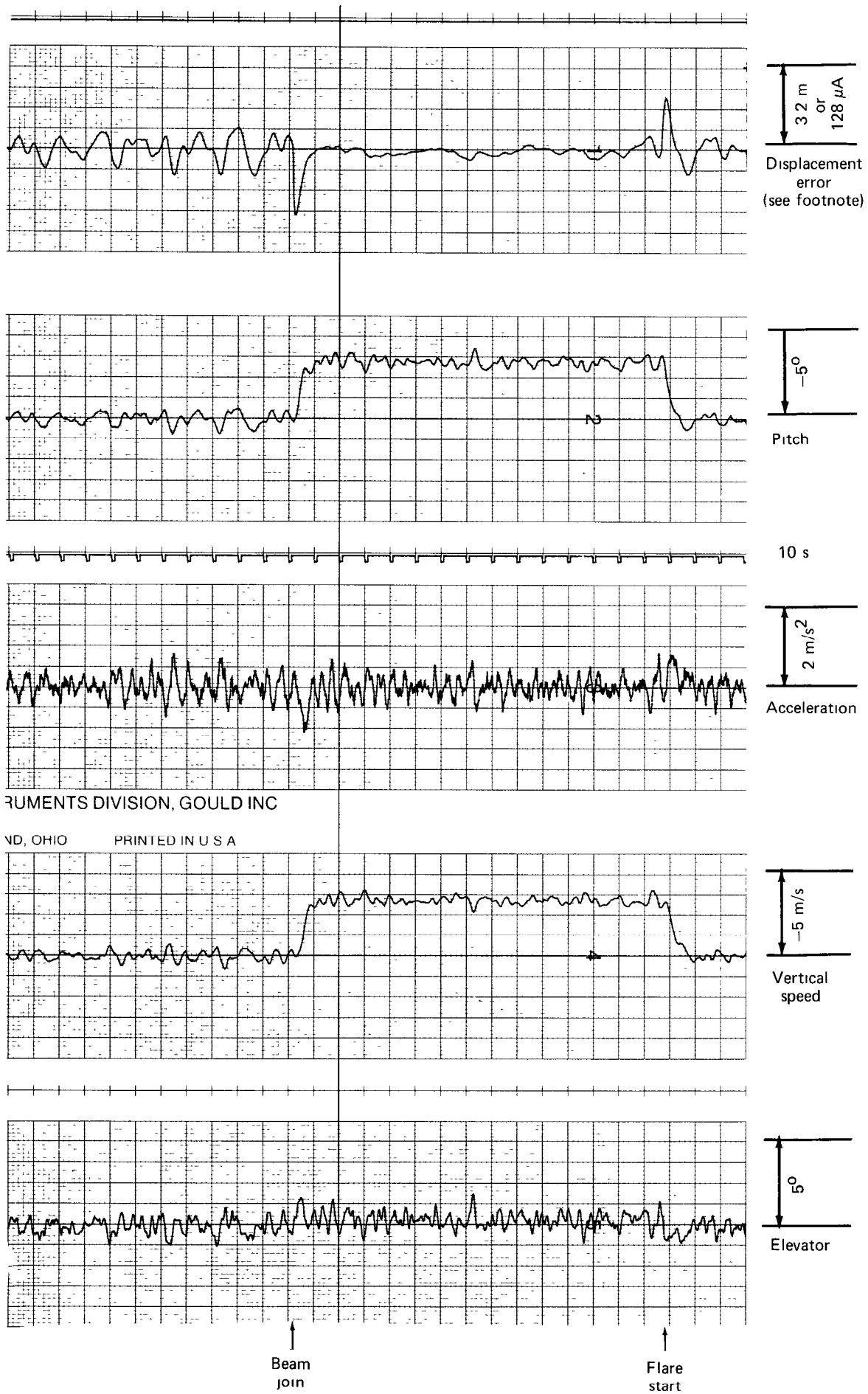
Fig.7 Bode diagrams of elevator amplitude caused by ILS noise via mixing filter





- $R=0.3\text{km}$
- x  $R=13\text{km}$  and unaltered poles
- - - 0.5 relative damping
- - 0.3 relative damping

Fig.8a Variation in pole positions for elevator only glide path system



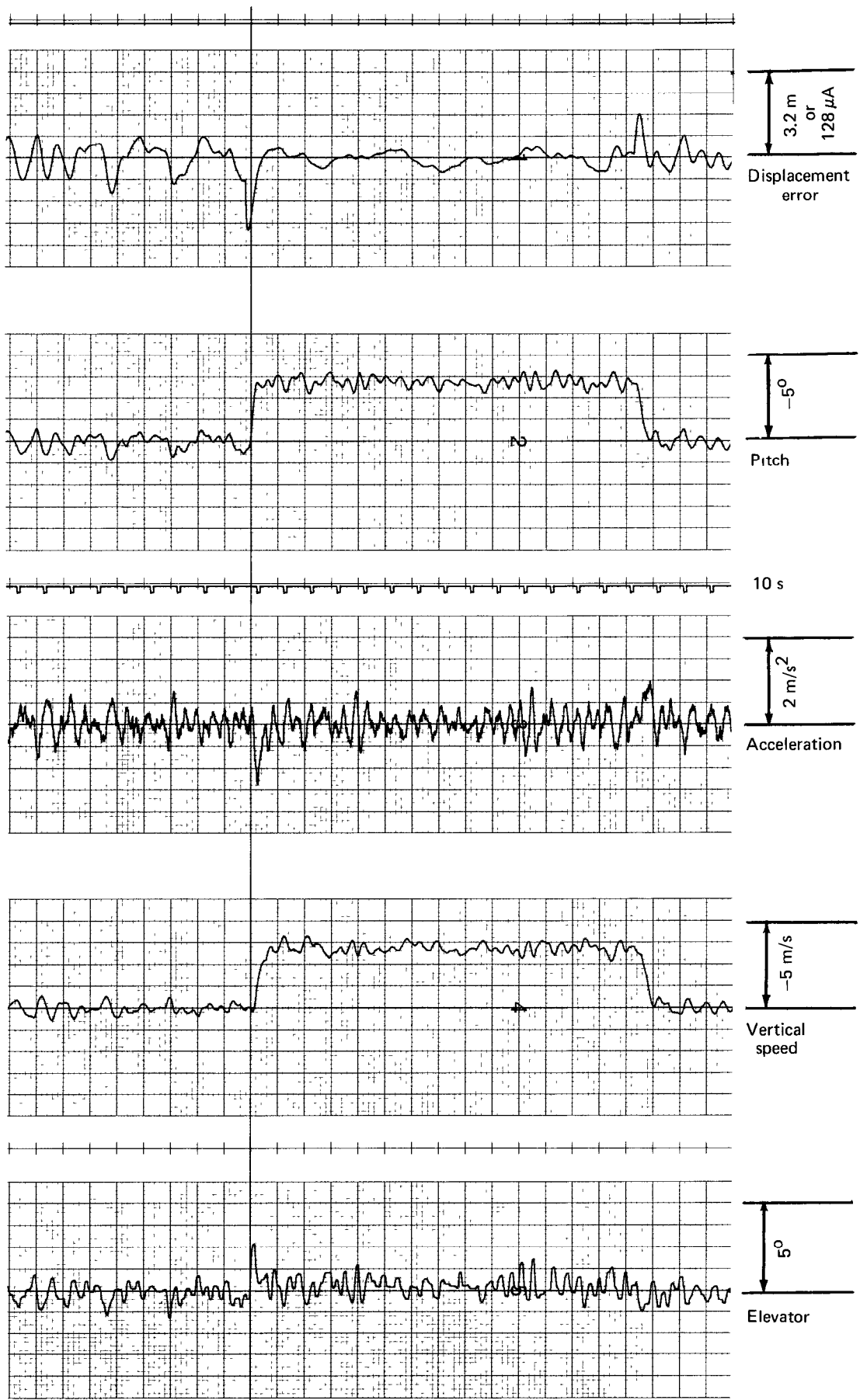
UMENTS DIVISION, GOULD INC

ND, OHIO PRINTED IN U S A

(a) Elevator only, no control non-linearities

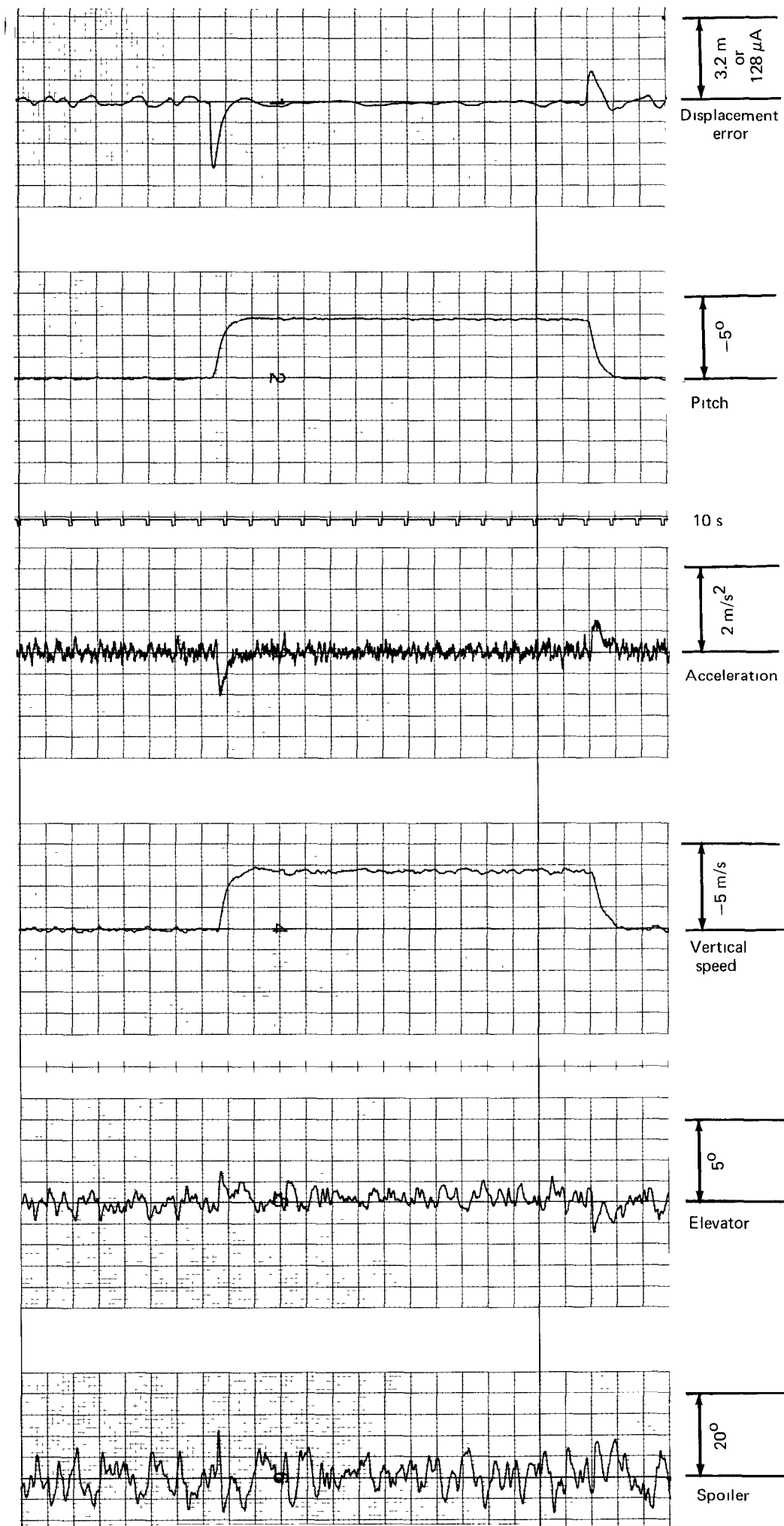
(Footnote: 3.2m scale for record to beam join and during flare)  
(128  $\mu\text{A}$  scale during glide path)

**Fig.9 Glide path hold and acquire: horizontal turbulence**



(b) Elevator only, with control non-linearities

Fig.9 (cont'd.)



(c) DLC, no control non-linearities nor limits

Fig.9 (cont'd.)

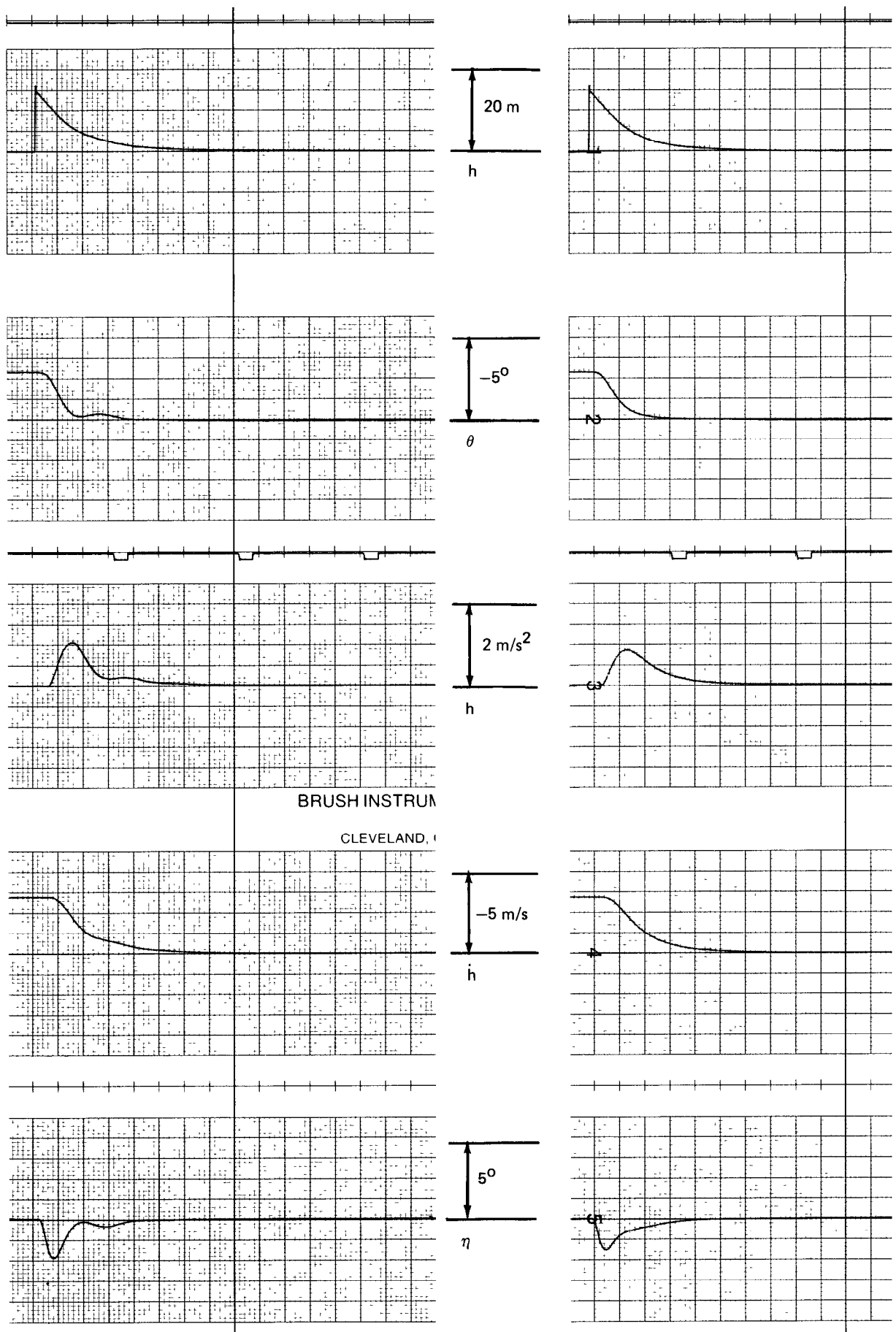
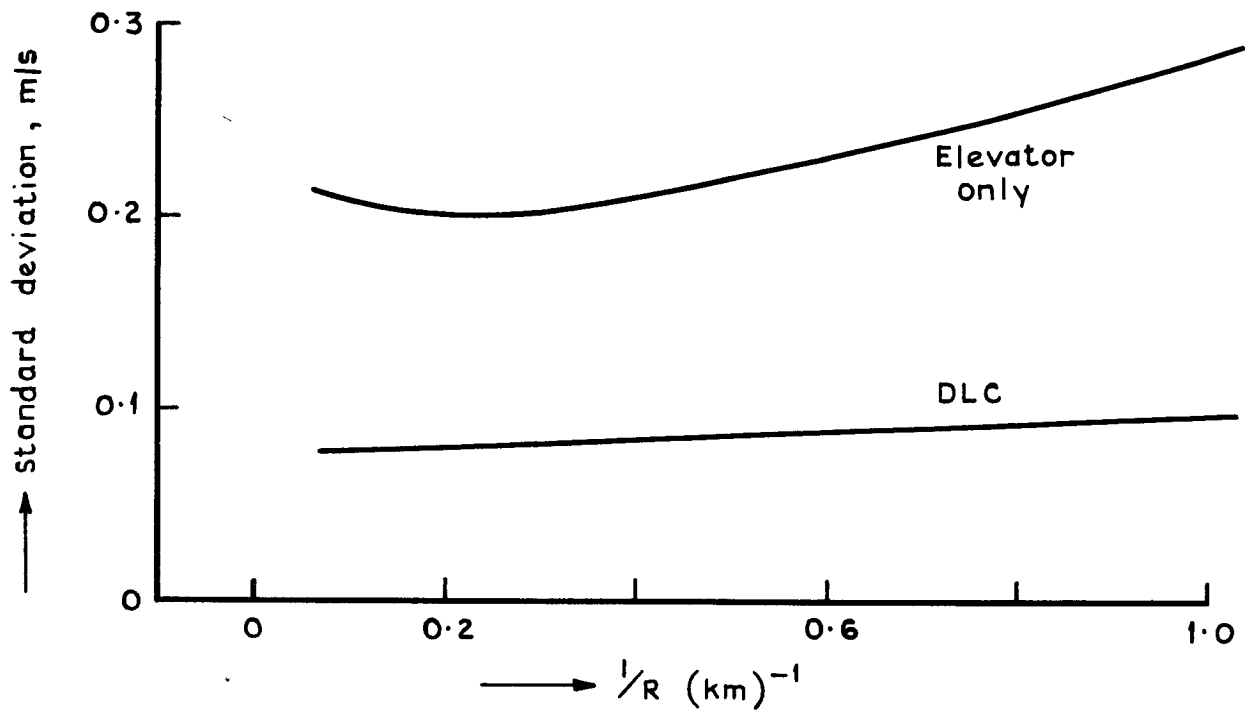
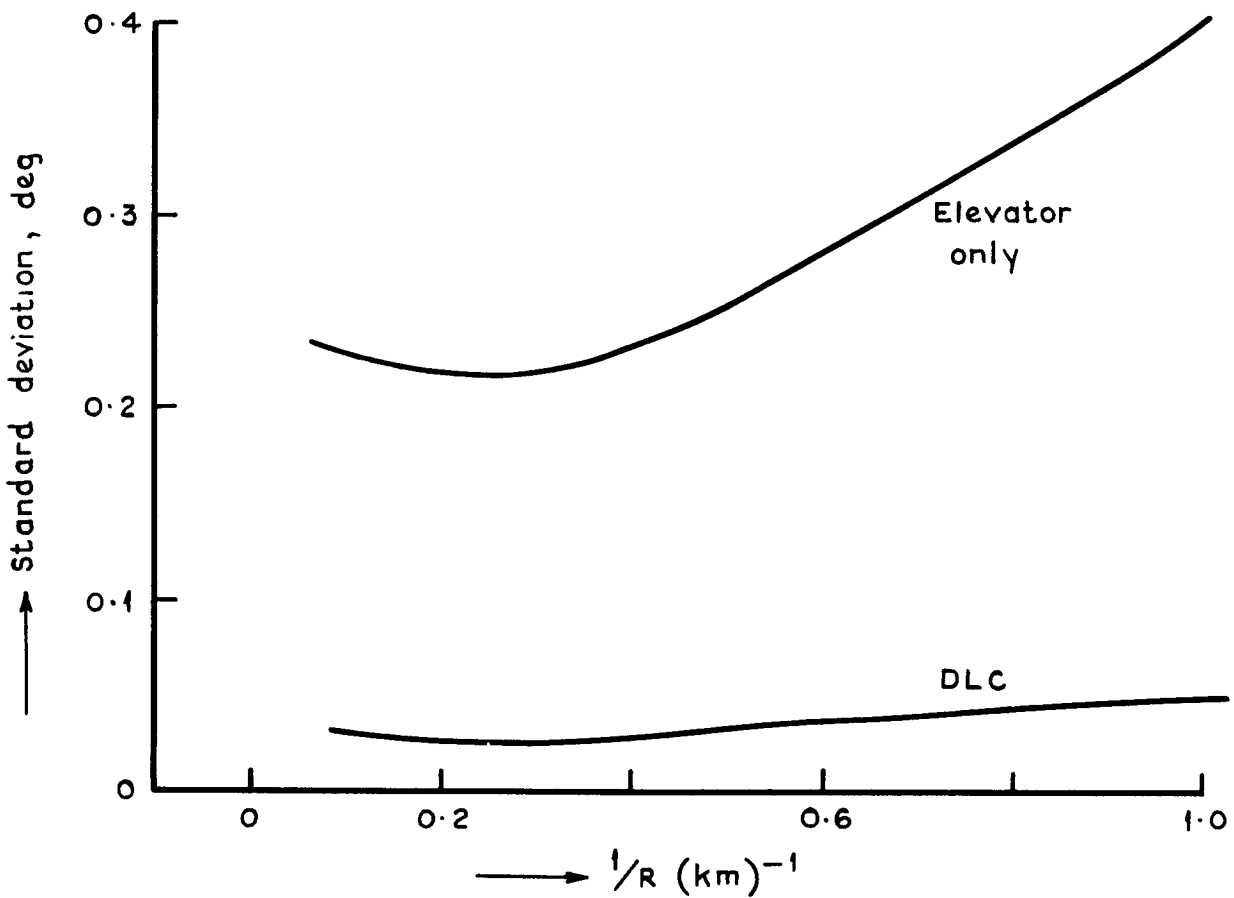


Fig.14 (cont'd.)

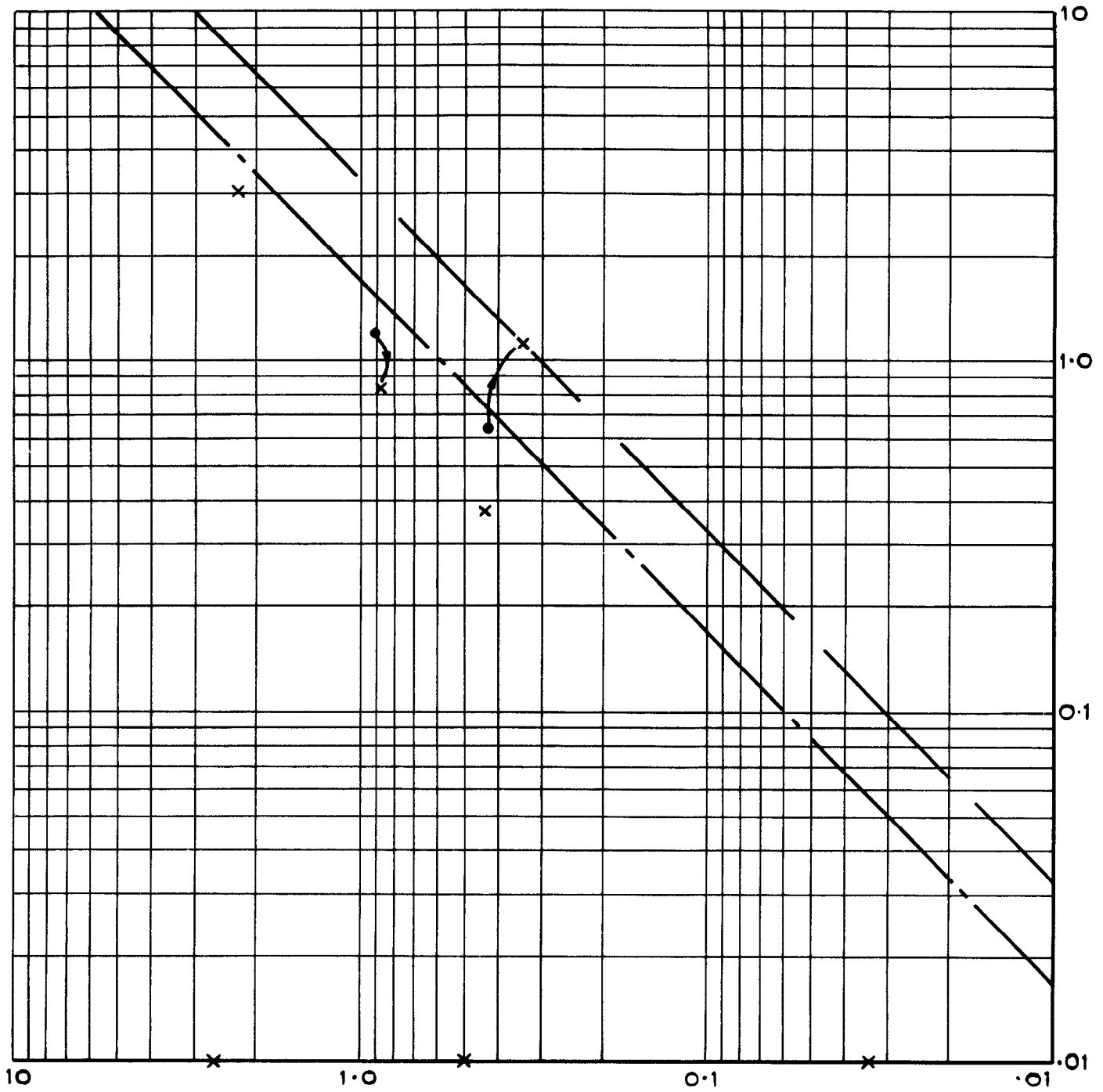


a Variation of vertical velocity errors



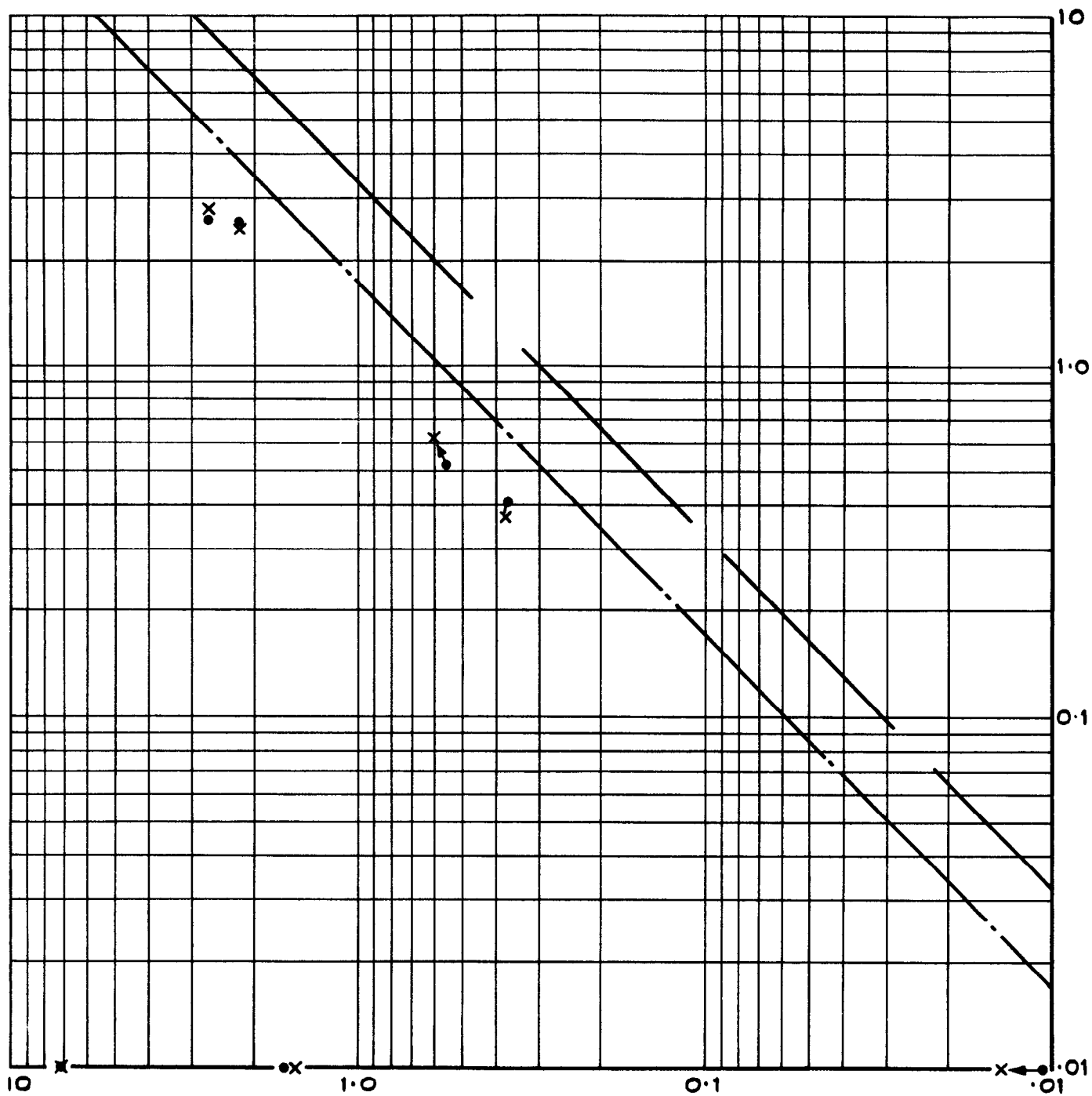
b Variation of pitching activity

Fig.10a & b Variation of performance with respect to horizontal turbulence on glide path hold



- 50ft
- x 7ft and unaltered poles
- - - 0.5 relative damping
- - - 0.3 relative damping

Fig. 11a Changes in pole positions with height:  
ground effect with elevator only flare system



- 50 ft above runway
- x 7 ft above runway
- - - 0.5 relative damping
- — 0.3 relative damping

Fig.11b Variation of pole positions with ground effect for D.L.C. system



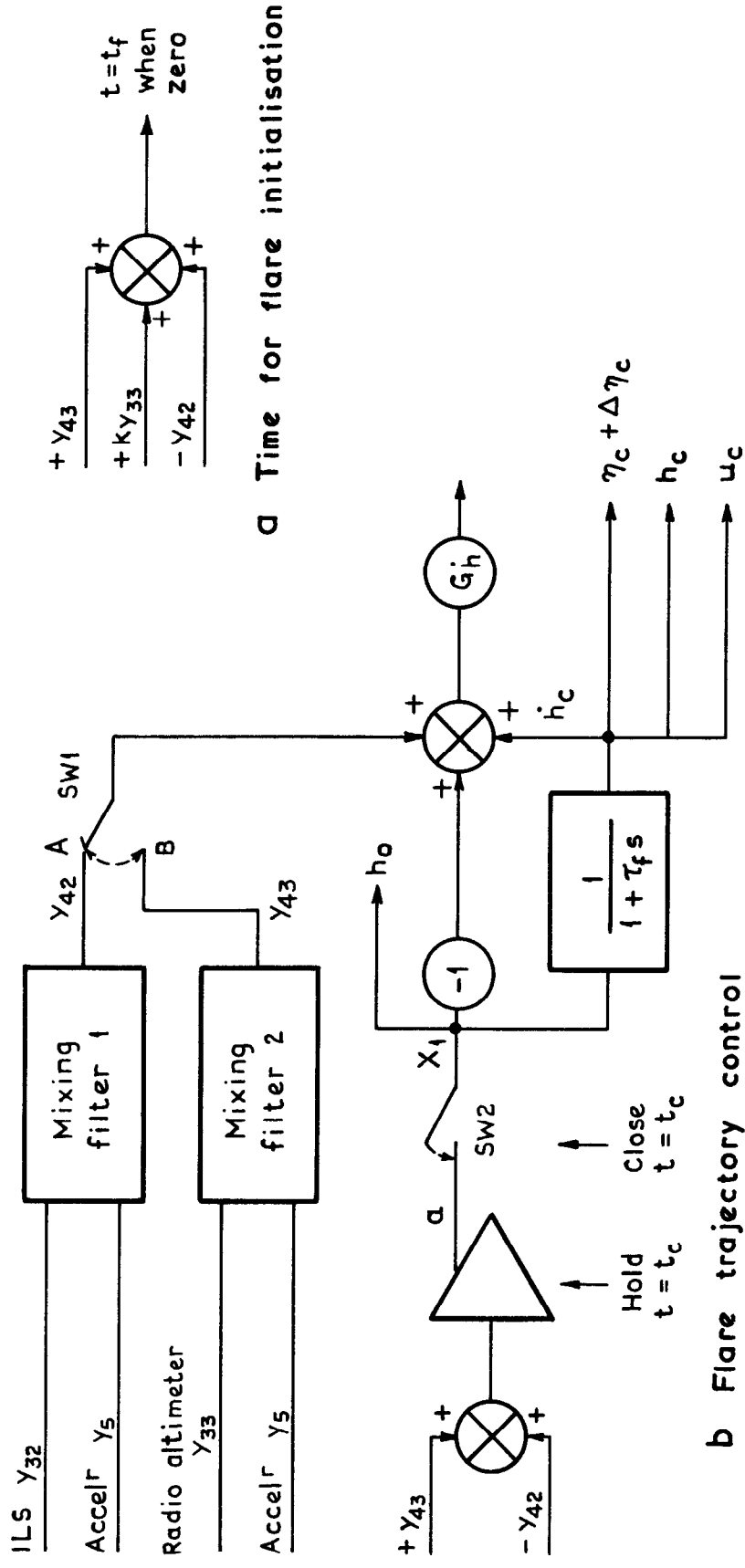
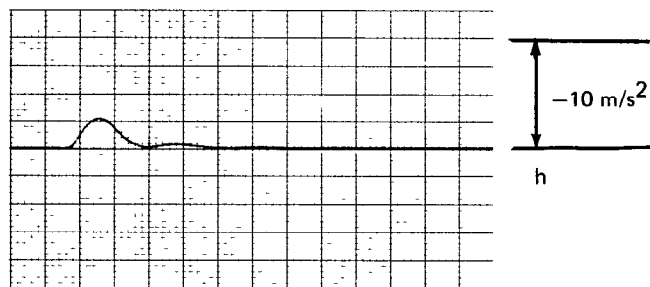
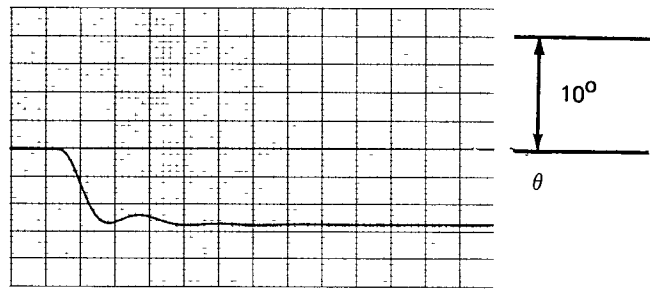
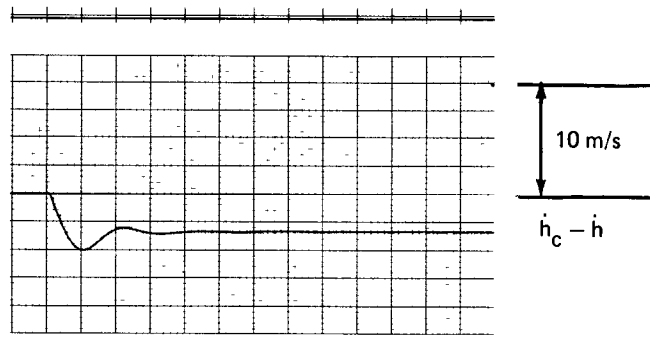
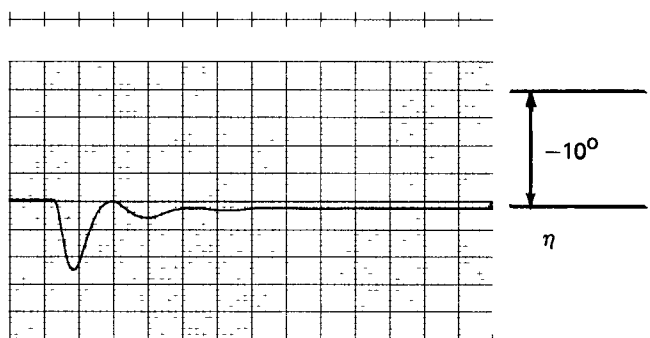
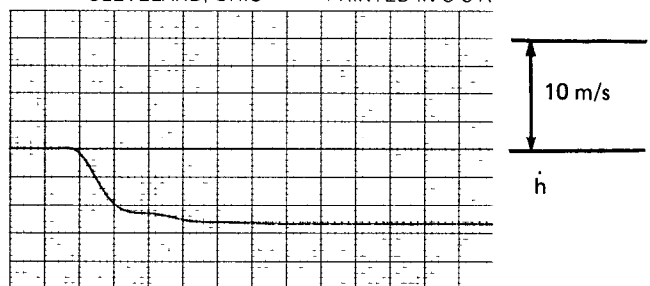


Fig.12 a & b Elements of producing flare



BRUSH INSTRUMENTS DIVISION, GOULD

CLEVELAND, OHIO PRINTED IN U.S.A.



(a)  $\dot{h}_c$  command signal only, with  $G_h = 0$

Fig.13 Change in vertical speed in displacement hold system

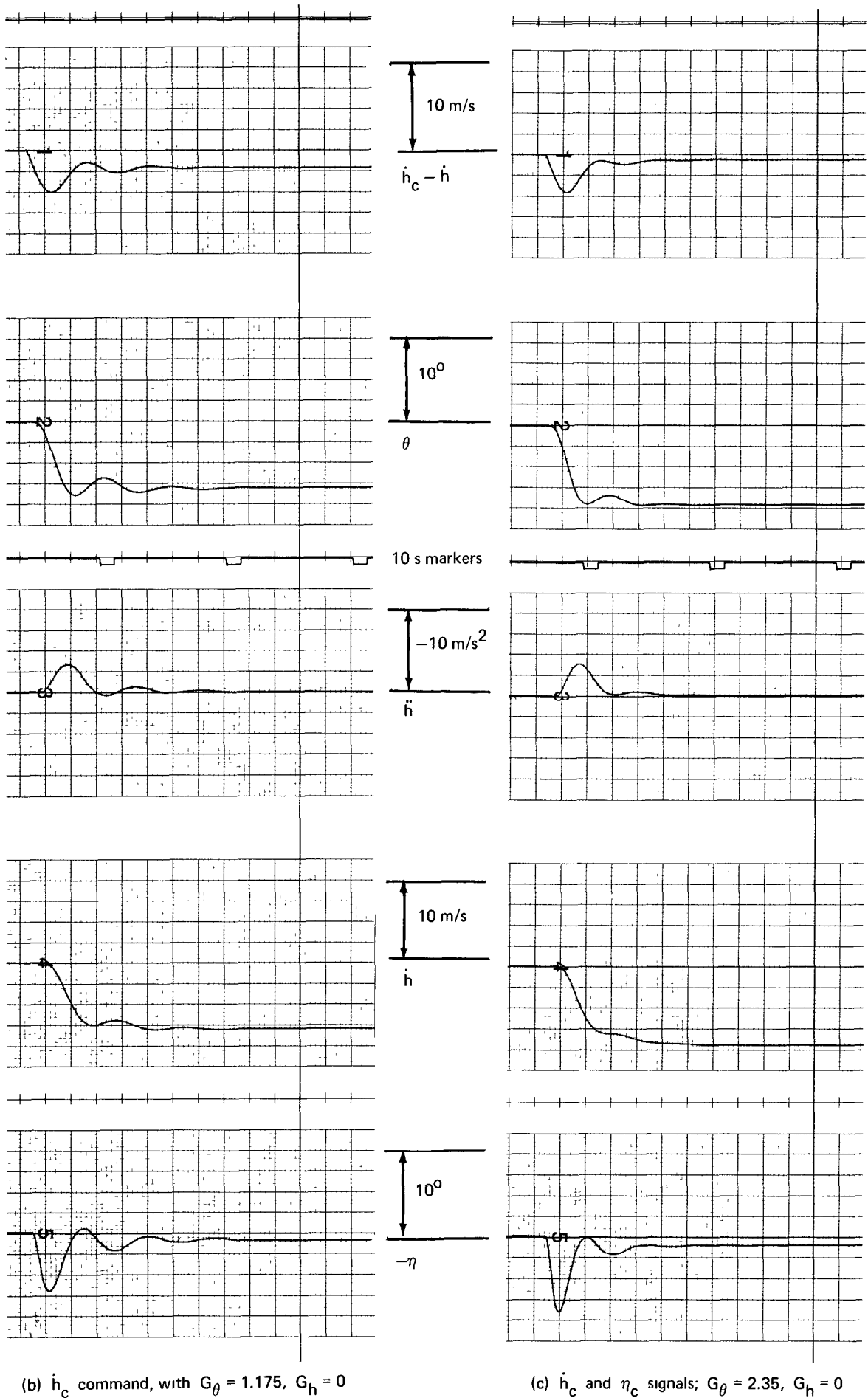
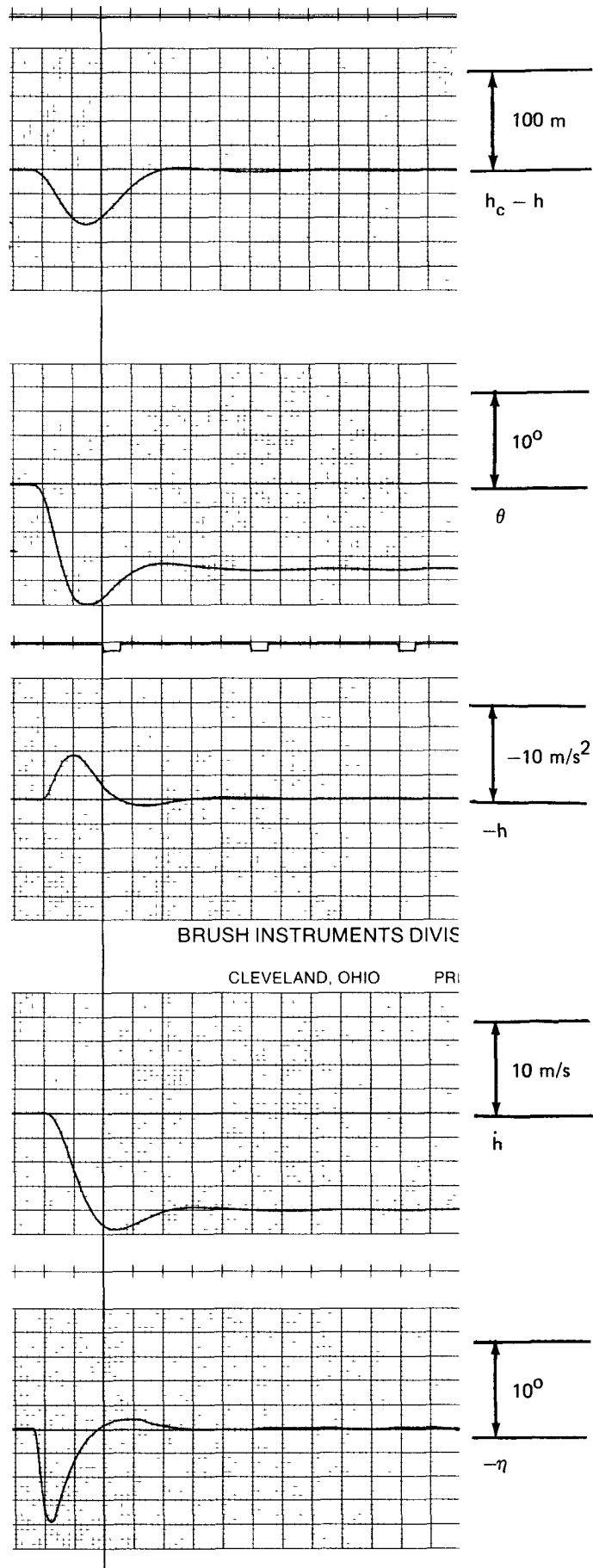
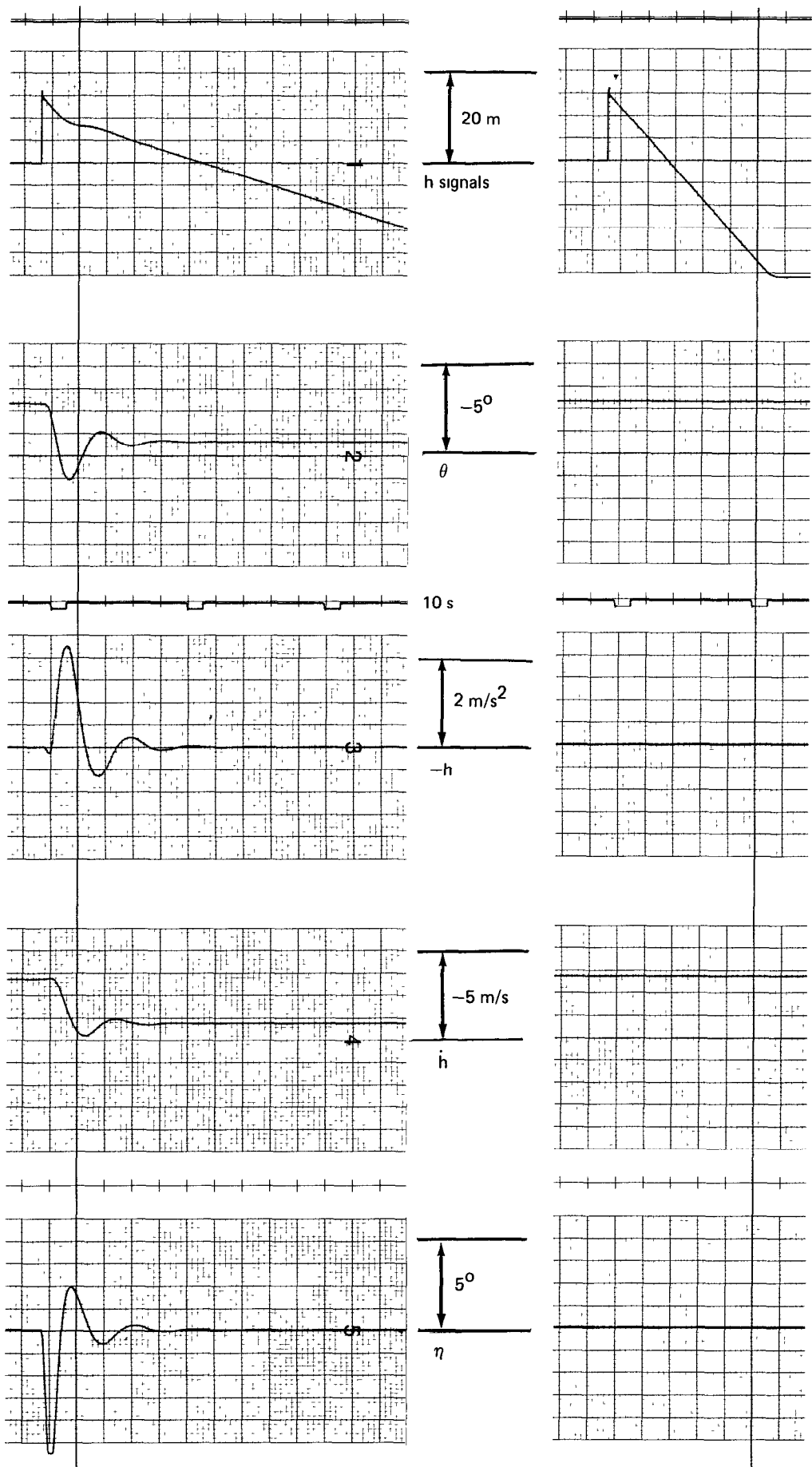


Fig.13 (cont'd.)



(d) Addition of  $G_h = 2.35^\circ/\text{m}$  acting on  $(h_c - h)$  to  $\dot{h}_c, \eta_c$  signals

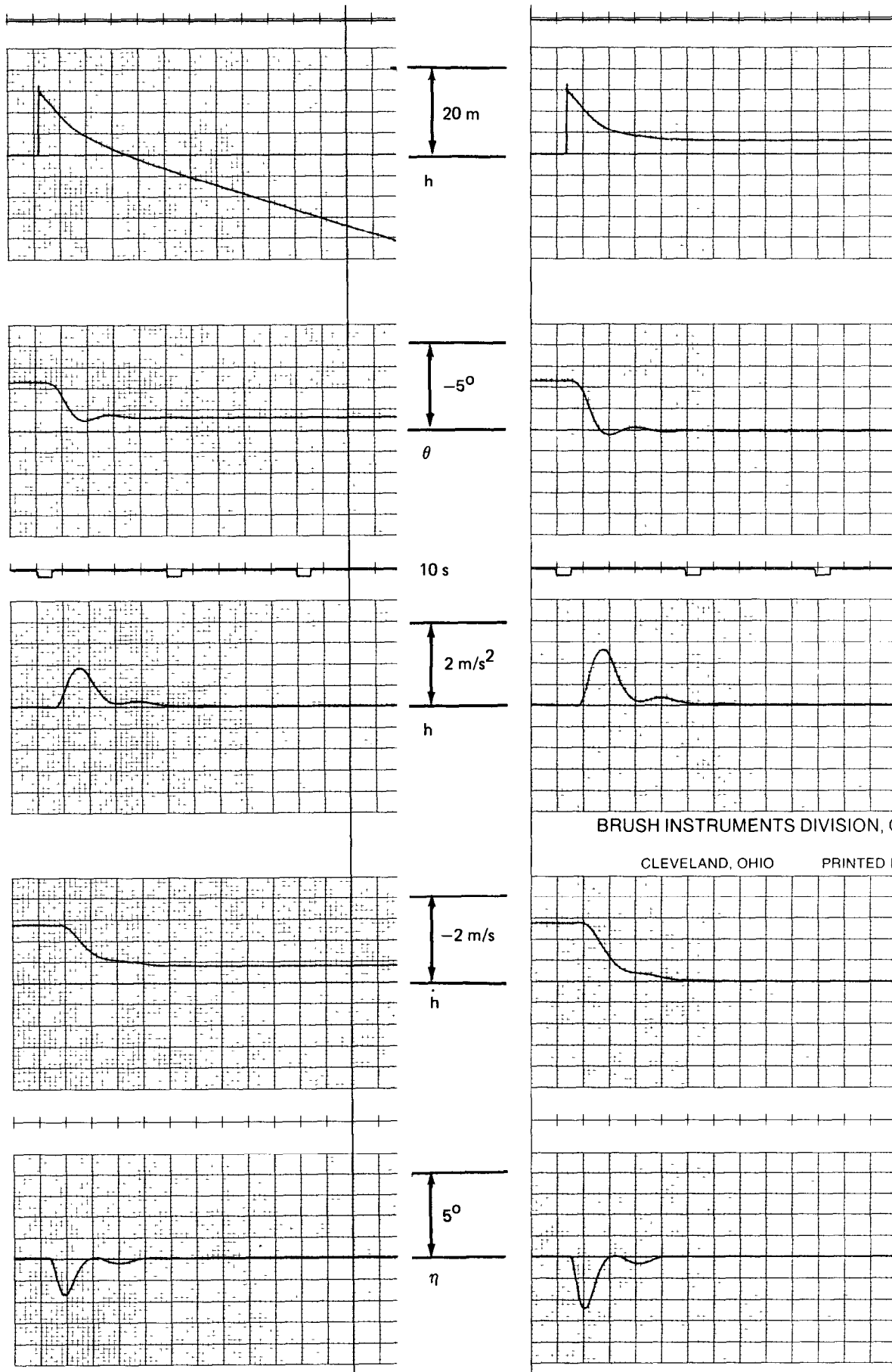
**Fig.13 (concl'd.)**



(a) Effect of step on  $h$  with  $G_h = 0$  during flare

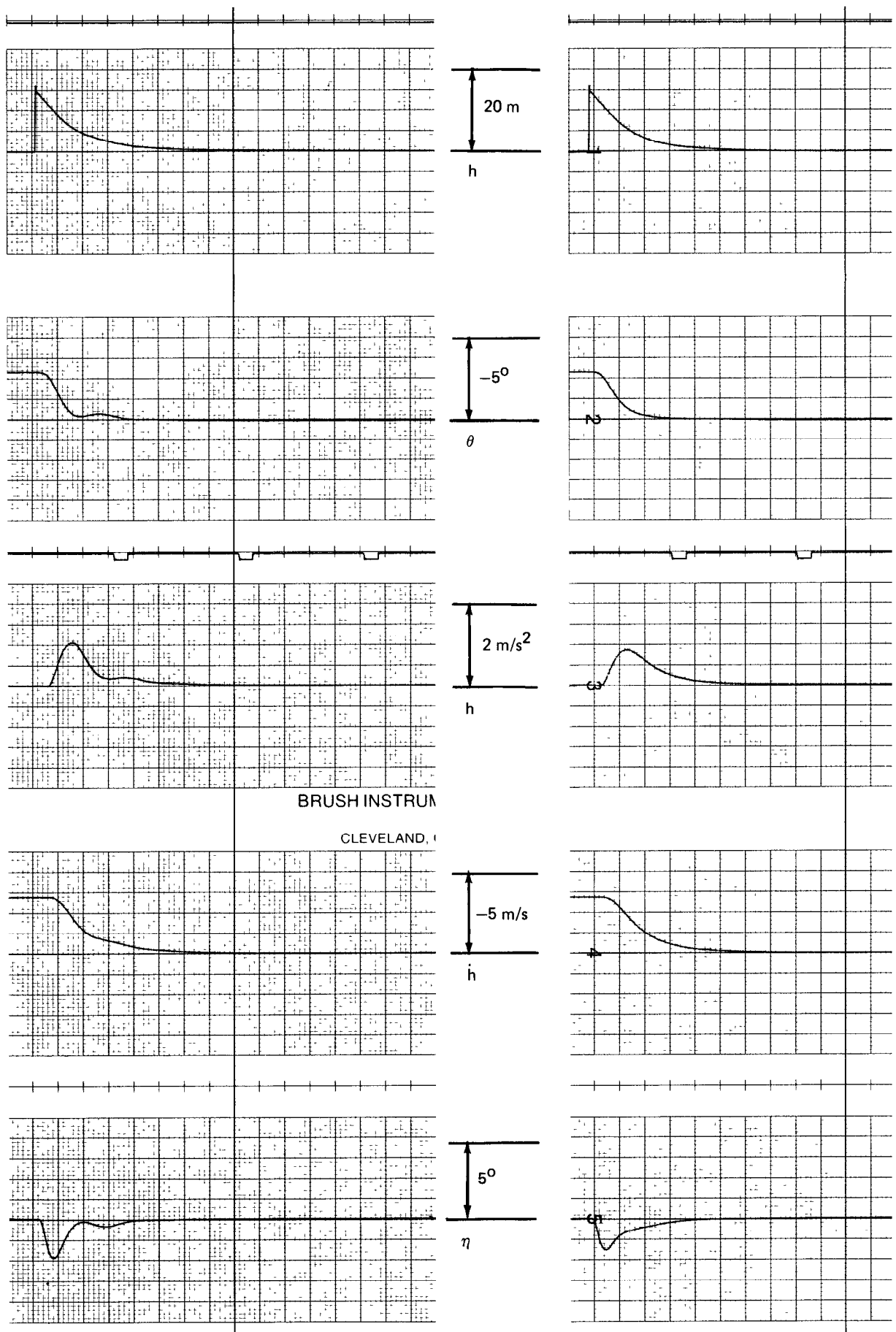
(b)  $\dot{h}$  step on switching is cancelled

Fig.14 Analysis of experimental flare system



(c) Addition of  $\dot{h}_C$ ;  $\tau_C = 2.23 \text{ s}$ ;  $G_h = 0$  during flare

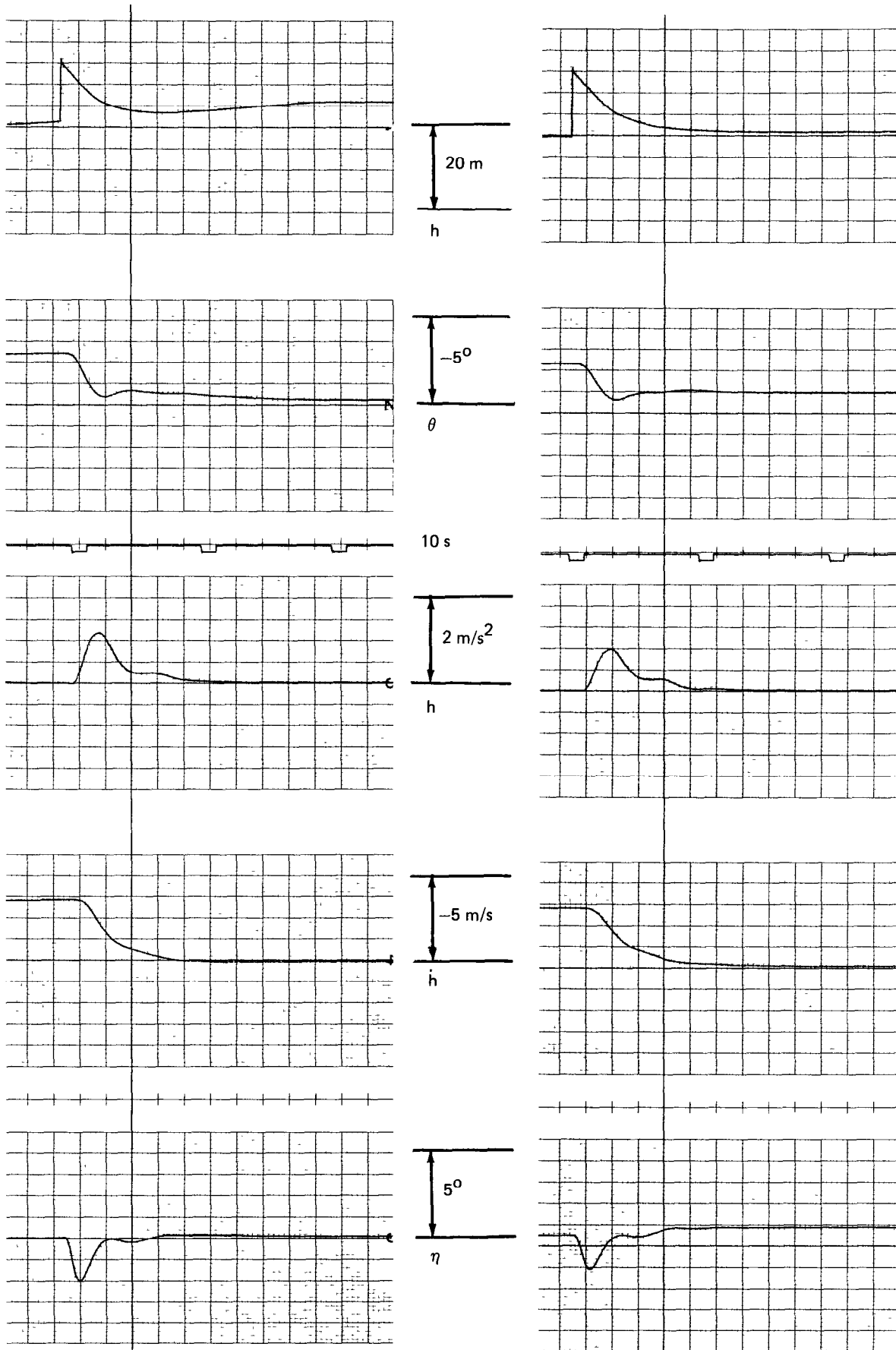
(d) Flare with  $\dot{h}_C, \eta_C$  signals;  $\tau_C = 2.23 \text{ s}$ ;  $G_h = 0$



(e) Change  $\tau_c$  to 3 s;  $G_h = 0$

(f) Introduce  $G_h = 2.35^\circ/\text{m}$  and  $h_c$  signal

Fig.14 (cont'd.)

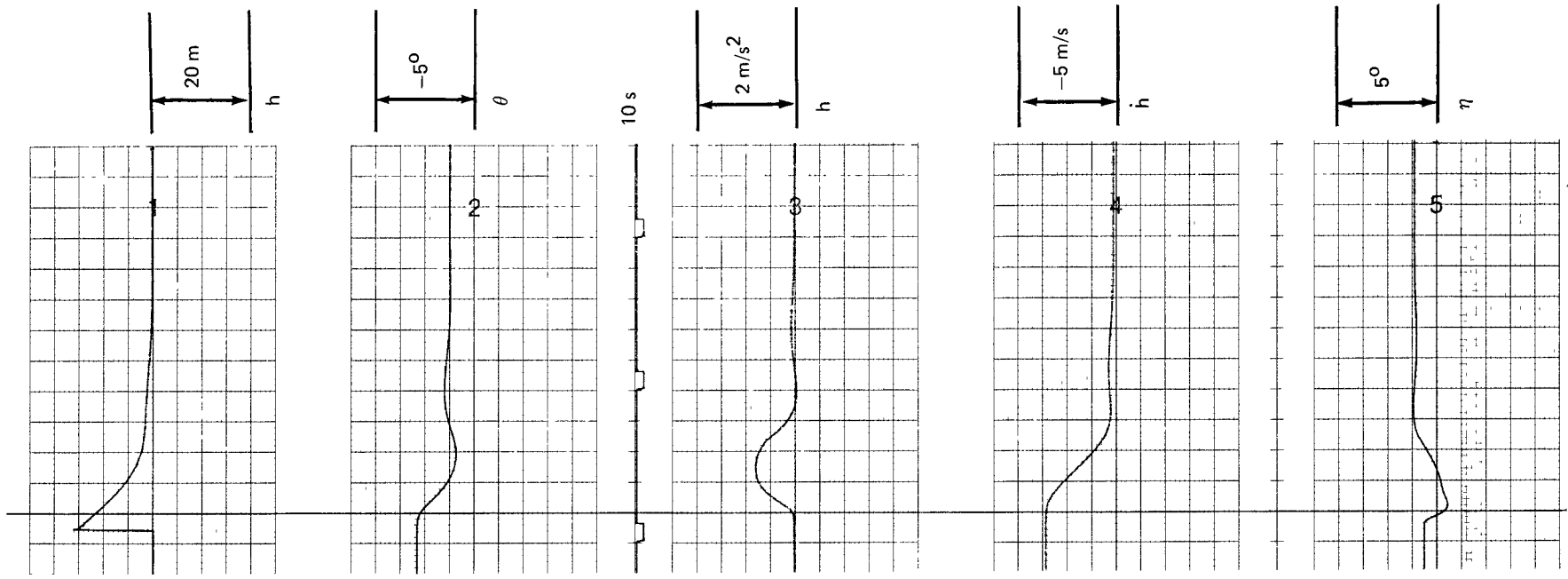


(g) Flare with ground effect  
 $\eta_c = \frac{G_\theta \cdot h_c}{1.14}$ ;  $G_h = 0$

(h) Flare and ground effect  
 $\eta_c = 1.06 h_c$ ,  $G_h = 0$

Fig.14 (cont'd.)





(i) Flare and ground effect,  $\eta_c = 1.06h_c$ ,  $G_h = 2.35^\circ/\text{m}$

Fig.14 (concl'd.)



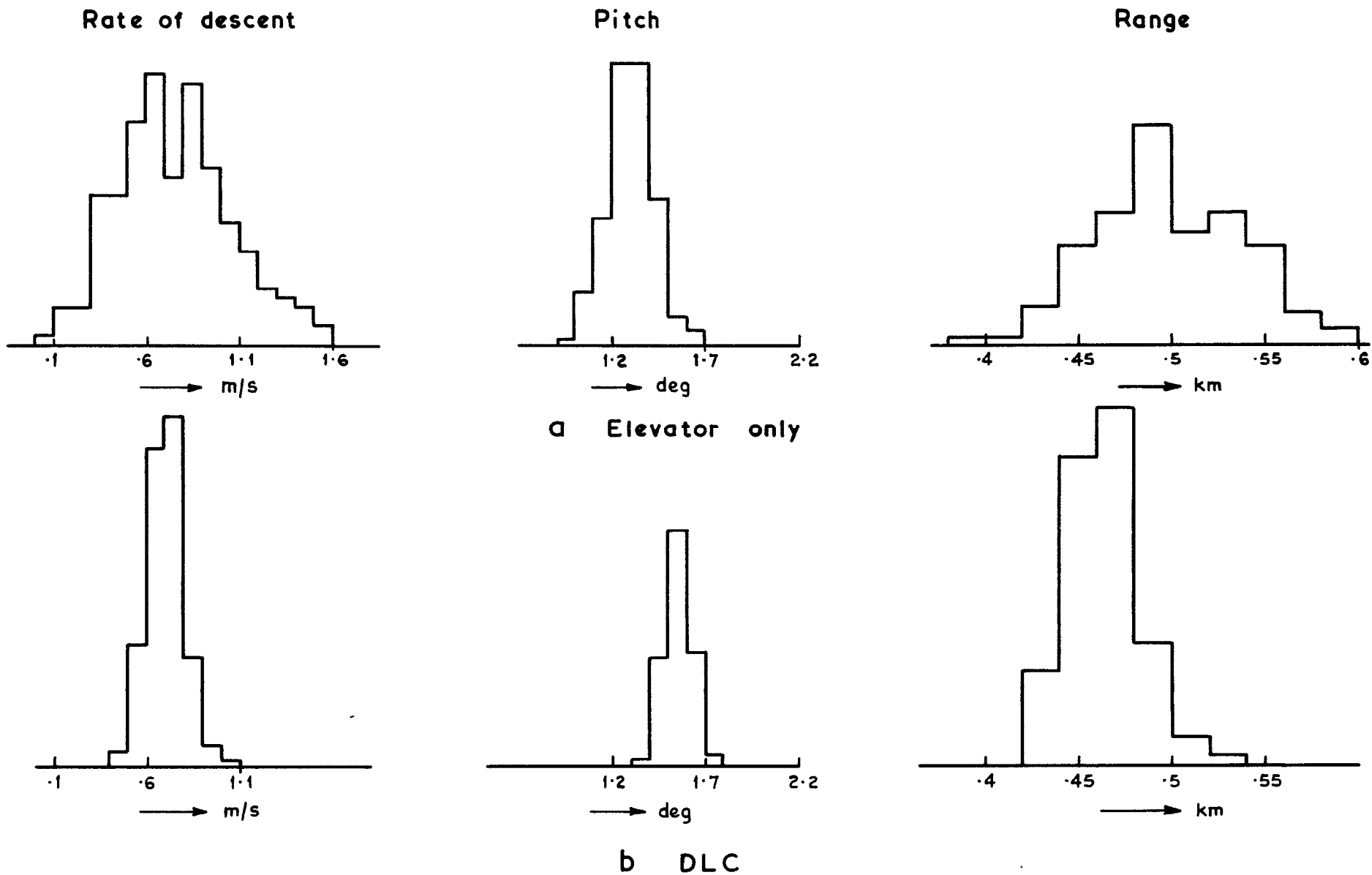
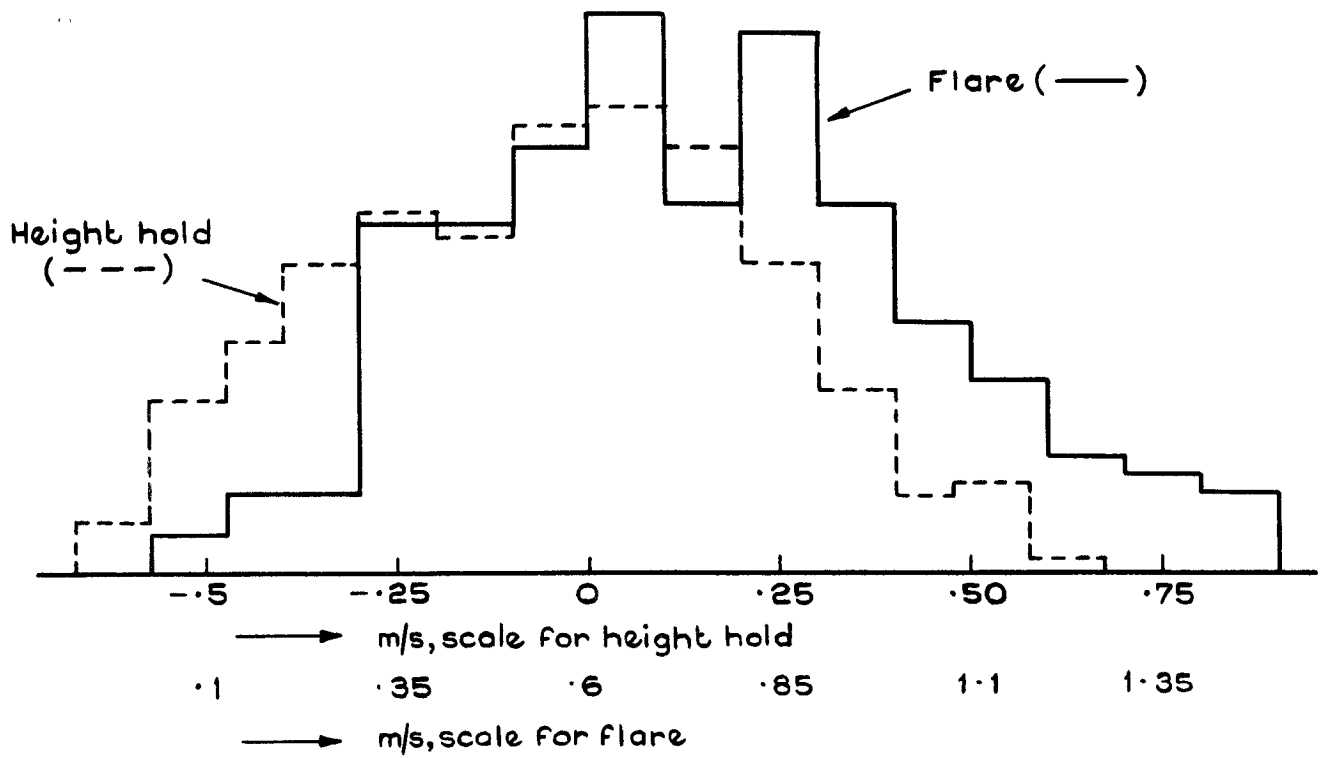
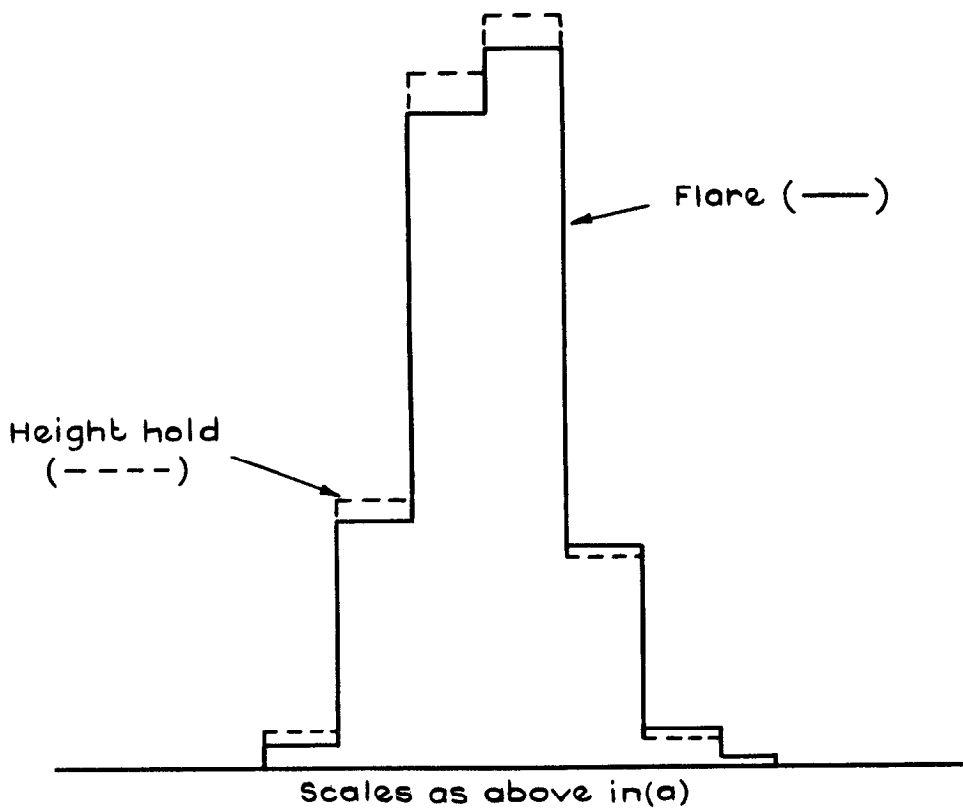


Fig.16 a & b Distribution of touchdown errors : horizontal turbulence (linear control)

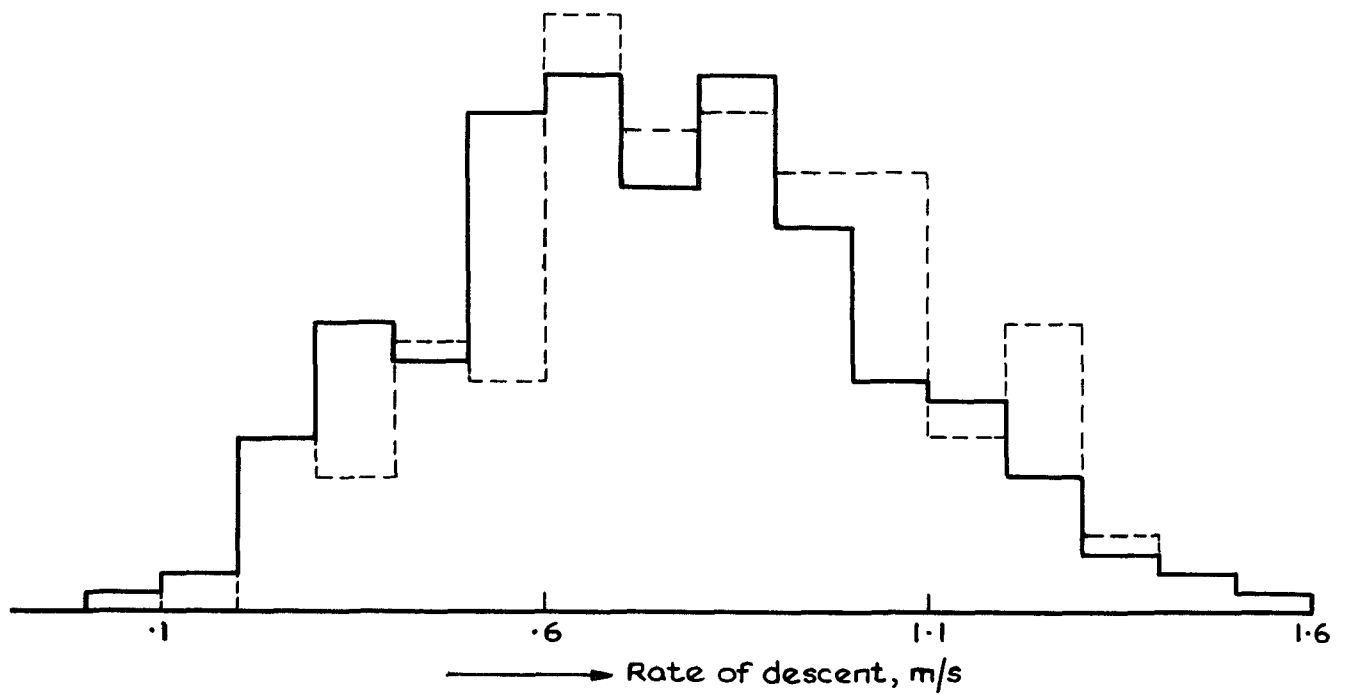


a Elevator only

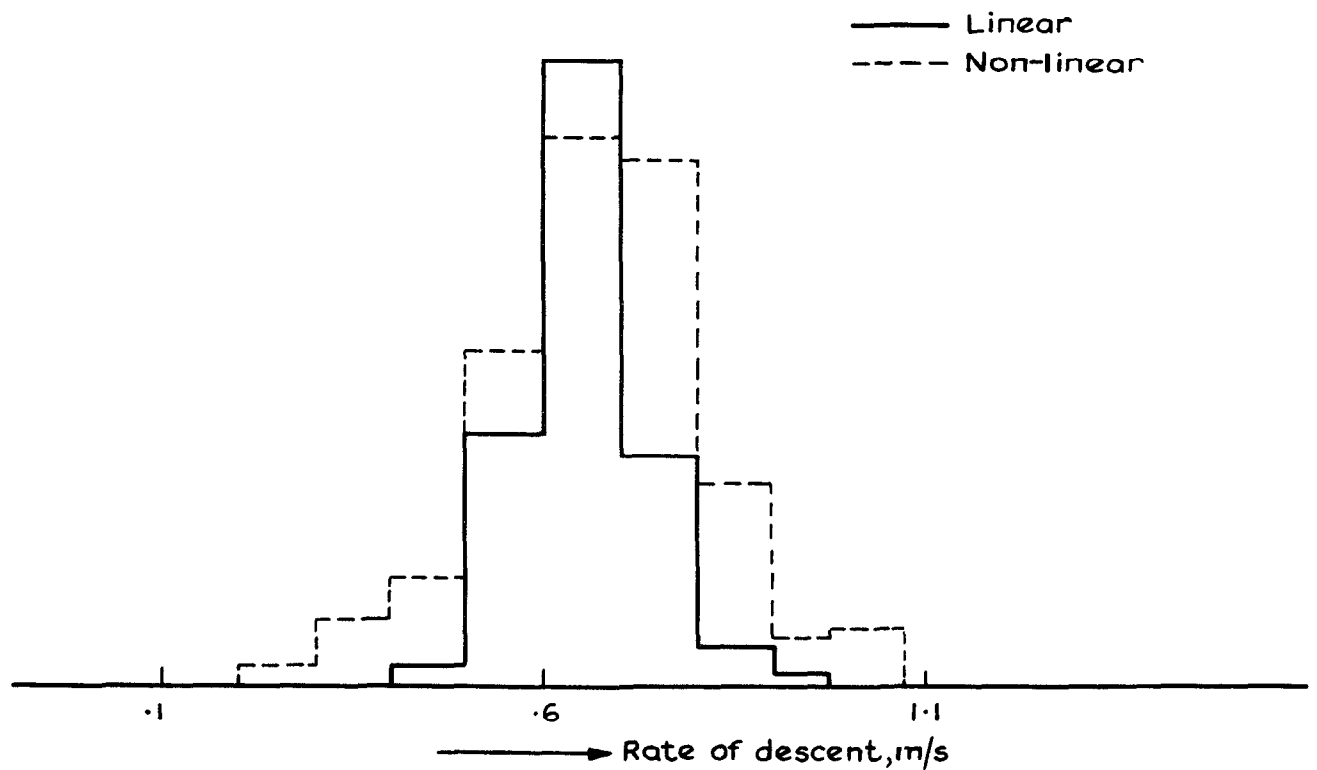


b DLC

Fig.17a&b Comparison of distribution: of vertical speed errors due to horizontal turbulence, height hold and flare



a Elevator only



b DLC (7° amplitude limit)

Fig.18a&b Effect of control non-linearities on distribution of rate of descent at touchdown due to horizontal turbulence

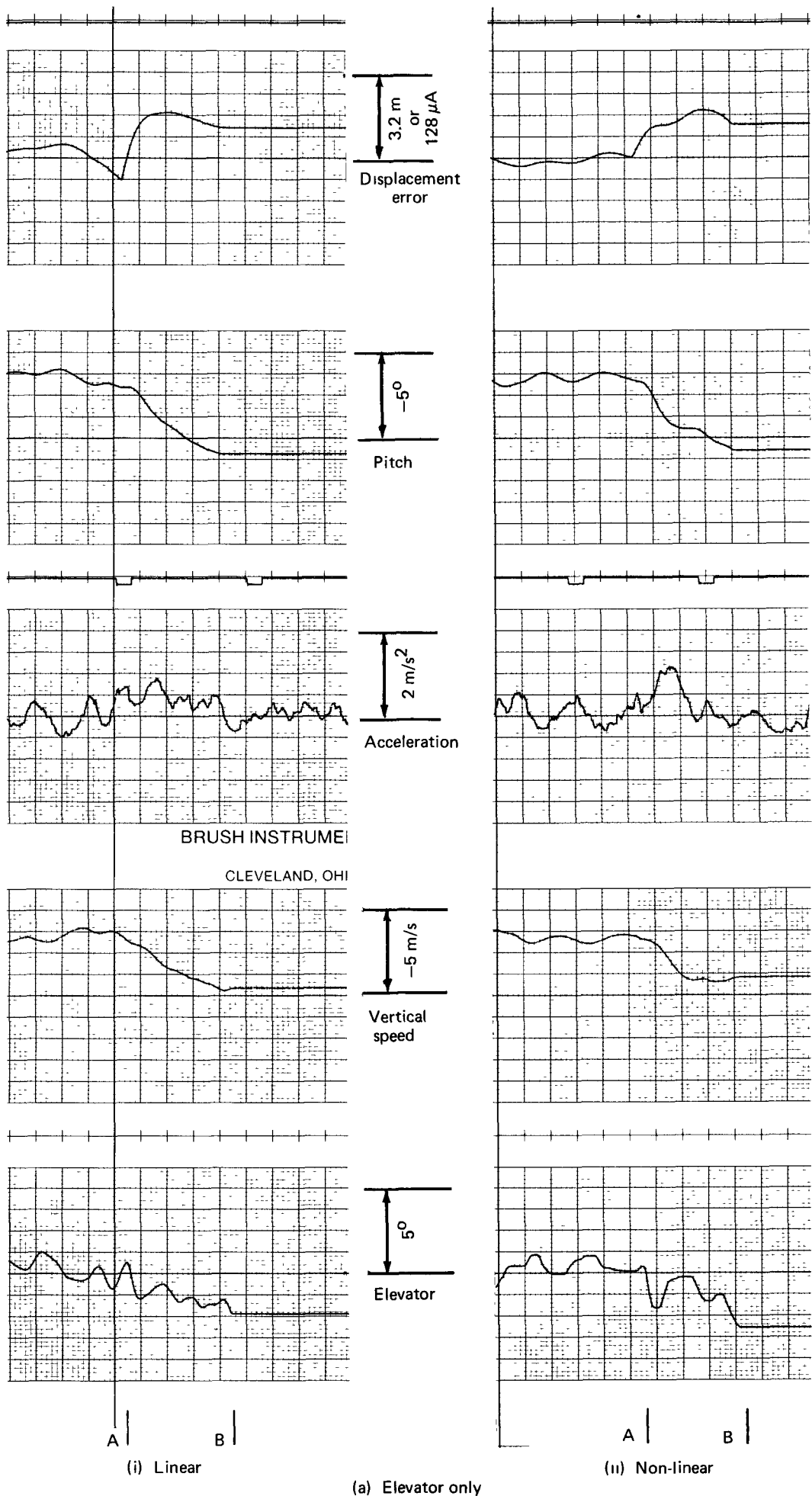


Fig.19 Horizontal turbulence during flare

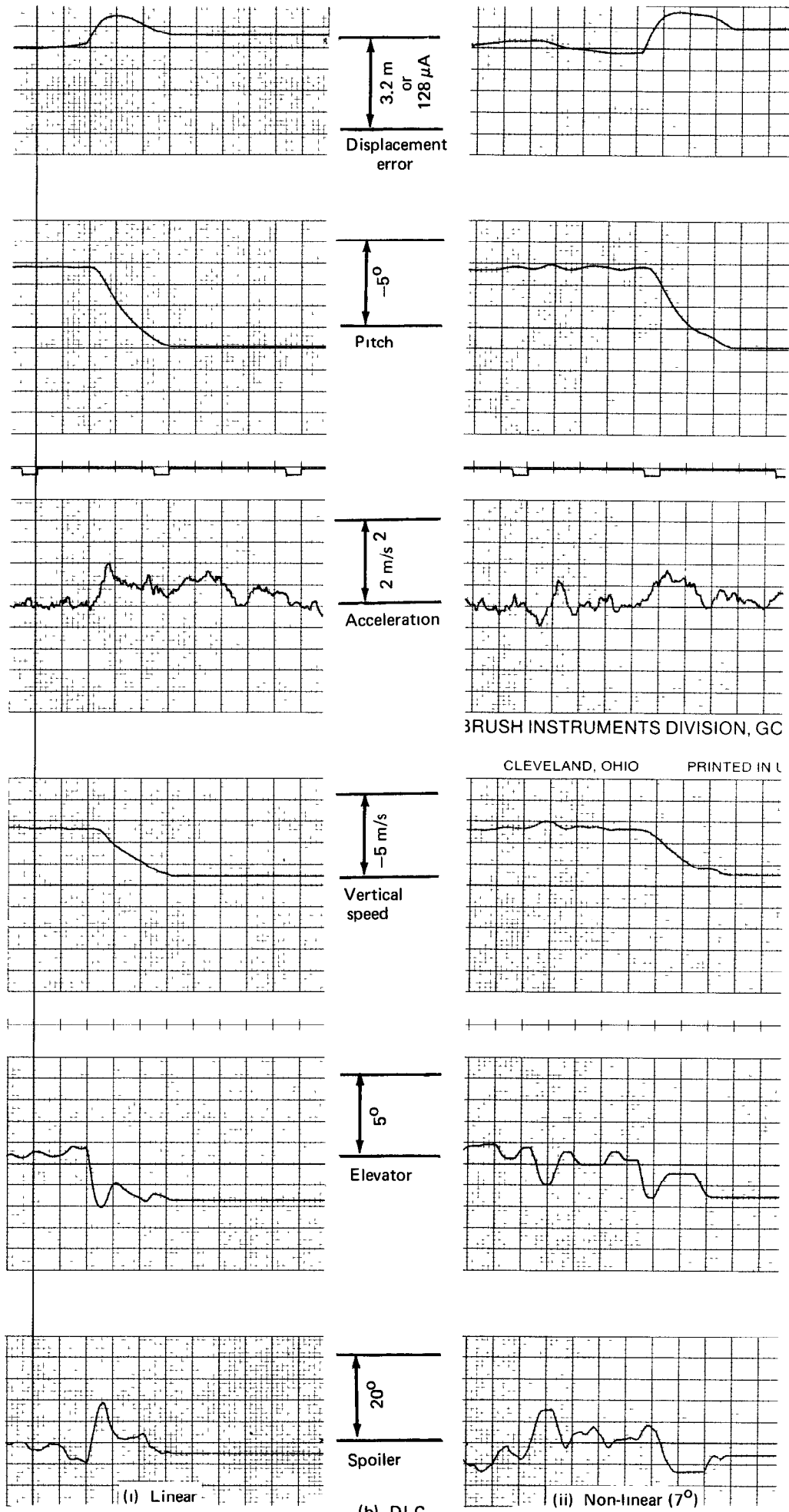
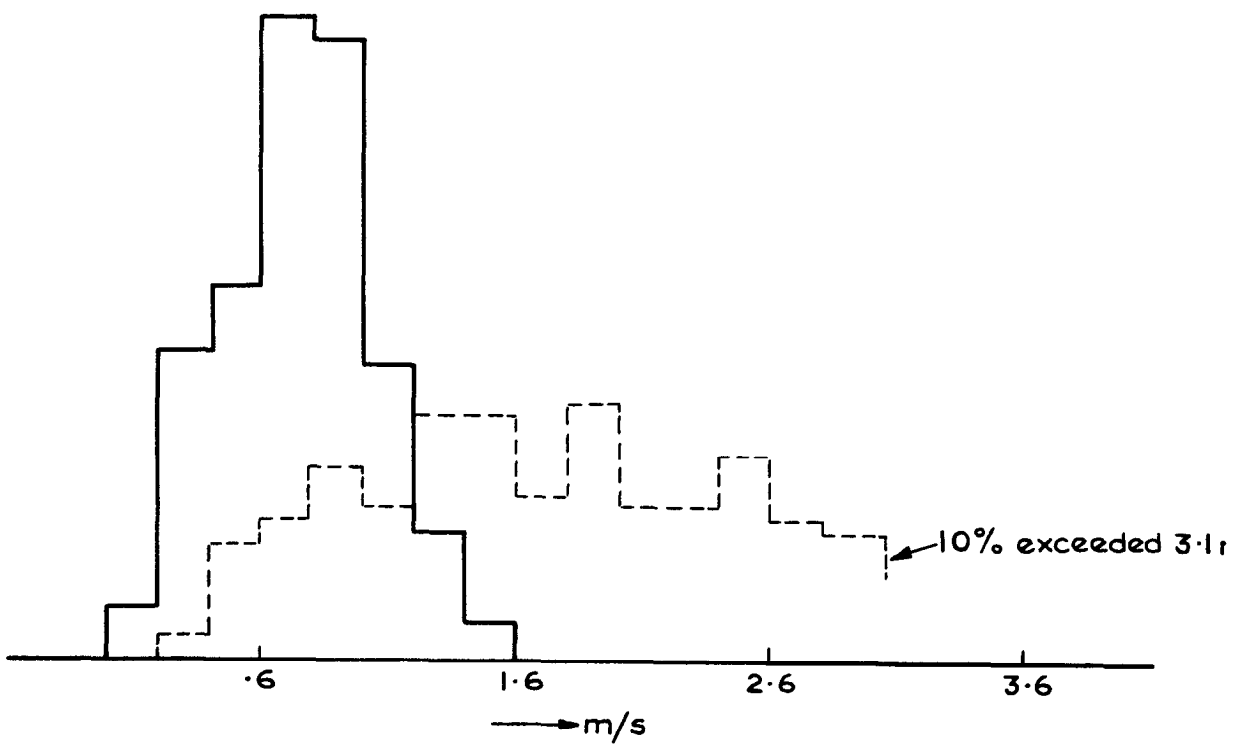
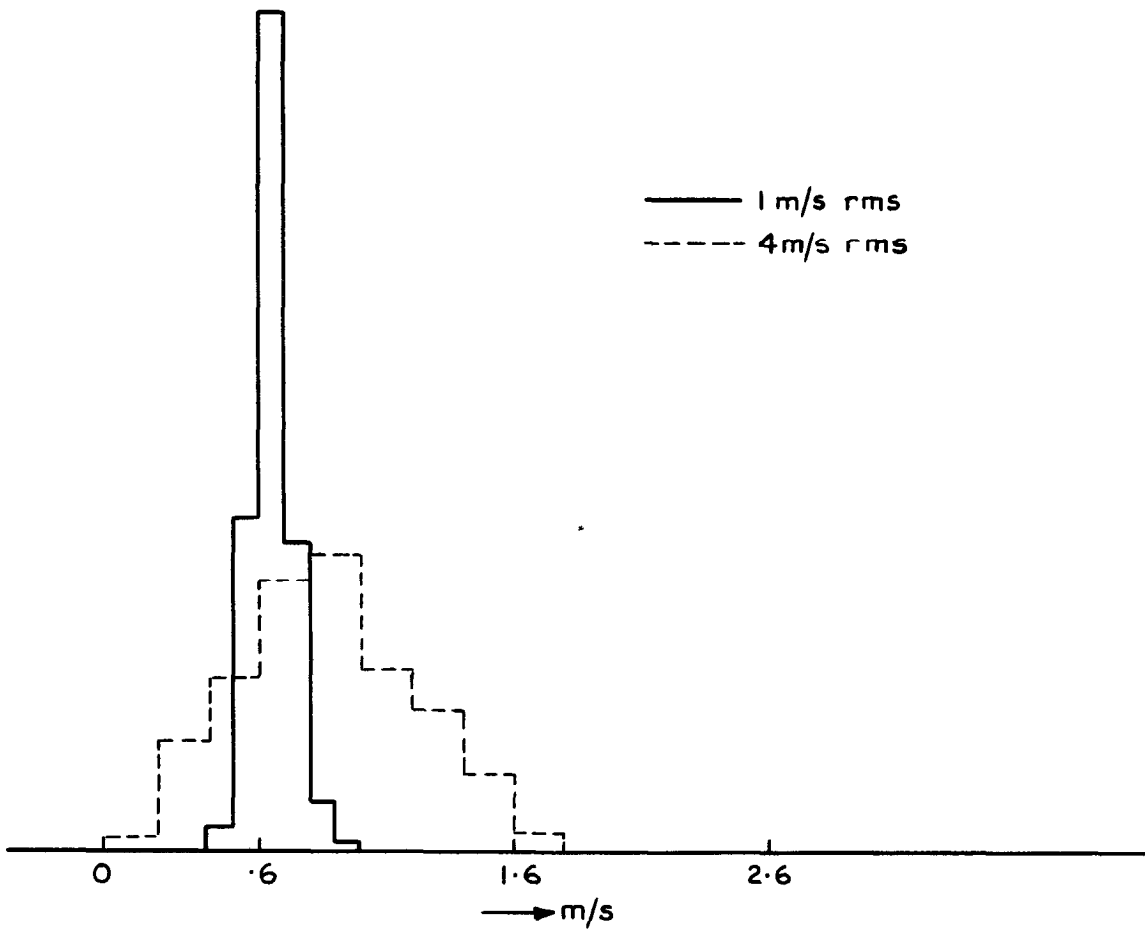


Fig.19 (cont'd.)



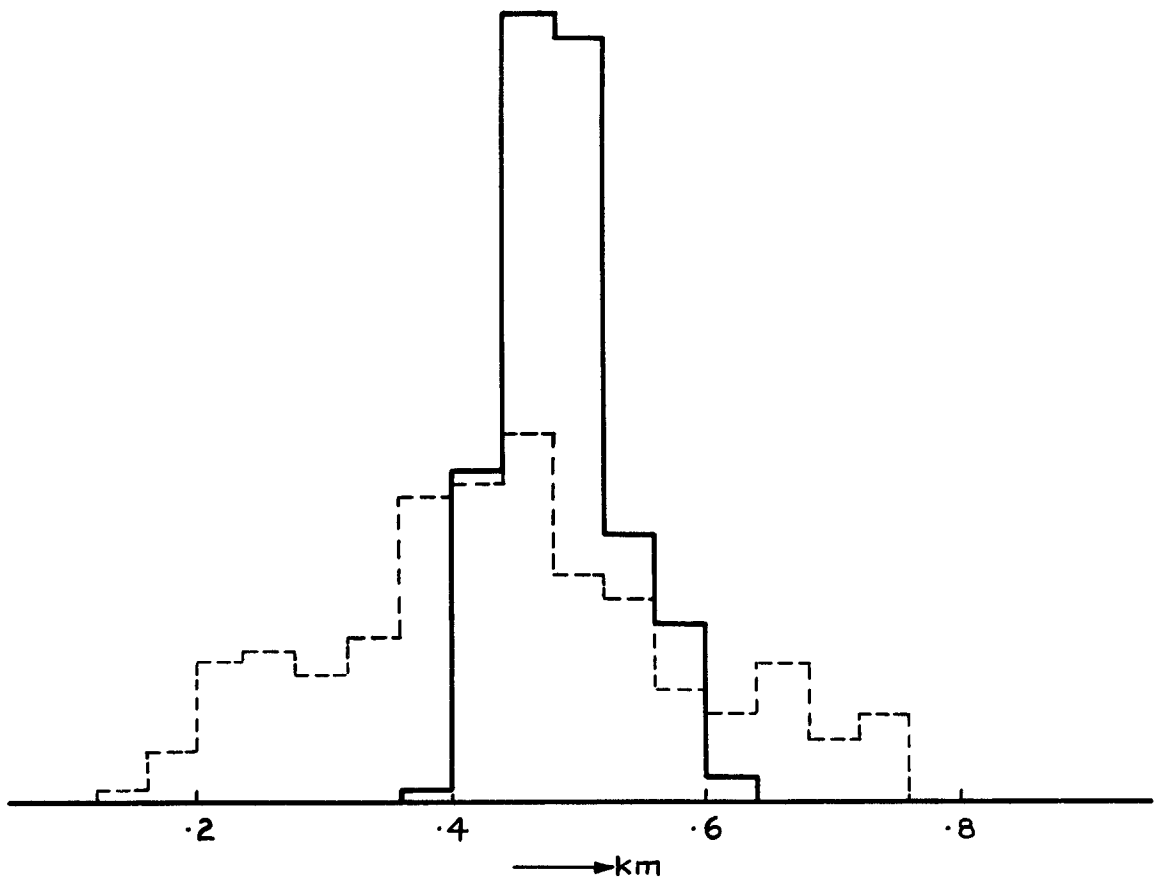
a Elevator only



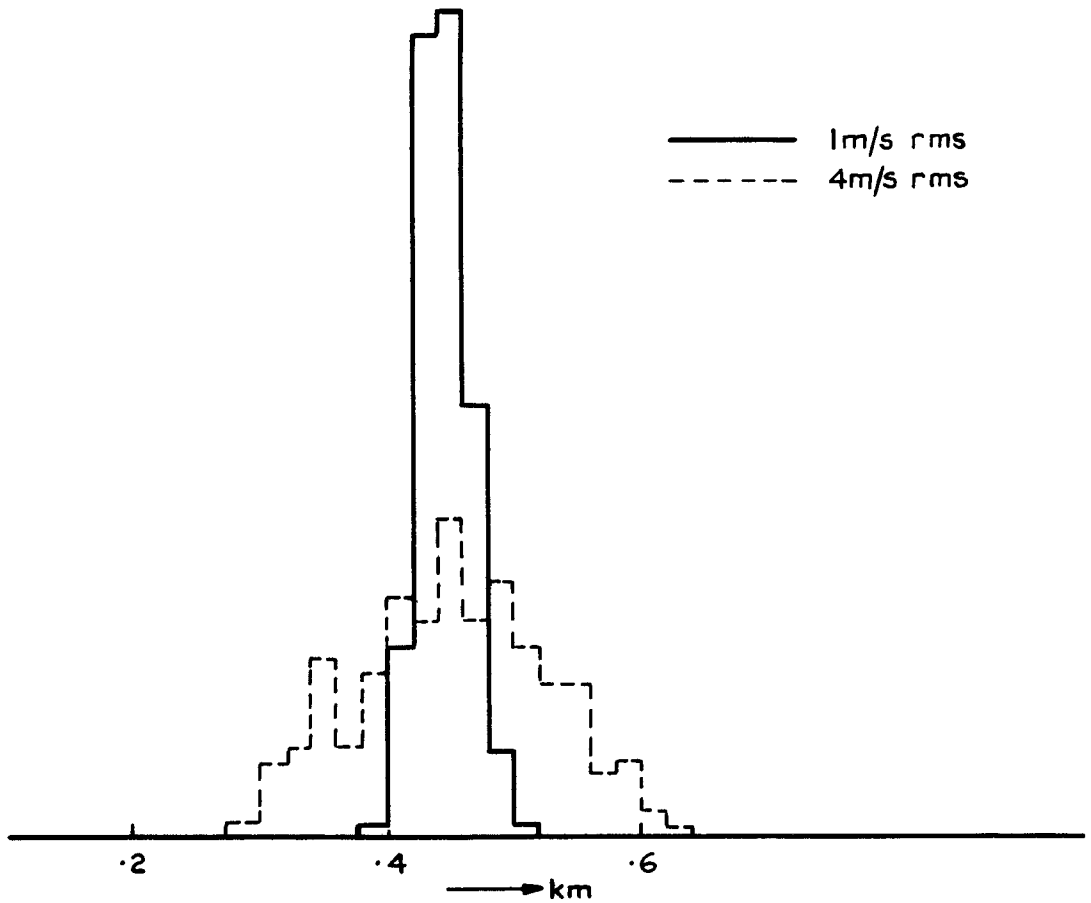
b DLC (NB linear)

Fig. 20a&b Effect of increasing level of horizontal turbulence on touchdown rate of descent



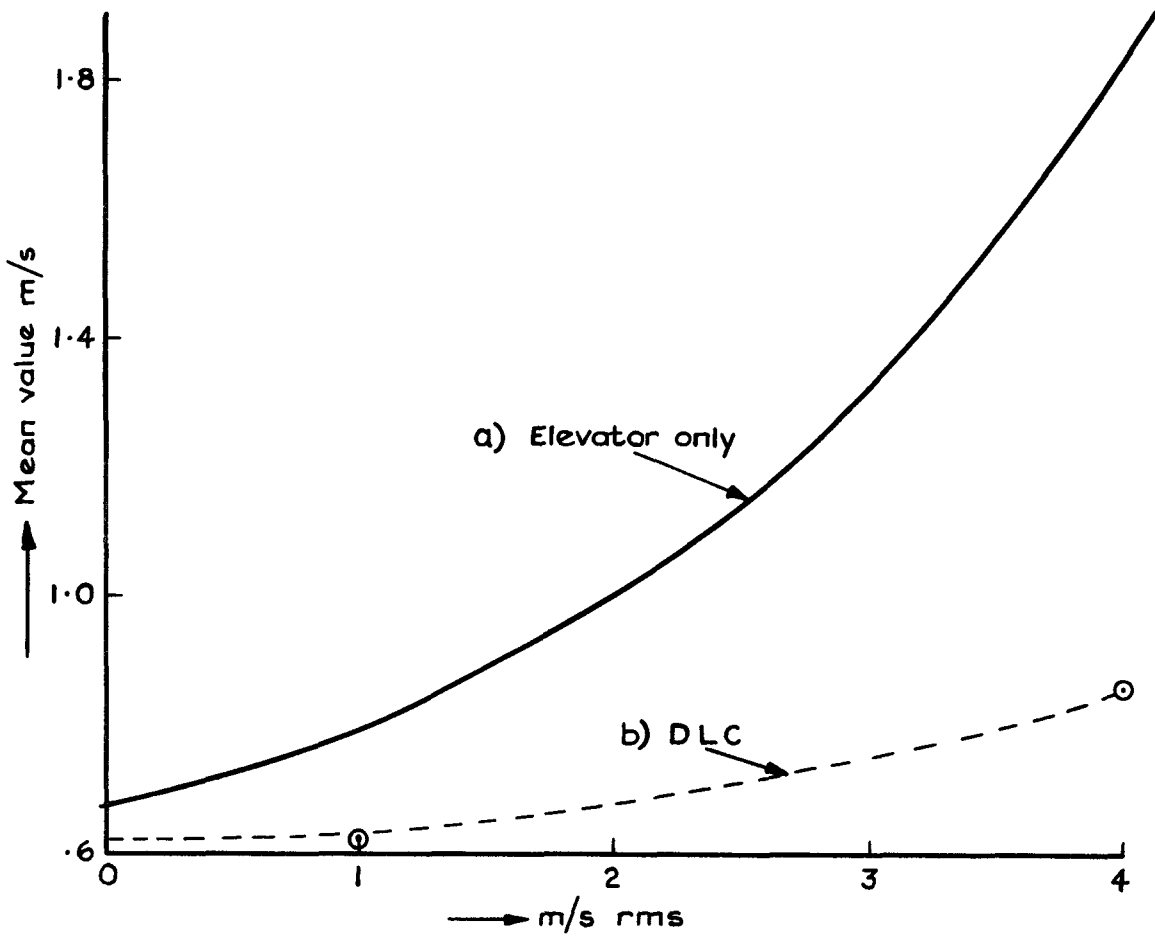


a Elevator only

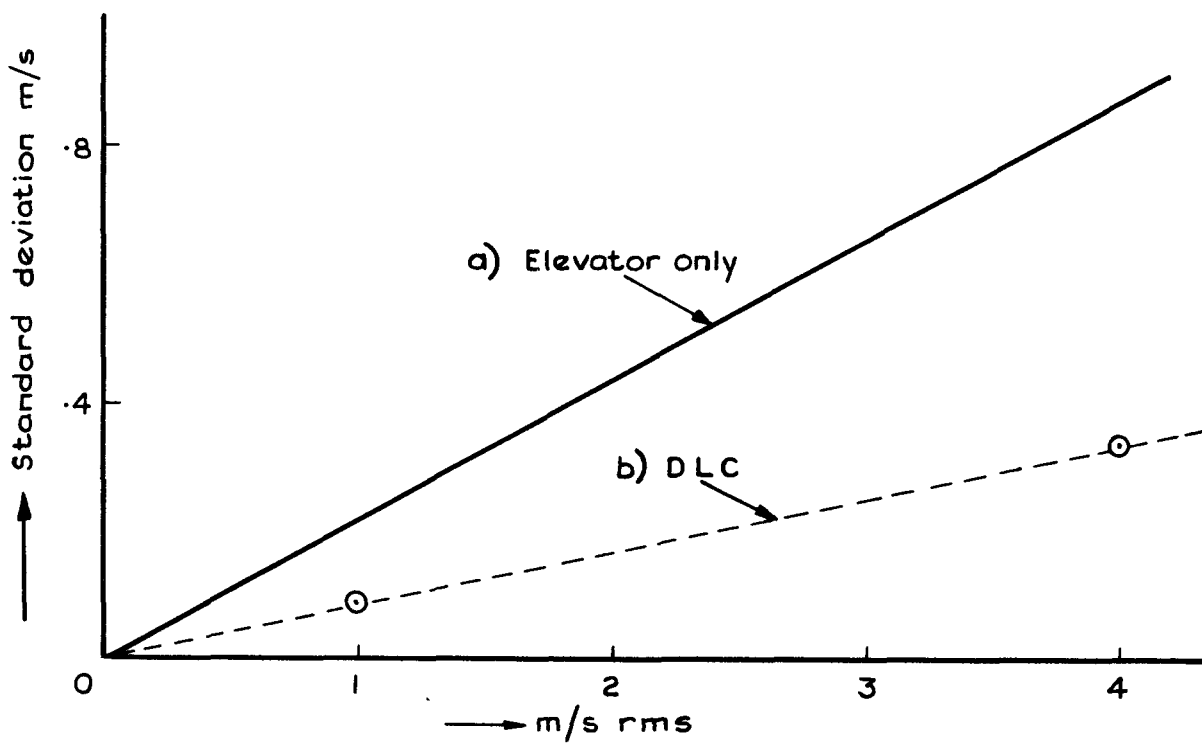


b DLC (linear)

Fig. 21a&b Effect of increasing level of horizontal turbulence on touchdown range (from threshold)



a Mean touchdown rate of descent



b Standard deviation

Fig. 22a&b Variation of touchdown rate of descent with level of horizontal turbulence

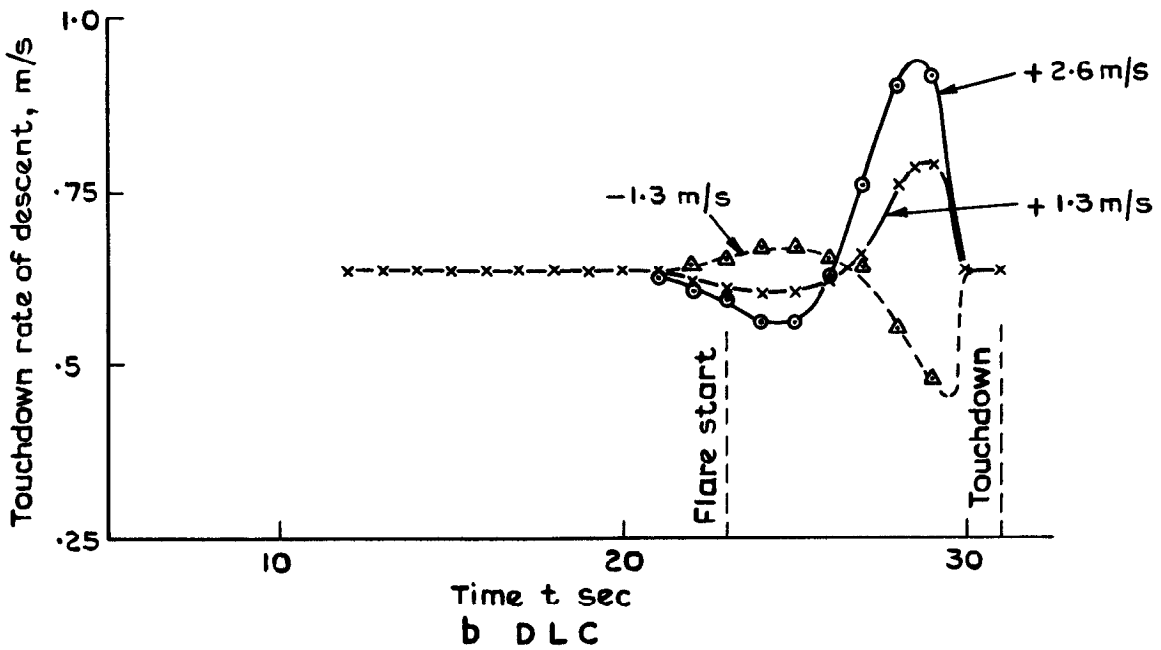
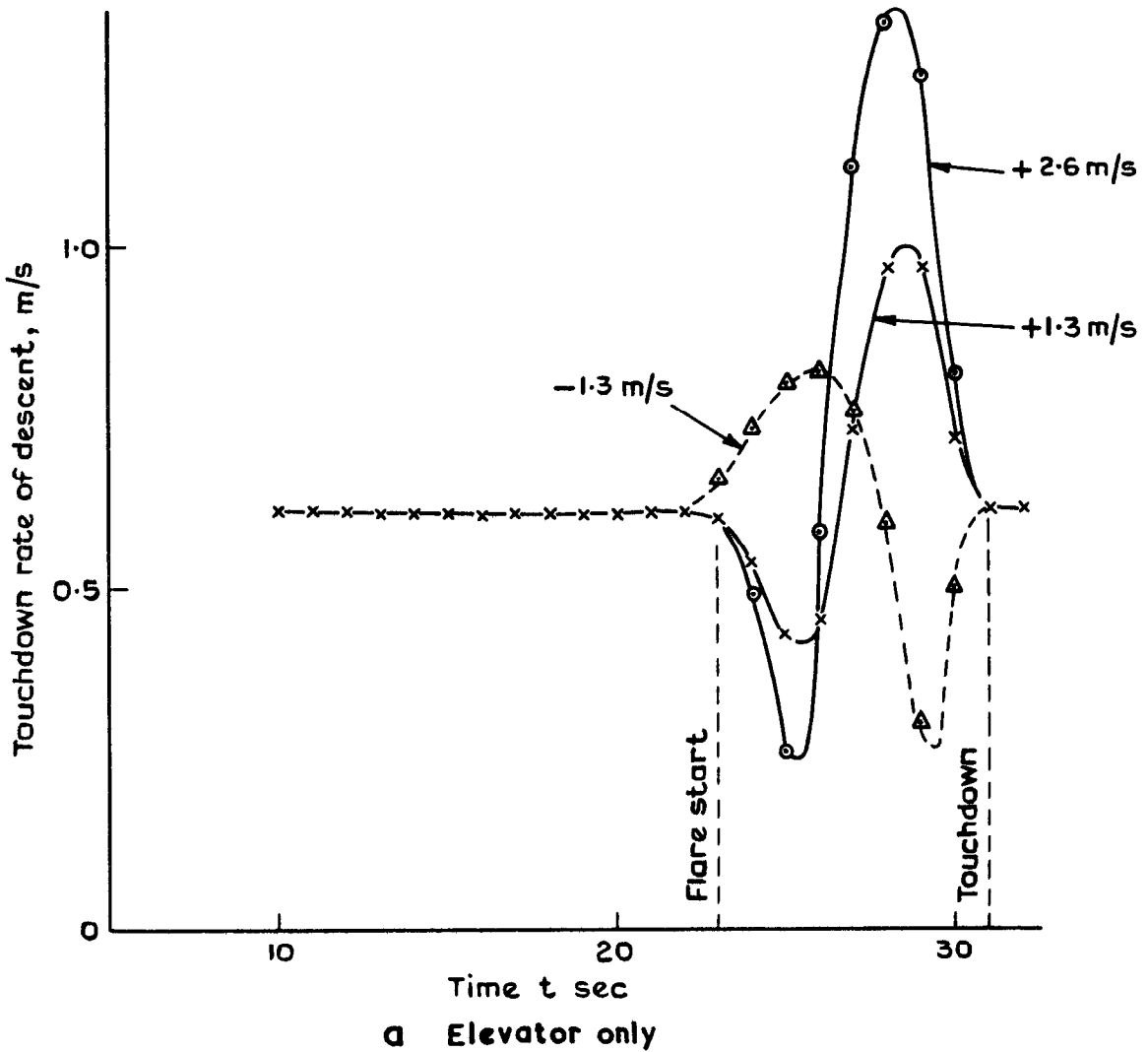


Fig.23 a&b Touchdown rate of descent due to step horizontal gusts applied at different times

ARC CP No.1337  
January 1974

621.396.933.23 :  
629.13.087

Gill, F. R.  
Corbin, M. J.

DESIGN AND THEORETICAL ASSESSMENT OF EXPERIMENTAL  
GLIDE PATH AND FLARE SYSTEMS FOR A BAC 1-11 AIRCRAFT  
(INCLUDING DIRECT LIFT CONTROL)

Two experimental glide path and flare systems are described, one using spoilers installed in the aircraft to provide direct lift control. The various longitudinal control modes, altitude hold, glide path and flare, have similar feedback control gains whose values were determined by parameter optimisation.

An assessment of the performance of these two systems is described. Using elevator and throttle control only, there was little improvement over current flare systems, but use of high gain direct lift control can give significant improvement.

ARC CP No.1337  
January 1974

621.396.933.23 :  
629.13.087

Gill, F. R.  
Corbin, M. J.

DESIGN AND THEORETICAL ASSESSMENT OF EXPERIMENTAL  
GLIDE PATH AND FLARE SYSTEMS FOR A BAC 1-11 AIRCRAFT  
(INCLUDING DIRECT LIFT CONTROL)

Two experimental glide path and flare systems are described, one using spoilers installed in the aircraft to provide direct lift control. The various longitudinal control modes, altitude hold, glide path and flare, have similar feedback control gains whose values were determined by parameter optimisation.

An assessment of the performance of these two systems is described. Using elevator and throttle control only, there was little improvement over current flare systems, but use of high gain direct lift control can give significant improvement.

DETACHABLE ABSTRACT CARDS

ARC CP No.1337  
January 1974

621.396.933.23 :  
629.13.087

Gill, F. R.  
Corbin, M. J.

DESIGN AND THEORETICAL ASSESSMENT OF EXPERIMENTAL  
GLIDE PATH AND FLARE SYSTEMS FOR A BAC 1-11 AIRCRAFT  
(INCLUDING DIRECT LIFT CONTROL)

Two experimental glide path and flare systems are described, one using spoilers installed in the aircraft to provide direct lift control. The various longitudinal control modes, altitude hold, glide path and flare, have similar feedback control gains whose values were determined by parameter optimisation.

An assessment of the performance of these two systems is described. Using elevator and throttle control only, there was little improvement over current flare systems, but use of high gain direct lift control can give significant improvement.

ARC CP No.1337  
January 1974

621.396.933.23 :  
629.13.087

Gill, F. R.  
Corbin, M. J.

DESIGN AND THEORETICAL ASSESSMENT OF EXPERIMENTAL  
GLIDE PATH AND FLARE SYSTEMS FOR A BAC 1-11 AIRCRAFT  
(INCLUDING DIRECT LIFT CONTROL)

Two experimental glide path and flare systems are described, one using spoilers installed in the aircraft to provide direct lift control. The various longitudinal control modes, altitude hold, glide path and flare, have similar feedback control gains whose values were determined by parameter optimisation.

An assessment of the performance of these two systems is described. Using elevator and throttle control only, there was little improvement over current flare systems, but use of high gain direct lift control can give significant improvement.

DETACHABLE ABSTRACT CARDS

- Cut here -

- Cut here -

© *Crown copyright*

1975

Published by  
HER MAJESTY'S STATIONERY OFFICE

*Government Bookshops*

49 High Holborn, London WC1V 6HB  
13a Castle Street, Edinburgh EH2 3AR  
41 The Hayes, Cardiff CF1 1JW  
Brazennose Street, Manchester M60 8AS  
Southey House, Wine Street, Bristol BS1 2BQ  
258 Broad Street, Birmingham B1 2HE  
80 Chichester Street, Belfast BT1 4JY

*Government Publications are also available  
through booksellers*